ENVIRONMENTAL MAGNETISM: PRINCIPLES AND APPLICATIONS

Qingsong Liu,[1] Andrew P. Roberts,[2] Juan C. Larrasoaña,[3] Subir K. Banerjee,[4] Yohan Guyodo,[5] Lisa Tauxe,[6] and Frank Oldfield[7]

Received 15 March 2012; revised 9 July 2012; accepted 13 August 2012; published 6 November 2012.

[1] In environmental magnetism, rock and mineral magnetic techniques are used to investigate the formation, transportation, deposition, and postdepositional alterations of magnetic minerals under the influences of a wide range of environmental processes. All materials respond in some way to an applied magnetic field, and iron-bearing minerals are sensitive to a range of environmental processes, which makes magnetic measurements extremely useful for detecting signals associated with environmental processes. Environmental magnetism has grown considerably since the mid 1970s and now contributes to research in the geosciences and in branches of physics, chemistry, and biology and environmental science, including research on climate change, pollution, iron biomineralization, and depositional and diagenetic processes in sediments to name a few applications. Magnetic parameters are used to routinely scan sediments, but interpretation is often difficult and requires understanding of the underlying physics and chemistry. Thorough examination of magnetic properties and of the environmental processes that give rise to the measured magnetic signal is needed to avoid ambiguities, complexities, and limitations to interpretations. In this review, we evaluate environmental magnetic parameters based on theory and empirical results. We describe how ambiguities can be resolved by use of combined techniques and demonstrate the power of environmental magnetism in enabling quantitative environmental interpretations. We also review recent developments that demonstrate the mutual benefit of environmental magnetism from close collaborations with biology, chemistry, and physics. Finally, we discuss directions in which environmental magnetism is likely to develop in the future.

Citation: Liu, Q., A. P. Roberts, J. C. Larrasoaña, S. K. Banerjee, Y. Guyodo, L. Tauxe, and F. Oldfield (2012), Environmental magnetism: Principles and applications, *Rev. Geophys.*, *50*, RG4002, doi:10.1029/2012RG000393.

1. INTRODUCTION

[2] Environmental magnetism is an interdisciplinary subject that integrates research on a wide range of topics [*Evans and Heller*, 2003]. The basic principle of environmental magnetism involves linking magnetic properties of mineral assemblages to the environmental processes that control them. Environmental changes, including climate, occur over variable time scales and can influence the mode of sediment transport, deposition, and/or diagenetic reactions [e.g., *Thompson et al.*, 1980; *Thompson and Oldfield*, 1986; *Oldfield*, 1991; *Verosub and Roberts*, 1995; *Maher and Thompson*, 1999]. The magnetic properties of many minerals in different domain states have been systematically investigated since the development of paleomagnetism [*Dunlop and Özdemir*, 1997]. The initial purpose of rock and mineral magnetic studies was to investigate the directional stability of remanence carried by magnetic minerals over geological time scales. Magnetic stability relies not only on the domain states of the constituent rock-forming magnetic minerals [*Dunlop and Özdemir*, 1997] but also on how those minerals formed and were subsequently preserved or transformed. Insights from rock and mineral magnetism that relate magnetic properties to magnetic mineralogy and changes in their concentration, grain size or grain shape,

[1]State Key Laboratory of Lithospheric Evolution, Institute of Geology and Geophysics, Chinese Academy of Sciences, Beijing, China.
[2]Research School of Earth Sciences, Australian National University, Canberra, ACT, Australia.
[3]Instituto Geológico y Minero de España, Unidad de Zaragoza, Zaragoza, Spain.
[4]Institute for Rock Magnetism, University of Minnesota, Twin Cities, Minneapolis, Minnesota, USA.
[5]Institut de Minéralogie et de Physique des Milieux Condensés, UMR 7590, CNRS-UPMC-IPGP-UPD-IRD, Paris, France.
[6]Scripps Institution of Oceanography, University of California, San Diego, La Jolla, California, USA.
[7]School of Environmental Sciences, University of Liverpool, Liverpool, UK.

Corresponding author: Q. Liu, State Key Laboratory of Lithospheric Evolution, Institute of Geology and Geophysics, Chinese Academy of Sciences, 19 Beitucheng Xi Rd., Chaoyang, Beijing, China. (liux0272@yahoo.com)

8755-1209/12/2012RG000393
Paper number 2012RG000393

therefore serve as the foundation for what has come to be known as "environmental magnetism" [*Thompson et al.*, 1980; *Thompson and Oldfield*, 1986; *Verosub and Roberts*, 1995].

[3] In 1986, Roy Thompson and Frank Oldfield published the seminal textbook *Environmental Magnetism*, which defined the basic scope of the subject. After a decade, *Verosub and Roberts* [1995] summarized new developments and foresaw a bright future for environmental magnetism, pointing out the inherent advantages of magnetic techniques. For example, magnetic measurements are efficient, nondestructive, sensitive, and, most important, they can address significant issues that cannot be resolved with other techniques. The 1997 textbook by David Dunlop and Özden Özdemir, *Rock Magnetism: Fundamental and Frontiers*, systematically explained the physical basis for different magnetic parameters in detail. *Maher and Thompson* [1999] summarized developments in environmental magnetic analysis of Quaternary settings in their textbook *Quaternary Climates, Environments and Magnetism.* More recently, *Evans and Heller* [2003] outlined the range of themes addressed by environmental magnetism and treated developments such as biomagnetism and magnetic monitoring of pollution in greater depth than previous reviews. *Tauxe* [2010] updated the rock magnetic toolkit available to environmental magnetism and described recent applications.

[4] The fields of rock and environmental magnetism have grown considerably over the past 30 years. Advances have been driven by the fact that iron-bearing minerals are sensitive to many environmental processes, which makes magnetic analysis extremely useful in studies of climate change (e.g., assessing paleoclimate fluctuations recorded by loess-paleosol sequences and lake and marine sediments (see section 4)), pollution, iron biomineralization, and in understanding depositional and diagenetic processes in sediments. The wide range of geological, biological and environmental processes that can produce and mix magnetic minerals means that increasing efforts have been made in recent years to unravel complex magnetic signals to understand the respective significance and the environmental processes from which they result. Furthermore, minute quantities of magnetic minerals are easily detected with modern magnetic measurement systems. These facts will ensure the widespread use of environmental magnetism and its techniques to address many problems in the geosciences, and in branches of physics, chemistry, biology and environmental science. Pioneering studies on the subject have been well summarized by *Verosub and Roberts* [1995]. In this paper, we focus on recent progress in rock and environmental magnetism. First, we evaluate environmental magnetic parameters, based on theory and empirical results. We show how ambiguities can be resolved by combining techniques and we demonstrate their power for enabling quantitative environmental interpretations. We also review recent developments in environmental magnetism, to demonstrate how it has benefited from collaborations with biology, chemistry and physics and how it has also had impact in these fields. We conclude with a perspective on how environmental magnetism is likely to develop in the near future.

2. FUNDAMENTALS OF ROCK AND ENVIRONMENTAL MAGNETISM

[5] Magnetic parameters provide information on the concentration, domain state (or indirectly the magnetic grain size), and mineralogy of magnetic particles in a sample, all of which are related to original geological or subsequent environmental processes. The physics of magnetism and physical interpretation of many magnetic parameters have been previously well summarized [e.g., *Thompson and Oldfield*, 1986; *Hunt et al.*, 1995a; *Verosub and Roberts*, 1995; *Dekkers*, 1997; *Dunlop and Özdemir*, 1997; *Walden et al.*, 1999; *Maher and Thompson*, 1999; *Peters and Dekkers*, 2003; *Evans and Heller*, 2003; *Liu et al.*, 2007a; *Tauxe*, 2010]. In this section, we briefly sketch the main concepts for uninitiated readers. Readers who are familiar with rock and environmental magnetic techniques may wish to proceed directly to Section 3. For simplicity, we use the term "oxide" to include both iron oxides and oxyhydroxides. Thus, magnetite, maghemite and hematite, as well as ferrihydrite, goethite and lepidocrocite classify as "oxides" when this term is used with quotation marks.

2.1. The Physical Framework for Interpretation of Magnetic Parameters

2.1.1. Room Temperature Properties

2.1.1.1. Magnetic Susceptibility

[6] One of the most widely used magnetic properties is the low-field magnetic susceptibility (χ, mass specific, or κ, volume specific). χ is defined as the ratio between the magnetic response (or the induced magnetization, M) of a material to an applied magnetic field (H), $\chi = dM/dH$. Unlike magnetic remanence, all materials contribute to the bulk χ of a sample. Therefore, despite its widespread use, χ is a complex parameter that reflects contributions from minerals that retain a strong remanent magnetization in the absence of an applied field (i.e., ferromagnetic materials, *sensu lato*, e.g., magnetite, maghemite), a weak remanent magnetization (i.e., antiferromagnetic materials, e.g., hematite and goethite), and those that are "nonmagnetic," which include paramagnetic (e.g., silicates, clays), and diamagnetic (e.g., quartz, carbonate) materials. Therefore, to characterize the ferrimagnetic (χ_{ferri}) component (e.g., due to magnetite, pyrrhotite, greigite) in samples, contributions from paramagnetic (χ_{para}) and imperfect antiferromagnetic minerals (e.g., hematite and goethite) must be subtracted from the bulk χ. The magnetization of ferrimagnetic minerals tends to saturate in large applied magnetic fields. The susceptibility in saturating fields (i.e., the high-field slope, χ_{high}) is frequently used as a proxy for the nonferrimagnetic contribution to susceptibility (i.e., the combined paramagnetic and diamagnetic contributions). The ferrimagnetic susceptibility is then given by: $\chi_{ferri} = \chi - \chi_{high}$. χ_{ferri} is mildly grain size dependent owing to the effects of complex spin structures that depend on the size and shape of magnetic particles. For example, at sizes larger than a few hundred nanometers,

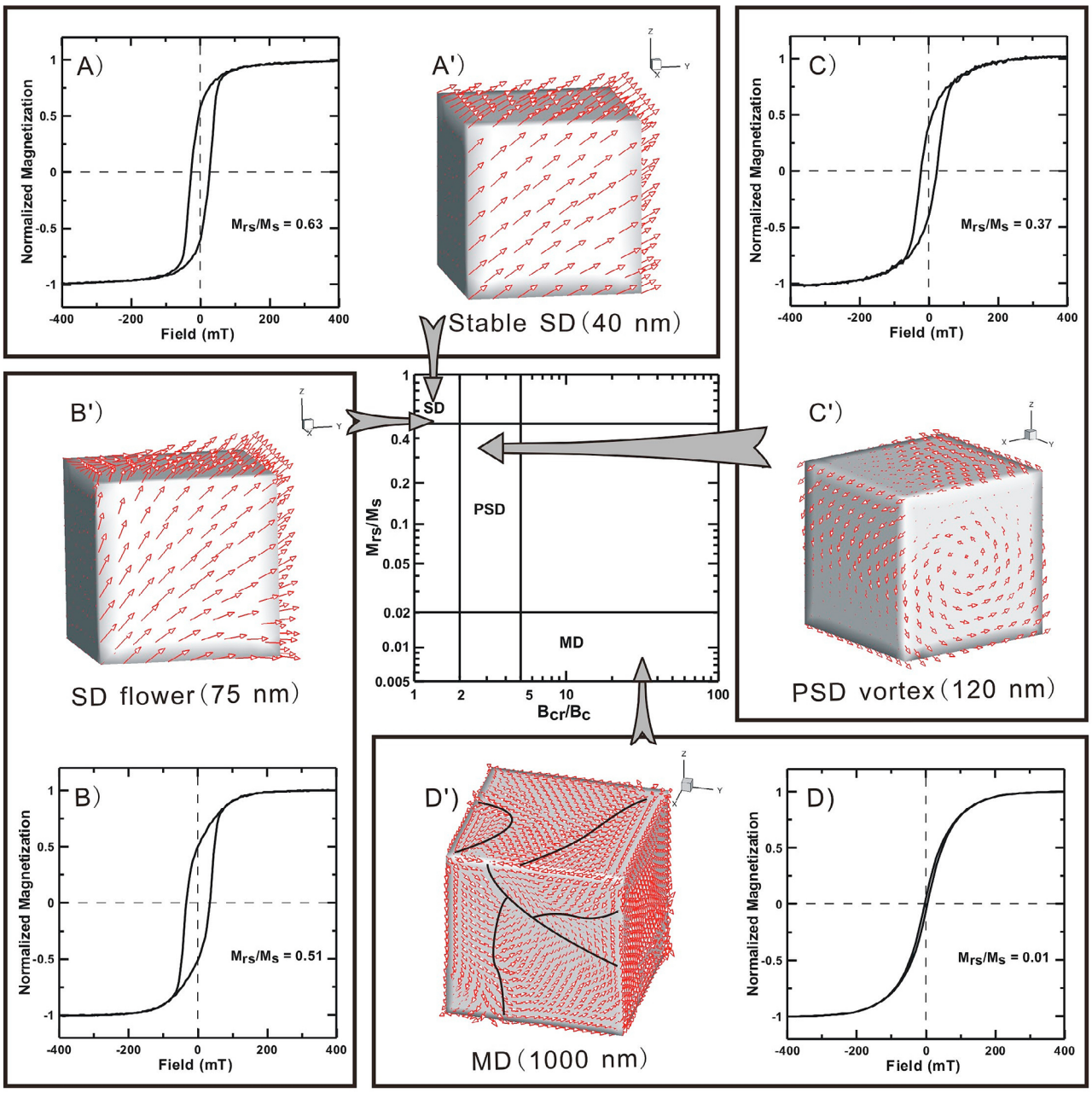

Figure 1. (a–d) Hysteresis loops and associated theoretical micromagnetic states for a uniaxial magnetite cube with different sizes. With increasing grain size, spin structures evolve from uniaxial (Figure 1a) to flower (Figure 1b), to vortex (Figure 1c), and to multidomain states (Figure 1d). The central subfigure is a plot of grain size–dependent ratios of hysteresis parameters [*Day et al.*, 1977] with data ranges for M_{rs}/M_s versus B_{cr}/B_c (usually named the Day plot) that divides the region into SD, PSD, and MD fields. For a more detailed explanation of the Day plot, readers are referred to *Dunlop* [2002a, 2002b].

magnetite crystals break into regions of uniform magnetization (magnetic domains) to reduce the overall magnetic energy [*Dunlop and Özdemir*, 1997; *Tauxe*, 2010]. Domain walls can migrate through a crystal in response to changing external field and temperature conditions (domain structures are illustrated in Figure 1). Grains with magnetic domain walls, which are known as multidomain (MD) grains, therefore, respond differently to applied fields than magnetically ideal single domain (SD) grains that are uniformly magnetized and that have no domain walls. At the small end of the grain size spectrum, SD grains have magnetic moments that are strongly constrained to lie along particular directions within the grain, which limits their χ. But the magnetization of the smallest SD grains can be dominated by thermal fluctuations; their moments are not constrained and they exhibit what is known as superparamagnetic (SP) behavior and have much higher χ than SD grains. For hydrothermally grown magnetites with grain sizes >∼100 nm, *Heider et al.* [1996] found that χ is independent of grain size, which could be

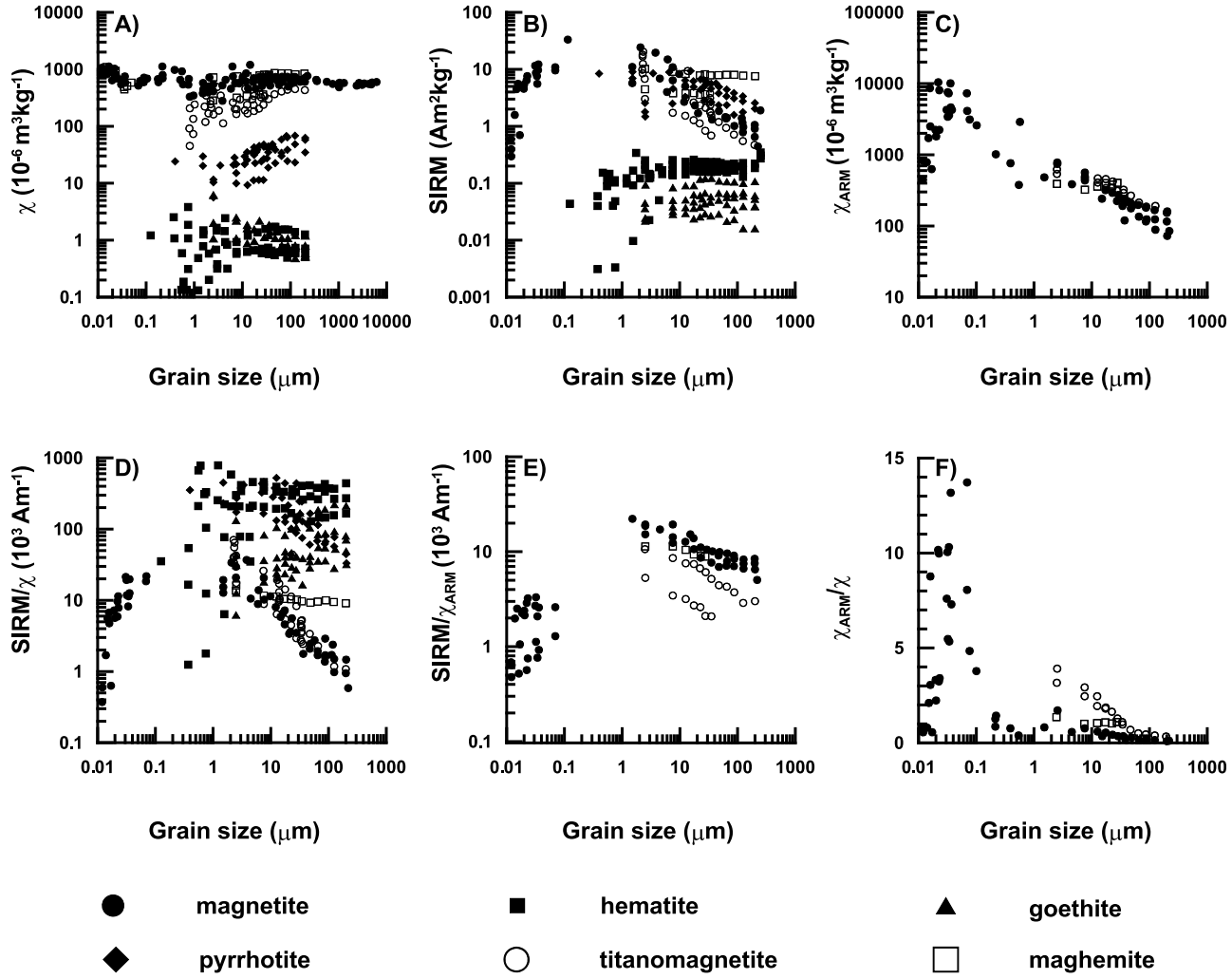

Figure 2. Grain size dependence of various magnetic properties. (Reprinted from *Peters and Dekkers* [2003], with permission from Elsevier.)

because internal stress in these particles is low compared to natural minerals.

[7] The ability of the magnetic moment to respond to changes in the external field is time and temperature dependent. χ therefore depends on the measurement frequency used or the length of time over which measurements are made. Generally, the magnetic properties of MD and SD materials reflect fundamentally different magnetization mechanisms, and are controlled by nucleation, annihilation, pinning and movement of domain walls, or by rotation of magnetization, respectively. As a result, these types of grains can be easily distinguished. However, SP and MD particles have many similarities in their magnetic response because they are both less stable than SD grains. The environmental processes that dictate the presence of coarse versus fine grains can be vastly different. It is therefore crucially important to be able to clearly distinguish SP from MD grains in environmental magnetic studies (see below).

[8] Grains of an intermediate size, which are too small to separate into domains, yet are too large to be uniformly magnetized, exhibit complex electronic spin patterns (Figure 1). For example, instead of two domains separated by a domain wall, the grain may be almost entirely occupied by a domain wall–like structure known as a vortex [*Schabes and Bertram*, 1988; *Williams and Dunlop*, 1989]. Smaller grains may have spins that fan out in "flower" structures. These grains exhibit behaviors that are transitional between those of true MD and SD grains and are termed pseudo single-domain (PSD) grains [e.g., *Stacey*, 1962; *Stacey and Banerjee*, 1974; *Williams and Dunlop*, 1995].

[9] Organization of internal configurations of magnetic spins as SD, PSD, or MD structures means that χ_{ferri} varies mildly with grain size (Figure 2) as well as with magnetic mineral concentration for strongly magnetic minerals [*Peters and Dekkers*, 2003]. Near the SP/SD boundary (~20–25 nm for magnetite) [*Maher*, 1988; *Worm*, 1998], things become more complex. The threshold at which a particle transforms from stable SD to SP behavior is controlled by the time over which it can respond to external forcing by an applied field, and is therefore both time and temperature dependent. By decreasing temperature or the time span of observation, grains near the SP/stable SD boundary can change from the SP state to the stable SD state [*O'Reilly*, 1984; *Worm*, 1998]. In practice, this can be done by increasing the observation

frequency (e.g., from 470 Hz to 4700 Hz, the two operating frequencies for the commonly used Bartington Instruments magnetic susceptibility meter). Changing from the SP to the stable SD state causes a sharp decrease in χ [*Thompson and Oldfield*, 1986; *Worm*, 1998; *Till et al.*, 2011]. Therefore, the absolute frequency-dependent susceptibility χ_{fd} ($= \chi_{470\ Hz} - \chi_{4700\ Hz}$) is used to determine the concentration of magnetic particles over a small grain size window across the SP/stable SD boundary [*Liu et al.*, 2005a]. χ_{fd} can be normalized by χ_{ferri} ($\chi_{fd}\% = \chi_{fd}/\chi_{ferri} \times 100\%$). χ_{fd} and $\chi_{fd}\%$ are both used to detect the presence of SP particles [*Zhou et al.*, 1990; *Worm*, 1998; *Liu et al.*, 2005a]. $\chi_{fd}\%$ is also related to the grain size distribution of the SP/SD particle assemblage [*Worm*, 1998]. SP behavior is extremely temperature dependent, which means that it is useful to measure χ as a function of temperature [e.g., *Dunlop*, 1973; *Liu et al.*, 2005a].

2.1.1.2. Anhysteretic Remanent Magnetization

[10] The smallest stable SD particles have the lowest χ_{ferri}, but have the highest ability to retain a magnetic remanence [*Banerjee et al.*, 1981; *King et al.*, 1982; *Hunt et al.*, 1995a]. One such remanence, the anhysteretic remanent magnetization (ARM), is imparted by placing a sample in an alternating field (e.g., AF = ~100 mT) with a superimposed small biased direct current field (e.g., DC = ~50 microtesla, μT). ARM is proportional to the DC bias field, therefore, it is frequently expressed as the susceptibility of ARM (χ_{ARM} = ARM/DC bias field). The different behaviors of χ and ARM (or χ_{ARM}) with grain size (Figures 2a and 2c) led *Banerjee et al.* [1981] to propose that plots of χ versus χ_{ARM} (the Banerjee diagram) are useful for detecting grain size changes (Figure 2f). *King et al.* [1982] proposed that χ_{ARM} can be plotted versus χ_{ferri} in a modified Banerjee diagram known as the King diagram.

[11] While ARM is a useful parameter, interpretations involving ARM are not without complication. For example, the relationship between χ_{ARM} and χ_{fd} (or $\chi_{fd}\%$) can be sensitive to the relative concentration of SP and stable SD particles. Moreover, χ_{ARM} assumes that ARM is linearly related to the DC bias field. This assumption is rarely tested and fails at DC fields >~80 μT [*Tauxe*, 1993]. ARM is strongly dependent on magnetic particle concentration; ARM can decrease with increasing concentration due to interactions among magnetic particles [*Sugiura*, 1979]. Finally, ARM acquisition depends on differences in equipment, magnitudes of applied AF and DC fields, decay rates [*Yu and Dunlop*, 2003], and on other experimental factors used to impart ARM in different laboratories [*Sagnotti et al.*, 2003].

2.1.1.3. Isothermal Remanent Magnetization

[12] When a sample is exposed to a virtually instantaneously applied large magnetic field (i.e., over nanoseconds or milliseconds), it becomes remagnetized along the applied field direction. This magnetization is termed an isothermal remanent magnetization (IRM). The IRM increases with increasing applied field until the response is saturated and the sample acquires a room temperature saturation IRM (SIRM or M_{rs}). A DC field of 1 T is usually used, although such a field will not saturate imperfect antiferromagnetic materials (hematite, goethite). Therefore, an IRM imparted at 1 T is often specified as $IRM_{1\ T}$ rather than as SIRM. Higher maximum applied fields (>1.5–2 T) are preferable, although even these fields will still not fully saturate hematite or goethite; the latter mineral (without Al substitution) does not even saturate in an applied field of 57 T [*Rochette et al.*, 2005].

[13] SIRM can reflect magnetic mineral concentration when the magnetic grain size and mineralogy remain relatively constant. Similar to the χ_{ARM}/χ_{ferri} ratio, χ_{ARM}/SIRM is also grain size dependent [*Peters and Dekkers*, 2003]. In some cases, χ_{ARM}/SIRM is a superior parameter to χ_{ARM}/χ_{ferri} because the former is affected only by particles that carry a permanent magnetization (i.e., those with stable SD and larger grain sizes), whereas χ_{ARM}/χ_{ferri} is also strongly affected by SP particles. The SIRM/χ ratio is also frequently used as an indicator of SD greigite particles in sedimentary environments [e.g., *Snowball*, 1991; *Roberts and Turner*, 1993; *Roberts*, 1995], where enhanced SIRM values compared to χ indicate the superior magnetic recording capability of SD particles.

2.1.1.4. Saturation Magnetization (M_s)

[14] Like the remanent magnetization, the induced magnetization (M) also increases with increasing applied field. At a critical field (~300 mT for magnetite), the electronic spins are fully aligned and M no longer responds to increasing applied fields. The resulting magnetization is the saturation magnetization (M_s). Unlike other parameters, M_s is independent of grain size, and is therefore an excellent proxy for the concentration of magnetic minerals. M is measured in the presence of an applied field, therefore M_s in samples with significant paramagnetic content needs to have the paramagnetic susceptibility (estimated from the high-field slope) subtracted. M_s can also be combined with other parameters. For example, χ_{ferri}/M_s is sensitive to the presence of SP grains [*Hunt et al.*, 1995a; *Liu et al.*, 2003] because of the enhanced response of M_s to SP grains relative to SD grains.

2.1.1.5. Coercivity-Dependent Parameters

[15] The magnetization of ferrimagnetic minerals (magnetite, maghemite, titanomagnetite, pyrrhotite, greigite) can be more than 2 orders of magnitude higher than that of antiferromagnetic minerals (hematite and goethite). The signal of these weakly magnetic minerals is therefore often masked by the presence of other strongly magnetic minerals [e.g., *Liu et al.*, 2002]. Nevertheless, their magnetic signals can be isolated by exploiting their different degrees of magnetic "hardness" (i.e., coercivity). The energy required to overcome the tendency of magnetic moments to lie in certain "easy" directions within the crystal can be supplied either by thermal energy or by an external field. The field required to flip the magnetization in an individual grain from one easy direction to another is called the microcoercivity. In a magnetic mineral assemblage, the field that can drive a magnetization from saturation to zero is the coercivity of the sample, which is referred to as H_c (with units of A/m) or B_c (with units of T).

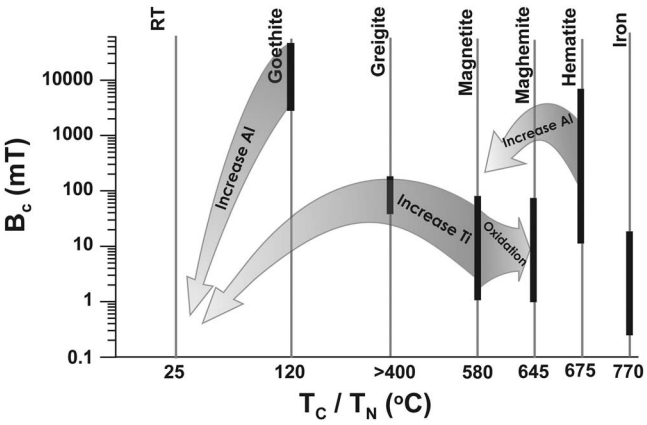

Figure 3. A schematic correlation of B_c and T_C (T_N) variations for different magnetic minerals. Arrows indicate the effects of isomorphous substitution and oxidation on the corresponding magnetic properties of these minerals. RT indicates room temperature.

[16] For a population of randomly oriented hematite grains, B_c is typically >100–300 mT (that of goethite is even harder), whereas for magnetite (maghemite) it is only several tens of mT. To isolate signals due to hematite and/or goethite from those of magnetite (maghemite) in terms of coercivity, the "hard" IRM (HIRM) is often used (HIRM = (SIRM + $IRM_{-0.3T}$)/2, where $IRM_{-0.3T}$ is the IRM remaining after exposure to a reversed field of −0.3 T after SIRM acquisition in the opposite direction). The S ratio is defined as S = ($-IRM_{-0.3T}$/SIRM) [*King and Channell*, 1991]. HIRM is used as a measure of the mass concentration of high-coercivity magnetic minerals, e.g., hematite and goethite, while the S ratio is a measure of the relative abundance of high-coercivity minerals in a mixture with ferrimagnetic minerals (e.g., magnetite, maghemite). When the S ratio approaches unity, ferrimagnetic minerals are dominant. As the concentration of hematite (goethite) increases, the S ratio gradually decreases. Variations in the relative concentration of high- and low-coercivity phases indicated by the S ratio are nonlinear and interpretation of the S ratio is nonunique [e.g., *Heslop*, 2009]. Quantitative interpretation therefore requires constraints from other parameters. *Liu et al.* [2007b] proposed the L ratio (= (SIRM + $IRM_{-0.3T}$)/(SIRM + $IRM_{-0.1T}$)) to determine how the hardness of hematite affects HIRM and the S ratio. Only when the L ratio is stable can HIRM and S ratio be interpreted conventionally. Variable L ratio values indicate changes in the grain size (coercivity) distribution of the high-coercivity component, which could reflect changes in provenance or other factors that influence the properties or relative proportions of hematite and goethite [*Liu et al.*, 2007b].

2.1.2. Temperature-Dependence of Magnetic Properties

[17] The most important temperature-dependent property (determined by measuring χ or M_s) is the Curie temperature (T_C) for ferrimagnets or the Néel temperature (T_N) for imperfect antiferromagnets, at which the mineral suddenly becomes paramagnetic because thermal energy overcomes the magnetic exchange interaction. For stoichiometric magnetic minerals, T_C is widely used to determine the composition of the mineral phase. Below T_C, thermal energy can overcome the magnetic anisotropy until the remanence blocks in at the blocking temperature T_b ($<T_C$). SP behavior results when grains are above their blocking temperatures. With increasing grain size, T_b approaches T_C. When a grain goes through its T_b, it will exhibit a sudden increase in χ, as discussed earlier, which results in a χ peak below T_C (known as the Hopkinson peak). Natural samples usually have a distribution of grain sizes so that the maximum T_b is often equivalent to T_C.

[18] Magnetite and hematite have T_C and T_N values of 580°C and 675°C, respectively [*Dunlop and Özdemir*, 1997], but T_C and T_N are affected by nonstoichiometry (isomorphous cation substitution and vacancies) (Figure 3). In natural environments, hematite is often not pure and is affected by Al substitution (Al-hematite) [*Cornell and Schwertmann*, 2003]. Al substitution reduces T_N so that it gradually approaches the T_C of magnetite. In most cases, the coercivity of Al-hematite remains higher than for magnetite [e.g., *Roberts et al.*, 2006; *Liu et al.*, 2007b]. Goethite has a low T_N of ∼120°C, which approaches room temperature with increasing Al content; the corresponding coercivity can sharply decrease from >10–20 T for goethite down to values comparable to those for magnetite (several tens of mT or less [*Liu et al.*, 2006a]). Maghemite has a theoretical T_C of 645°C [*Dunlop and Özdemir*, 1997]; however, it is thermally unstable and converts to other magnetic minerals (usually magnetite or hematite) below this temperature. For example, χ–T curves for paleosols from the Chinese Loess Plateau decrease between ∼300°C and 450°C, which is widely used to indicate the presence of maghemite in paleosols [e.g., *Liu et al.*, 2005b]. The T_C of titanomagnetite is lower than for magnetite, and decreases as Ti content increases; cation substitution can often be determined with high-temperature measurements [*Akimoto*, 1962; *Nishitani and Kono*, 1983]. For monoclinic pyrrhotite, T_C = 325°C [*Dekkers*, 1989a], while T_C remains undetermined for greigite. It exceeds 400°C [*Chang et al.*, 2008; *Roberts et al.*, 2011a], but thermal alteration above 280°C [e.g., *Snowball and Thompson*, 1988; *Krs et al.*, 1992; *Roberts*, 1995; *Dekkers et al.*, 2000] makes determination of T_C mainly a matter of theoretical interest. One disadvantage of high-temperature treatment is that the magnetic signal can be obscured by new magnetic minerals that form during heating/cooling.

[19] T_C values or thermal alteration temperatures in the 300°C–400°C temperature range for multiple minerals means that titanomagnetite with moderate Ti contents or maghemite can be confused with other minerals, including iron sulfides (greigite and pyrrhotite), if thermomagnetic measurements are the only analyses undertaken to determine magnetic mineralogy [e.g., *Roberts and Pillans*, 1993]. However, iron sulfides and iron oxides can be distinguished using SEM observations; pyrrhotite and greigite have distinct microtextures and compositions [e.g., *Roberts et al.*, 2010, 2011a]. In addition, measurement of the magnetic response of a sample using first-order reversal curve (FORC) diagrams

[*Pike et al.*, 1999; *Roberts et al.*, 2000] (see section 2.3) can reveal strongly magnetically interacting SD particles. Such features are routinely used to indicate the presence of magnetic iron sulfides [e.g., *Rowan and Roberts*, 2006; *Roberts et al.*, 2006], although interactions will not always be present [e.g., *Roberts et al.*, 2011a]. Overall, however, interpretational ambiguities associated with high-temperature measurements mean that they have drawbacks for uniquely determining magnetic mineralogy.

[20] Low-temperature magnetic measurements provide additional constraints on magnetic mineralogy because the dynamics of magnetic structures vary strongly below room temperature. For example, the crystallographic directions preferred by magnetic moments within magnetite crystals change profoundly at ~120 K. This phase transition is known as the Verwey transition [*Verwey*, 1939] and the transition temperature is denoted as T_V. Similarly, the Morin transition (T_M, ~250 K) (when present) is a key indicator of the presence of hematite [*Morin*, 1950]. Monoclinic pyrrhotite experiences a magnetic transition at 30–34 K [*Dekkers*, 1989a; *Rochette et al.*, 1990] that is now referred to as the Besnus transition [*Rochette et al.*, 2011]. These transitions have considerable diagnostic value. A reduced T_V (~110 K) [*Pan et al.*, 2005; *Li et al.*, 2009a, 2009b], combined with a FORC diagram indicative of noninteracting SD particles, points to the presence of biogenic magnetite [cf. *Egli et al.*, 2010; *Roberts et al.*, 2011b]. Similarly, a T_N of ~675°C combined with evidence of a Morin transition (if present) indicates the presence of hematite. While positive identification of these transitions can be diagnostic of magnetic mineralogy, minerals such as greigite have no low-temperature transition [e.g., *Chang et al.*, 2009], and absence of evidence for a transition is not a diagnostic indicator. In contrast, goethite also lacks a low-temperature transition, but its distinctive low-temperature behavior [e.g., *Dekkers*, 1989b; *Rochette and Fillion*, 1989; *Liu et al.*, 2004b, 2006a; *Guyodo et al.*, 2006a] has diagnostic value.

[21] For stoichiometric magnetite, T_V is generally fixed at ~120–122 K, but the amplitude of the magnetization decrease at T_V is gradually depressed as grain size decreases from the MD to the SD state [*Dunlop and Özdemir*, 1997]. For oxidized magnetite, the transition becomes smeared (both T_V and the intensity drop at T_V) until it disappears with higher degrees of oxidation [*Özdemir et al.*, 1993; *Cui et al.*, 1994]. Generally, increased nonstoichiometry (e.g., isomorphous cation substitution) shifts T_V to lower temperatures and depresses and broadens the transition.

[22] At the Morin transition (T_M), sublattice spins in hematite switch from the basal plane above T_M to the c axis below it because the anisotropy constant changes sign. T_M is affected by multiple factors, including particle size, morphology, and impurities, and is inhibited for grain diameters <10–20 nm [*Bando et al.*, 1965; *Ayyub et al.*, 1988]. Impurities or vacancies, strain accumulation, and crystal defects can also reduce T_M [*Morin*, 1950; *Morrish*, 1994]. Moreover, grain morphology plays an important role in controlling T_M [*Mitra et al.*, 2009].

2.2. Disentangling Mixed Magnetic Mineral Assemblages

[23] Natural samples usually contain mixed magnetic-mineral assemblages with components potentially having different origins and grain sizes. Each magnetic component must therefore be identified physically, chemically, or by mathematical unmixing. It is especially useful to unmix bulk magnetic signals to identify components and their causal links to specific environmental processes.

[24] Much commonly available equipment provides relatively crude parameters (e.g., χ, ARM, IRM at different fields, and various interparametric ratios such as HIRM, S ratio and L ratio). Some authors have argued that the main magnetic minerals in samples can be efficiently distinguished using a small number of sequential magnetic measurements [e.g., *Roberts et al.*, 1995; *Maher and Thompson*, 1999, p. 42]. However, the effects of variable domain state and cation substitution mean that there are many ambiguities when identifying magnetic minerals using nonintrinsic magnetic properties. *Lowrie* [1990] proposed a method that can be performed in any laboratory with basic equipment in which an IRM is imparted with different applied fields along three mutually orthogonal axes, followed by stepwise thermal demagnetization. Thermal treatment enables discrimination among the unblocking temperature spectra of high-, medium- and low-coercivity components along the three axes. *Roberts et al.* [1995] and *Maher and Thompson* [1999] provided flowcharts for identifying magnetic minerals by integrating information concerning coercivity, thermal stability, and grain size distributions. Similar ideas were also adapted by *France and Oldfield* [2000] in which sequential treatments involving a high-field IRM (>2 T) are followed by orthogonal demagnetization and cooling and heating of the SIRM over the −196°C to 680°C temperature range. High coercivity features are useful for detecting and separating information about hematite and goethite [*France and Oldfield*, 2000; *Maher et al.*, 2004].

[25] Magnetic extraction is frequently used to separate strongly magnetic minerals from the nonmagnetic matrix [e.g., *Petersen et al.*, 1986; *Stolz et al.*, 1986; *Hesse*, 1994; *Hounslow and Maher*, 1996]. However, weakly magnetic minerals (e.g., hematite and goethite) are often left in the residue and are not successfully extracted [*Liu et al.*, 2003]. Gravitational settling can also be used to divide a sample into discrete particle size fractions. In particular, heavy liquid separation can concentrate magnetic minerals with a wide range of coercivities that can be representative of the entire magnetic assemblage [*Franke et al.*, 2007].

[26] Measuring the magnetic properties of particle size fractions can often overcome the inadequacies of magnetic extraction procedures and place source-sediment comparisons on a more secure footing. Combined sieving and pipetting, preceded by sediment disaggregation using sodium hexametaphosphate and ultrasonic treatment, yields sediment fractions that are suitable for magnetic measurement. For dusts and aerosols, this approach permits more realistic comparisons between deposited materials and potential sources [*Lyons et al.*, 2012]; for paleosols, it helps to disentangle the

meaning of bulk measurements, thus allowing separate appraisal of detrital and pedogenic (soil forming) components [*Hao et al.*, 2008]. For lake sediments, removal of biogenic components can provide a reliable basis for sediment source identification [*Hatfield and Maher*, 2009].

[27] Along with physical treatments, chemical treatments can also be useful. For soil/paleosol samples, the citrate-bicarbonate-dithionite (CBD) method preferentially dissolves fine-grained Fe^{3+}-bearing minerals, including hematite, goethite, maghemite [*Mehra and Jackson*, 1958; *Verosub et al.*, 1993], and possibly fine-grained magnetite [*Hunt et al.*, 1995c]. When lithogenic components have a strong influence on bulk soil magnetic properties, CBD-extractable Fe is a better measure of pedogenesis [*Liu et al.*, 2010]. Poorly crystalline "oxide" soil components (e.g., ferrihydrite) can be removed as acid ammonium oxalate-extractable Fe [*Cornell and Schwertmann*, 2003].

[28] Low- and high-temperature thermal treatment is also an efficient approach to decompose bulk magnetic signals because different minerals have inherently different thermal stability. Using thermal unblocking characteristics of a low-temperature SIRM for magnetic particles with different domain states, *Banerjee et al.* [1993] quantitatively estimated the concentration of SP particles. Similarly, by taking advantage of the difference in low-temperature behavior between SP + SD magnetic particles and MD magnetite, *Liu et al.* [2004d] separated Verwey transition signals typical of MD magnetite from the SP + SD background. Goethite often carries a stable remanence, which cannot be easily removed by AF demagnetization, but it can be efficiently demagnetized by thermal treatment at 150°C. Maghemite and magnetite have different thermal stability. Nano-sized maghemite of pedogenic origin can be transformed into hematite by thermal treatment at >300°C. Therefore, the loss of magnetization (or χ) at 300°C has been used to quantify the maghemite content of soils [*Deng et al.*, 2001].

[29] Physical, chemical, and high-temperature treatments usually require destruction of bulk samples. Mathematical approaches have been developed to decompose magnetic signals of bulk samples; these approaches do not require destruction of samples and make use of routinely measured bulk magnetic properties. For example, IRM acquisition curves can be decomposed into different coercivity fractions [*Robertson and France*, 1994; *Kruiver et al.*, 2001; *Heslop et al.*, 2002; *Egli*, 2004a, 2004b, 2004c]. The high-coercivity fraction (e.g., several hundreds of mT or several T) can be assigned to hematite and/or goethite. To further discriminate between carriers of the high-coercivity component (hematite versus goethite), IRM acquisition curves can be measured at elevated temperatures (>150°C) to remove the influence of goethite, although goethite often does not carry a remanence because its Néel temperature is below room temperature due to Al substitution. In summary, a combination of treatments can reduce ambiguities caused by mixed magnetic signals. Regardless, it is often possible to unambiguously unmix room temperature IRM acquisition curves. *Egli* [2004a, 2004b, 2004c] provided important details for interpreting components identified through IRM acquisition curve unmixing. *Heslop and Dillon* [2007] also used the expectation that components within a mixed magnetic mineral assemblage have linearly additive magnetizations to develop end-member modeling of IRM acquisition curves for a collection of samples. Quantitative unmixing of IRM acquisition curves is being increasingly used to unlock details of environmental processes to shed light on eolian, fluvial and biogenic components in marine environments [e.g., *Köhler et al.*, 2008; *Roberts et al.*, 2011b; *Just et al.*, 2012].

[30] Magnetic hysteresis data also often reflect mixed magnetic mineral assemblages and such mixtures are often interpreted in the so-called Day plot in which M_r/M_s is plotted versus B_{cr}/B_c [*Day et al.*, 1977]. Data presented within the Day plot are fundamentally ambiguous and unmixing of hysteresis data is not straightforward. This fundamental ambiguity has led some workers to suggest alternative data presentations to the Day plot [e.g., *Tauxe et al.*, 2002]. However, pervasive use of the Day plot in rock and environmental magnetism, despite its obvious ambiguities, means that application of quantitative unmixing approaches are needed to enable more rigorous interpretation. *Heslop and Roberts* [2012a] developed an end-member unmixing method to enable unmixing of binary mixtures on the Day plot. *Dunlop* [2002a, 2002b] discussed the nature of binary mixtures on Day plots in detail, but an approach such as that of *Heslop and Roberts* [2012a] is needed to unlock quantitative interpretation of hysteresis data from mixed natural samples. The reality, however, is that natural magnetic mineral assemblages are often much more complicated than simple binary mixing systems. *Heslop and Roberts* [2012b], therefore, extended hysteresis end-member unmixing to multicomponent mixtures. As is the case for IRM unmixing, mathematical unmixing approaches now also hold promise for hysteresis and many other types of magnetic and nonmagnetic data sets and should unlock increasingly quantitative environmental interpretations.

[31] In an attempt to derive greater information from hysteresis measurements rather than only the conventional parameters used in the Day plot, *Pike et al.* [1999] and *Roberts et al.* [2000] proposed the use of detailed magnetization measurements from first-order reversal curves (FORCs) [cf. *Mayergoyz*, 1986] to construct FORC diagrams. A FORC diagram is a representation of the distribution of coercivity and interaction fields in a magnetic mineral assemblage. A large data catalog now exists to assist identification of magnetic mineral components in natural samples using FORC diagrams [e.g., *Roberts et al.*, 2000, 2006; *Pike et al.*, 2001a, 2001b; *Muxworthy et al.*, 2005; *Yamazaki*, 2009; *Egli et al.*, 2010]. However, quantitative unmixing of components in FORC diagrams remains unresolved; future such work would be extremely useful in environmental magnetism.

[32] Nonmagnetic techniques are also useful for assessing iron "oxide" concentration, e.g., Mössbauer spectra, scanning and transmission electron microscope (SEM and TEM) observations, X-ray diffraction (XRD), and diffuse reflectance spectroscopy (DRS). Quantitative end-member unmixing approaches have also been developed for DRS data [*Heslop*

et al., 2007]. We recommend integration of intrinsic (e.g., T_C, T_V) and nonintrinsic (e.g., coercivity) magnetic information and nonmagnetic techniques to definitively identify and quantify magnetic mineral concentrations in environmental magnetism.

2.3. New Techniques

[33] Environmental Magnetism has become an elaborate and quantitative discipline, owing to the increasing use of advanced measurement and data analysis methods. Among these tools, low-temperature measurements of remanence, induced magnetization in high field, and alternating current susceptibility avoid heating-induced mineralogical alterations associated with high-temperature (>100°C) analyses. These tools are well adapted to analysis of iron "oxide" nanoparticles along with temperature-dependent magnetic properties such as superparamagnetism and enhanced magnetic moments due to size effects.

[34] In addition to low-temperature methods, techniques that rely on absorption of X-ray photons produced at synchrotron radiation facilities are increasingly being used to investigate magnetic properties at the atomic scale. Synchrotron techniques allow identification of minerals and the oxidation state of cations, atomic structure, and magnetic properties. These techniques are independent of the physical state of a sample, contrary to, for instance, a classical XRD analysis. For example, magnetic properties of poorly crystalline nanoparticles can be analyzed just as easily as larger more crystalline particles. Synchrotron-based measurements can also be carried out at the same time scale as chemical reactions that reproduce redox reactions in nature. These advantages open many new opportunities for understanding processes important to environmental magnetism.

[35] Synchrotron measurements are made at specific facilities where electrons circulate in large storage rings. The electrons emit a polychromatic X-ray beam when their trajectory is deflected by magnetic fields produced by insertion devices such as bending magnets or undulators. The energy of the X-ray beam produced varies from a few hundred to tens of thousands of electron volts (eV). The X-ray beam is directed toward beam lines that surround the storage ring. These beam lines are equipped with different optics and experimental setups that are designed to perform a large spectrum of measurements. An important piece of equipment at each beam line is the monochromator, which allows selection of specific energies of the incident X-ray beam.

[36] Among the various applications of synchrotron radiation, X-ray absorption spectroscopy involves measuring the absorption coefficient of a sample as a function of the energy of the incident X-ray beam. As the energy increases, the absorption coefficient undergoes several jumps, known as absorption edges. The energy of each absorption edge corresponds to the binding energy of a core electron. The core electron is a 1*s* electron at the K edge, a 2*s* electron for the L_1 edge, and a 2*p* electron for the $L_{2,3}$ edge. Three regions are distinguished in the X-ray absorption spectrum (XAS). The *preedge* region provides information about the oxidation state of the absorber, and absorber-ligand bonding. The *X-ray absorption near edge structure* region (XANES) is sensitive to the arrangement of neighbors around the absorber, and can be used as a fingerprint to compare unknown samples to standards [*Dräger et al.*, 1988; *Bajt et al.*, 1994; *Fredrickson et al.*, 2000; *Mikhaylova et al.*, 2005]. The *extended X-ray absorption fine structure* region (EXAFS) can be analyzed to obtain information about the distance from the absorber to near neighbors, and about the number and type of neighbors. An example of the use of EXAFS at the iron K edge for an environmentally relevant magnetic mineral is provided by *Guyodo et al.* [2006b], who showed that three samples of poorly ordered six-line ferrihydrite with different average particle sizes had identical Fe-O and Fe-Fe average distances, which therefore have similar short-range order. Because of the similarities in both short-range and long-range ordering of these samples, proof was provided that observed differences in low-temperature magnetic properties observed between the three samples are due to size effects and not to mineralogical effects. A more recent EXAFS study of ferrihydrite indicated the presence of 20–30% tetrahedrally coordinated Fe^{3+} in the mineral structure [*Maillot et al.*, 2011], which confirms recent hypotheses [e.g., *Michel et al.*, 2007, 2010] but contradicts other studies [e.g., *Drits et al.*, 1993; *Jambor and Dutrizac*, 1998; *Manceau*, 2009, 2011]. X-ray magnetic circular dichroïsm (XMCD) measurements (Figure 4) performed at the iron K and $L_{2,3}$ edges on ferrihydrite [*Guyodo et al.*, 2012] demonstrate the existence of a significant amount of Fe^{3+} in tetrahedral sites in the magnetic structure of six-line ferrihydrite, therefore supporting the EXAFS results of *Maillot et al.* [2011].

[37] XMCD is a synchrotron technique that provides access to the magnetic moments of selected atoms (Fe, Ti, etc., depending on beam energy), which allows analysis of the magnetic coupling between atoms. XMCD [*Schütz et al.*, 1987] corresponds to a variation of the absorption coefficient with the direction of the circular polarization of the incoming X-ray beam for magnetized samples. In practice, an XMCD spectrum is obtained by calculating the difference spectrum from two X-ray absorption spectra successively collected with left- then right-circularly polarized X-rays in the presence of a large magnetic field (up to several Tesla). *Brice-Profeta et al.* [2005] used XMCD to investigate nanoparticles of maghemite with different sizes and surface coatings. Working at the iron $L_{2,3}$ edges, they observed the relative magnetic contributions of the iron atoms in octahedral and tetrahedral sites. Their results indicated that the three particle types have similar tetrahedral/octahedral site occupancy ratios, and that smaller particles and surface-coated nanoparticles have a larger disorder of Fe^{3+} octahedral spins. Their results also confirmed the hypothesis of a core/shell magnetic model for the magnetic properties of maghemite nanoparticles, with surface spins experiencing lower exchange interactions with their neighbors.

[38] *Carvallo et al.* [2008] performed XMCD experiments at the iron $L_{2,3}$ edge on magnetite nanoparticles cooled to 200 K. They showed that biogenic magnetite is characterized by a higher-Fe^{2+} content than coprecipitated (abiotic)

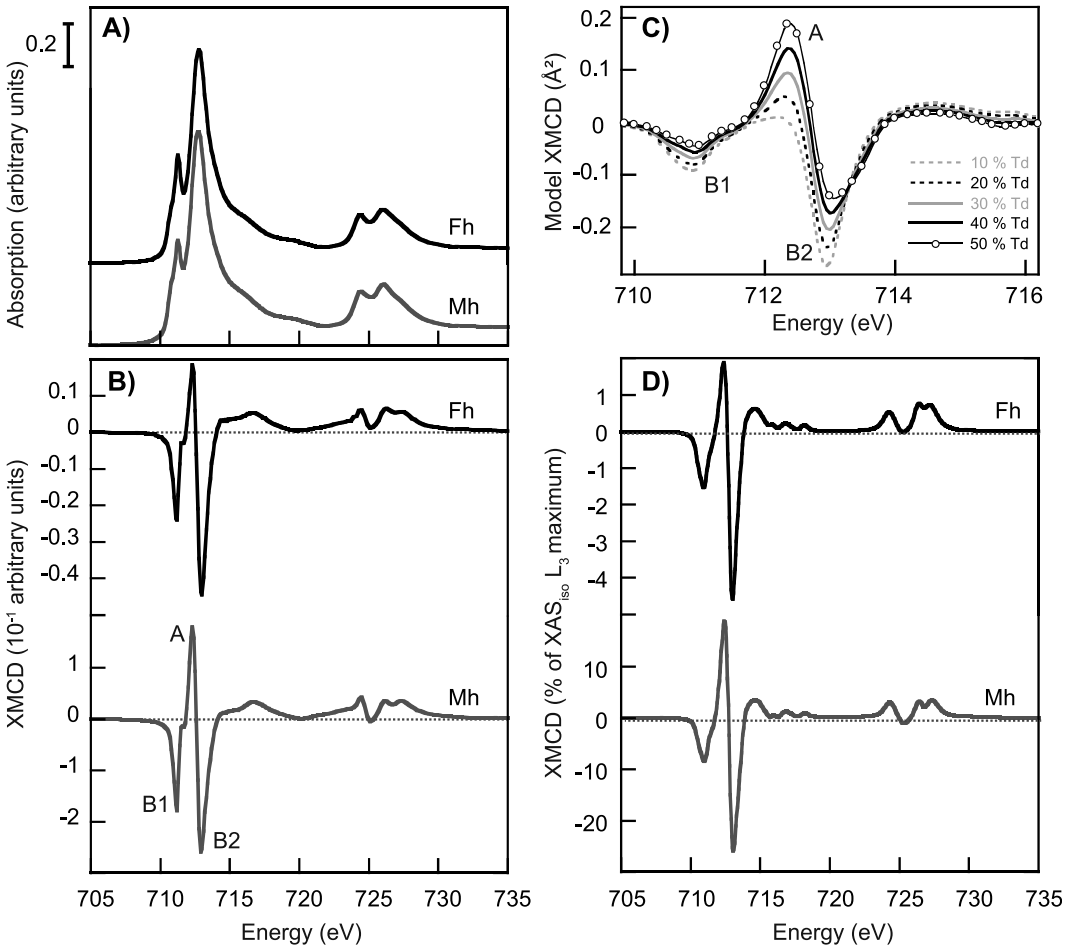

Figure 4. (a) $L_{2,3}$ edge isotropic X-ray absorption spectra (XAS) of synthetic samples of six-line ferrihydrite (Fh) and maghemite (Mh), acquired at 15 K at the Swiss Light Source (based on *Guyodo et al.* [2012]). (b) Corresponding XMCD spectra of Fh and Mh, obtained by taking the difference between XAS successively collected with left- then right-circularly polarized X-rays in the presence of a 6 T magnetic field. The data presented are averaged from multiple experiments. According to previous Ligand Field Multiplet theory calculations [*Brice-Profeta et al.*, 2005], the positive peak labeled as A is due to tetrahedral iron (Fe_{Td}), while the two negative peaks labeled as B1 and B2 are due to octahedral iron (Fe_{Oh}). The shape of the Fh XMCD spectrum is similar to that of Mh, which indicates the presence of a significant amount of Fe_{Td} in Fh. (c) Illustration of the effect of varying the amount of Fe_{Td} on the shape of XMCD spectra calculated using the Ligand Field Multiplet theory, which indicates that the A and B2 peaks have the greatest sensitivity to the Fe_{Td} contribution. (d) Best fit XMCD spectra with 28% and 37.5% of Fe_{Td} for Fh and Mh, respectively.

magnetite, which suggests that the high crystallinity and stochiometry of such nanoparticles is a signature of their biogenic origin. *Lam et al.* [2010] probed individual magnetosomes (chain-structured SD magnetic particles produced by magnetotactic bacteria from marine vibrio strain MV-1) using scanning transmission X-ray microscopy (STXM) and XMCD at the iron $L_{2,3}$ edge on a magnetotactic bacterium. Their results confirmed that such magnetosomes have excess Fe^{2+}.

[39] The advantage of synchrotron techniques is that they are site specific and they do not depend on the existence of long-range periodic structures. Low-crystallinity mineral phases and nanoparticles can be targeted. These are of particular interest to environmental studies, where many processes occur at particle surfaces. Improved understanding of atomic-scale magnetic properties of iron "oxides" helps to build more realistic models to explain bulk magnetic properties and how they respond to environmental variations. Better knowledge of the physical arrangement of atoms at poorly crystalline (i.e., high reactivity) mineral surfaces allows modeling of pathways of heavy metal adsorption, mineral dissolution/precipitation, or oxidation-reduction reactions [e.g., *Boily et al.*, 2001; *Rustad and Felmy*, 2005; *Casey and Rustad*, 2007]. Increased use of synchrotron techniques is likely in environmental magnetism because of their ability to probe environmentally relevant atomic-scale processes.

3. CYCLING OF IRON MINERALS IN NATURE

[40] Environmental magnetism is intimately linked to the global "iron cycle" through chemical, physical and

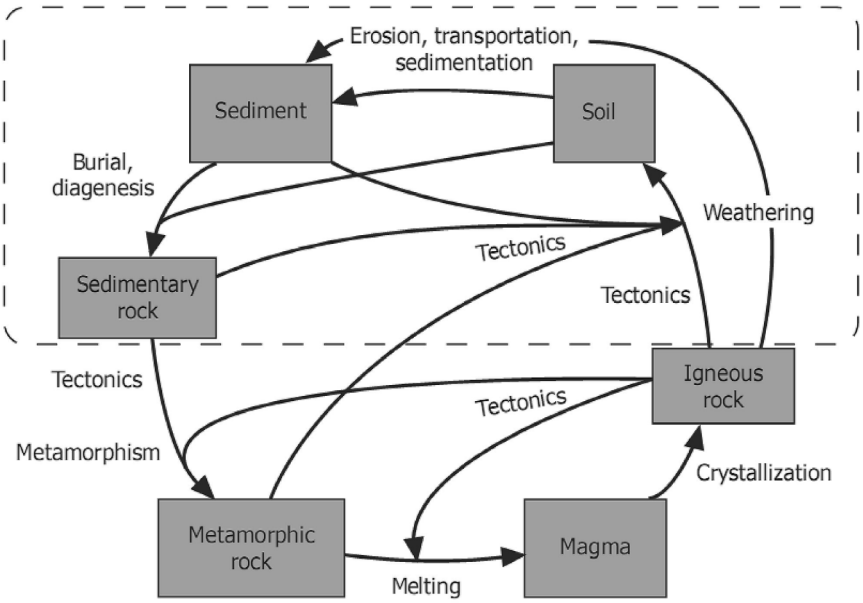

Figure 5. Tectonic rock cycle (based on *Wilson* [1966] and *Whitmeyer et al.* [2007]). The dashed box indicates the settings that are the focus of environmental magnetism.

biological mechanisms. The iron cycle operates at different scales including the global iron connections between desert dust, ocean biochemistry, and climate [*Jickells et al.*, 2005; *Maher et al.*, 2010], and the local or in situ transformation of iron oxides (e.g., magnetite, maghemite, ferrihydrite, goethite, lepidocrocite, iron sulfides, etc., that are common in soils, dusts, and other sediments) with or without effects of microbes in different environments [*Cornell and Schwertmann*, 2003; *Malki et al.*, 2006]. Below, we briefly discuss the global cycling of iron oxides in nature (Figure 5). We then discuss the physical chemistry of the iron cycle as it relates to environmental magnetism (Figure 6).

3.1. Global Iron Cycling

[41] We treat the global iron cycle by considering the fate of iron-bearing minerals in the rock cycle, of which magnetic minerals are of special interest in environmental magnetism (Figure 5). Magnetic minerals are formed by crystallization within igneous rocks while they cool. Magnetite is the most common magnetic mineral in continental and oceanic intrusive and plutonic rocks, either as a primary mineral or as a result of alteration of other minerals (i.e., through high-T oxidation, serpentinization, hydrothermal alteration) [*Dunlop and Özdemir*, 1997]. Continental intrusive and plutonic rocks also frequently contain monoclinic pyrrhotite. Titanomagnetite is common in subaqueous basalts, which typically also host titanomaghemite, whereas titanohematites are common in felsic volcanic rocks. Magnetic minerals in intrusive and plutonic rocks that cooled slowly within the Earth's crust typically have coarser grain sizes, whereas those in extrusive rocks that cooled rapidly at the Earth's surface typically have finer grain sizes [*Dunlop and Özdemir*, 1997].

[42] Once igneous rocks come into contact with air or water, they begin to undergo weathering. Soil formation can

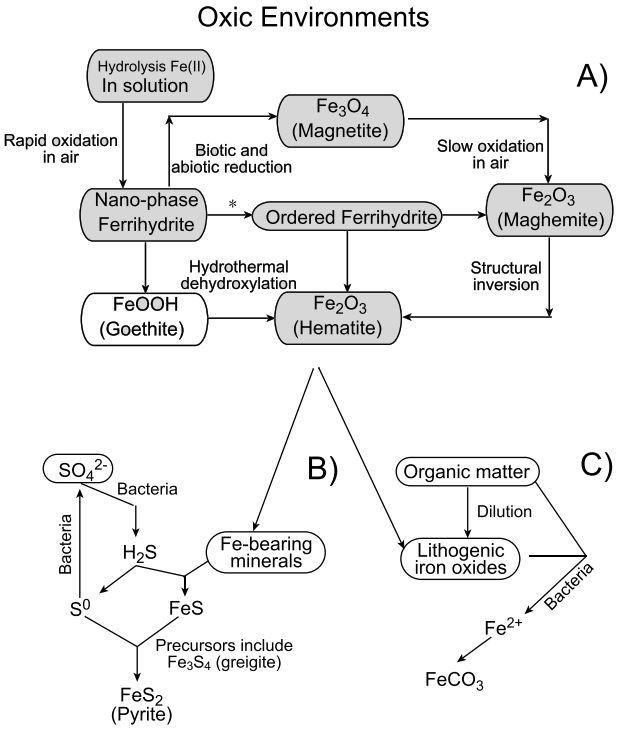

Figure 6. Transformation pathways for iron oxides and iron sulfides in (a) oxic, (b) sulfidic, and (c) nonsulfidic anoxic environments. The upper and lower panels indicate relevant iron cycling reactions for iron oxides, iron sulfides, and siderite, respectively. See section 3.2 for details. The asterisk indicates that the synthesis conditions for the conversion of ferrihydrite to ordered ferrihydrite require the presence of citrate and phosphorpus doping.

result under subaerial conditions. Preexisting magnetic minerals are then released from the parent rock and can be further altered, which results in formation of new (authigenic) magnetic minerals. The most common magnetic minerals in soils are maghemite, goethite, hematite and, to a lesser extent, magnetite. Oxidation of (titano)magnetite to (titano)maghemite in submarine basalts occurs widely during submarine weathering of magnetic minerals. Once preexisting and authigenic magnetic minerals within soils and their parent materials are eroded by water, ice or wind, they can be transported by a range of mechanisms with variable durations and then deposited in sediments under subaerial (terrestrial) or subaqueous (lacustrine or marine) conditions [*Maher*, 2011]. Magnetic minerals can be further altered chemically and by physical comminution during transportation, but coarse-grained lithogenic magnetic minerals are often well preserved after deposition.

[43] As sediments are buried, diagenetic processes under certain conditions can lead to replacement of detrital magnetic minerals by authigenic magnetic minerals through dissolution and recrystalization. Chemical changes can occur throughout the history of a rock even when the sediment is lithified and transformed into sedimentary rock. Authigenic minerals that typically form in oxic conditions include hematite and magnetite. Greigite and pyrrhotite grow under anoxic conditions. Deep burial or volcanic heating brings sedimentary rocks under the influence of metamorphism, which involves important chemical transformations that depend on pressure and temperature conditions. Magnetite and, to a lesser extent, pyrrhotite are the magnetic minerals that most commonly form in metamorphic rocks. Increased temperature or pressure causes melting, so that the rock cycle returns to its starting point (Figure 5).

[44] Repetitions of the rock cycle or parts of the cycle have given rise, throughout geological time, to the variety of soils, sediments, and rocks observed in nature, each of which contains a specific magnetic assemblage linked to the prevailing physical and chemical conditions during their formation. Biological activity can be intimately linked to, and can drive, mineralization processes. Examples of biological processes include degradation and fermentation of organic matter in soils and during early sedimentary diagenesis. Anthropogenic activity now also plays an active role in pedogenesis, sediment load production, or artificial (industrial) formation of magnetic minerals, among many other processes. Environmental magnetism is mainly concerned with processes that govern the iron cycle at the Earth's surface or at shallow depths (Figure 5), including (1) weathering and formation of soils; (2) erosion, transportation, and accumulation of sediments (including contributions from organisms, especially bacteria and humans); and (3) early diagenetic reactions in sediments. Processes that drive erosion, transportation and accumulation of magnetic minerals in sediments, e.g., physical iron cycling, carry a depositional signal that is linked to climate and environmental variability and to physical disturbance of the environment by human activities. In contrast, chemical cycling of iron provides information on mainly pedogenic, diagenetic, biogenic and anthropogenic processes, and concerning the environmental signals that they might encode. Beside these processes, other sources can also contribute primary magnetic minerals to sediments, e.g., atmospheric input from volcanic or anthropogenic aerosols, and extraterrestrial input [*Suavet et al.*, 2008]. Deep sea vents can also serve as important dissolved metal sources in the deep ocean [*Sander and Koschinsky*, 2011].

3.2. Physical Chemistry of Iron Cycling in Magnetic Minerals

[45] There are many natural archives of environmental change (e.g., soils, sediments, speleothems) that record climatic, hydrologic or anthropogenic signals. Environmental magnetism is an efficient interrogator of such changes via deposition and/or chemical alteration of Fe^{2+} or Fe^{3+} ions hosted in iron oxides (magnetite, maghemite, hematite), iron oxyhydroxides (goethite, ferrihydrite, lepidocrocite), iron sulfides (greigite, pyrrhotite) or carbonate (siderite) crystal lattices. Electron transfer between $Fe^{2+}$and Fe^{3+} is energetically highly favorable (only ~0.01 eV), and every transfer causes a change in magnetic moment of 1 Bohr magneton (9.27×10^{-24} Am^2) among local nonequivalent crystallographic sites in a compound. Magnetic techniques are highly sensitive to such minute changes and thus provide a sensitive tool for deciphering the history of environmental change [*Thompson and Oldfield*, 1986]. For example, conversion of iron oxides or oxyhydroxides to magnetite by reduction of ferric ions is important for tracking changes in iron species in soils [*Cornell and Schwertmann*, 2003; *Guyodo et al.*, 2006a] (Figure 6). Soils can thereby carry information about hydrologic changes [*Miller and White*, 1998], organic activity, or activity of iron-reducing microbes [*Insam and Domsch*, 1988]. Conversion of magnetite to greigite similarly carries information about environmental change in reducing environments brought about by organic matter degradation [e.g., *Karlin and Levi*, 1983; *Canfield and Berner*, 1987; *Roberts et al.*, 2011a].

[46] Iron cycling is a major factor in depositional records of environmental change. "Cycling" denotes migration of Fe ions from one crystal lattice (e.g., goethite) to another (e.g., magnetite), with the potential for reverse migration when environmental conditions reverse. Changes in environmental conditions can be expressed using variables such as acidity, alkalinity, ionic strength, temperature, organic carbon (C_{org}), or microfossil abundance (e.g., diatoms delivering silica). Iron cycling is accomplished by transfer of one electron from Fe^{2+} to Fe^{3+}; when the Fe^{2+} ion (magnetic moment of 4 Bohr magnetons at 0 K) becomes Fe^{3+} (5 Bohr magnetons at 0 K), a 25% magnetization increase occurs. Similarly, the magnetization will decrease by 25% for the reverse process. Magnetic particle size determination helps to identify such environmental changes. For example, iron reduction gives rise to magnetite or maghemite neoformation in topsoil as SP grains (diameter, $d < 20$ nm), which have high χ [*Zhou et al.*, 1990], or as slightly larger SD particles (20 nm < $d < 1$ μm) with large ARM values [*Liu et al.*, 2004a]. SD/SP particles in soils provide strong indications of iron cycling.

[47] Iron cycling in oxic environments within iron "oxides" is aided by two characteristics: (1) the presence of mixed valence iron "oxides" and (2) the prevalence of polyhedral chains of oxygen and hydroxyl ions within their crystal structures [*Waychunas*, 1991]. The mobility of Fe^{2+} and Fe^{3+} among local sites is aided by the low-activation energy of electron hopping that can convert Fe^{2+} to Fe^{3+} and vice versa. *Waychunas* [1991] demonstrated that long-range iron "oxide" structures are created by alternative types of packing (cubic (e.g., goethite and magnetite) and hexagonal (e.g., hematite)) and by missing chains of oxygen polyhedra. Goethite has two missing chains after every two chains along the [001] crystallographic direction. The lepidocrocite structure can be created from goethite by having one missing oxygen chain. In the case of magnetite versus hematite, there are no missing chains. By allowing these alternative polyhedral chain arrangements, coupled with valence change in Fe ions via electron hopping, iron can be cycled among all of these iron "oxides" except for ferrihydrite, which has a poorly crystalline arrangement of polyhedral chains.

[48] Electron transfer is also important for iron cycling in suboxic and anoxic sediments. In sedimentary environments, decomposition of buried organic matter involves the successive use of O_2, NO_3^- (under oxic conditions), MnO_2, Fe_2O_3, FeOOH (under suboxic conditions), SO_4^{2-}, and CO_2 (under anoxic conditions) as electron acceptors, which are used sequentially in an order opposite to the free energy that their reduction produces [*Froelich et al.*, 1979]. Degradation of organic matter continues during early burial diagenesis until all organic matter is exhausted or until all oxidants are consumed. When degradation of organic matter proceeds to, and especially beyond, suboxic conditions, magnetic lithogenic iron "oxides" (and other Fe-bearing minerals) will progressively dissolve [*Canfield and Berner*, 1987; *Karlin and Levi*, 1983, 1985; *Karlin*, 1990a,1990b; *Channell and Hawthorne*, 1990; *Rowan et al.*, 2009] as a result of sulfidization and pyritization (pyrite formation) reactions. Different iron "oxides" have different reactivity to sulfide, with the following order of reactivity (from most to least reactive): hydrous ferric oxides, lepidocrocite, goethite, magnetite, hematite [*Poulton et al.*, 2004]. Reaction of Fe^{2+} liberated by iron reduction with dissolved sulfide (H_2S and HS^-) created by reduction of SO_4^{2-} causes precipitation of authigenic iron sulfides, including ferrimagnetic greigite [*Roberts and Turner*, 1993; *Reynolds et al.*, 1994, 1999; *Roberts et al.*, 2011a]. Ferrimagnetic monoclinic pyrrhotite has often been erroneously identified as an intermediate authigenic product during early diagenetic pyrite formation [cf. *Sweeney and Kaplan*, 1973]. *Horng and Roberts* [2006] argued that while hexagonal pyrrhotite (which is antiferromagnetic at room temperature) can form during early diagenesis, modern sediments only contain monoclinic pyrrhotite as a detrital phase; authigenic monoclinic pyrrhotite grows during later diagenesis and will therefore carry a later magnetization [e.g., *Weaver et al.*, 2002; *Larrasoaña et al.*, 2007; *Roberts et al.*, 2010]. In anoxic, nonsulfidic environments, iron sulfide formation is inhibited, and siderite ($FeCO_3$) can form if the interstitial waters are saturated with respect to carbonate [*Berner*, 1981; *Roberts and Weaver*, 2005]. Excess Fe^{2+} can also diffuse upward in sediments until it finds oxic or suboxic conditions, where it precipitates again mainly in the form of iron oxides [*Karlin et al.*, 1987] or where it becomes available for biomineralization by magnetotactic bacteria [e.g., *Schüler and Baeuerlein*, 1996; *Tarduno and Wilkison*, 1996; *Flies et al.*, 2005; *Roberts et al.*, 2011b]. Alternatively, organic matter can be mostly degraded before burial in response to either low organic carbon fluxes to the seafloor or to high oxygen availability in bottom waters (or both). Such oxic conditions can drive authigenic iron oxide formation so that depositional signals associated with terrigenous sedimentation are preserved alongside later authigenic signals [e.g., *Henshaw and Merrill*, 1980].

[49] From this brief summary of the global iron cycle, it should be clear that small environmental changes can give rise to measurable changes in mineral magnetic properties. In environmental magnetism, we seek to detect and decipher these magnetic signals to understand the associated environmental changes. We now discuss specific cases where magnetic properties can improve our understanding of processes in different environments.

4. RECENT DEVELOPMENTS IN ENVIRONMENTAL MAGNETISM

[50] In this section, we provide an updated overview of how rock magnetic methods have contributed to unraveling environmental variations both in the geological past and in modern settings. Two categories of depositional signals are discussed depending on the type of environmental record concerned (continental or marine). Postdepositional (pedogenic, diagenetic) signals, biomagnetism and anthropogenic pollution are treated separately because they concern both continental and marine records of environmental variability.

4.1. Depositional Signals in Continental Records

4.1.1. Loess and Other Eolian Material

[51] Loess is a windblown (eolian) material that covers about 10% of the world's land surface, mainly in the midlatitudes (Figure 7). Loess forming dust can be transported over long distances (e.g., dust from the Tarim Basin (Taklimakan Desert) can be transported by westerlies to the remote Pacific Ocean [*Sun et al.*, 2008] and beyond; for example, Asia has been argued to be the source of dust in Greenland ice [e.g., *Biscaye et al.*, 1997]). Therefore, although loess originates from surrounding deserts, it is not necessarily straightforward to determine its provenance.

[52] The vast expanses ($\sim 500 \times 10^6$ km^2) of ancient windblown dust preserved in central China (100–300 m thick) provide good archives for paleoclimate [*Heller and Liu*, 1986; *Kukla et al.* 1988; *Maher and Thompson*, 1991, 1992, 1995; *Banerjee et al.*, 1993; *An and Porter*, 1997; *Ding et al.*, 2002] and paleomagnetic studies [*Heller and Liu*, 1982, 1984; *Heller and Evans*, 1995; *Zhu et al.*, 1999; *Evans and Heller*, 2001; *Pan et al.*, 2001] over the last 2.5 million years. Potential sources of loess deposits on the Chinese Loess Plateau (CLP) include the nearby Gobi desert

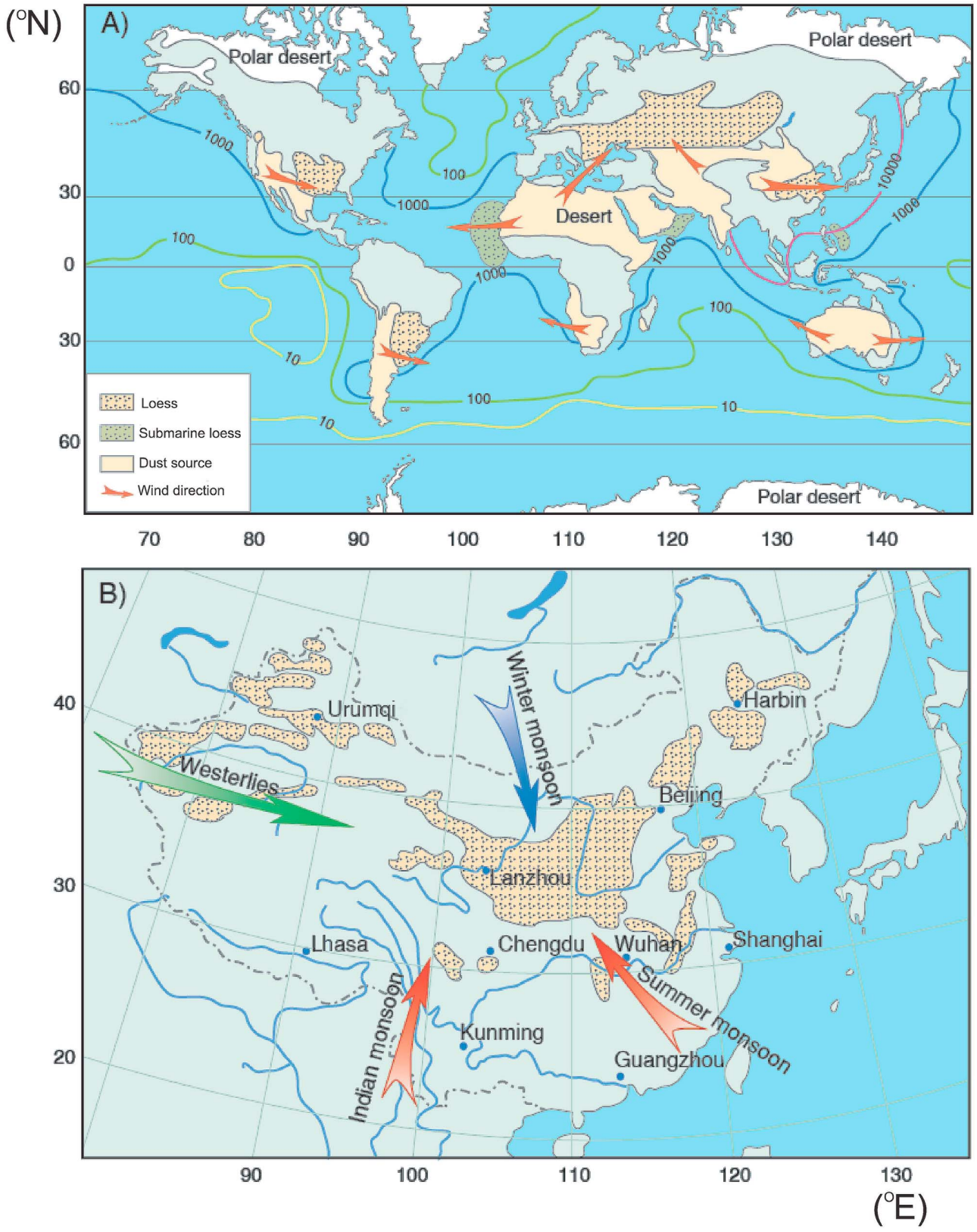

Figure 7. (a) Map of major global dust sources and deposits. Dust flux contours (mg m^{-2} yr^{-1}) are shown in oceans surrounding the dust sources [after *Duce et al.*, 1991]. (b) Map of loess deposits in China. Arrows indicate wind directions.

and three northwestern inland basins (the Junggar, Tarim, and Qaidam basins). Constrained by electron spin resonance signal intensity and crystallinity of fine-grained quartz, *Sun et al.* [2008] proposed that fine-grained loess on the CLP originates mainly from the north (the Gobi desert and sandy deserts in north China). In North America and Europe, most loess deposits originate from rock flour derived from recently glaciated regions. Thus, compared to loess deposits on the CLP, these deposits are thin (generally $<\sim$30 m). Although the source materials differ greatly among these regions, a common feature is that the background magnetic mineral concentration in fresh loess is low. In New Zealand [*Pillans and Wright*, 1990], Alaska [*Begét et al.*, 1990; *Lagroix and Banerjee*, 2004; *Lagroix et al.*, 2004], and Argentina [*Carter-Stiglitz et al.*, 2006; *Bidegain et al.*, 2009], loess deposits contain eolian volcaniclastic material, with variable magnetic properties that add complexity to interpretation of magnetic properties of loess/paleosol sequences. *Liu et al.* [2010] found that the magnetic susceptibility of the lithogenic component in Argentinian soils accounts for >60% of the total magnetic signal. Variations in magnetic properties of lithogenic and pedogenic components can therefore be ambiguous unless contributions from different magnetic minerals with variable grain sizes are discriminated. Environmental magnetic studies of loose surface sediments undergoing eolian deflation (including soils, sand dunes and alluvial sediments) have been conducted to assess the impact of climate variability on the magnetic mineralogy of source materials for eolian dusts [*Walden et al.*, 2000; *Lyons et al.*, 2010] and to identify source areas for dust that has accumulated in other eolian sediments, mainly loess [*Torii et al.*, 2001; *Maher et al.*, 2009a, 2009b].

4.1.2. Alluvial and Fluvial Sediments

[53] Alluvial and fluvial sediments can accumulate over prolonged periods of time (tens of Myr) in thick successions (up to several thousand m). Such sediments are often enriched in iron oxides whose concentration and grain size variations can reflect long-term climate changes that are otherwise elusive to assess because of the generally widespread lack of high-resolution paleoenvironmental (e.g., paleontologic) data from such environments. Regardless, most alluvial and fluvial sediments have been the focus of environmental magnetic studies not for their intrinsic interest but mostly because they constitute the material from which lithogenic sediment is partially derived and on which pedogenic processes have acted (see Section 4.1.3) [*White and Walden*, 1997; *Pope and Millington*, 2000; *Bógalo et al.*, 2001; *Kumaravel et al.*, 2005; *Sinha et al.*, 2007; *Franke et al.*, 2009; *Gómez-Paccard et al.*, 2012]. In addition to their environmental significance, fluvial sediments have been studied in source to sink studies [e.g., *Salomé and Meynadier*, 2004; *Horng and Roberts*, 2006; *Horng and Huh*, 2011] to aid interpretation of marine sedimentary records. For example, it is crucial to know whether magnetic minerals deposited in marginal marine sediments have a detrital or diagenetic origin. Tracing magnetic minerals through fluvial systems is a powerful way of determining their origin, especially at locations where intense river discharge associated with typhoon or storm events brings about rapid transportation from source to sink [*Salomé and Meynadier*, 2004; *Horng and Roberts*, 2006; *Horng and Huh*, 2011].

4.1.3. Lake Sediments

[54] Lake sediments are important because they can record high-resolution continuous terrestrial paleoclimatic signals. Application of magnetic techniques to lake sediments can be traced back to the 1920s [*Ising*, 1943]. In pioneering studies on varved clay deposits in lakes, *Ising* [1943] found that the concentration of magnetite is much higher in spring layers than in other seasonal layers, which strongly indicated that the magnetic properties of lake sediments are controlled by environmental factors, although the exact mechanism behind this relationship was not fully understood at that time. Major breakthroughs in environmental magnetic studies of lake sediments occurred in the 1960s–1980s, which were mostly led by British groups [e.g., *Thompson*, 1973; *Thompson et al.*, 1975, 1980; *Dearing and Flower*, 1982; *Sandgren and Snowball*, 2002]. Since then, lake sediment studies using environmental magnetic approaches have become internationally important. Changes in the magnetic iron "oxide" content (in terms of mineralogy, concentration, and grain size) in lake sediments are linked to climate via processes such as soil development in the catchment, the erosive agent (e.g., water, ice), and erosion in catchment areas, and through organic carbon supply and postdepositional processes within the lake. Soil development and the type of erosion affect the lithogenic components in a magnetic mineral assemblage, whereas biologic productivity changes control organic carbon contents that contribute to destruction of lithogenic iron oxides and biogenic and authigenic growth of secondary magnetic minerals (e.g., biogenic magnetite and greigite). Nonsteady state diagenesis, with alternations between oxic and anoxic states, can be paleoenvironmentally controlled and can also be readily detected with sediment magnetic properties [e.g., *Williamson et al.*, 1999] (see section 4.3.2). Processes that control the transportation, deposition, and postdepositional alteration of magnetic minerals in lake catchment systems are summarized in Figure 8.

[55] It has been shown that there exists a strong teleconnection between Greenland/North Atlantic and continental climatic/environmental changes. By investigating biogenic silica records from Lake Baikal, *Colman et al.* [1995] found that the continental interiors interact with the global climate system dominantly through nonlinear ocean/ice sheet responses to orbital forcing (100 kyr cycle) as well as partly through insolation forcing. *Thouveny et al.* [1994] observed a striking millennial-scale correlation between the χ record from maar lake deposits in the Massif Central, France, and oxygen isotope records from the Greenland Ice Core Project (GRIP) and Greenland Ice Sheet Project 2 (GISP2) ice cores. Activity of mountain glaciers, which are often linked to North Atlantic climate variability, has been also disentangled on the basis of bulk magnetic properties of proglacial sediments [*Lie et al.*, 2004; *Nesje et al.*, 2006; *Larrasoaña et al.*, 2010]. Although there is no doubt that to first order, local climate/environment changes in lakes are

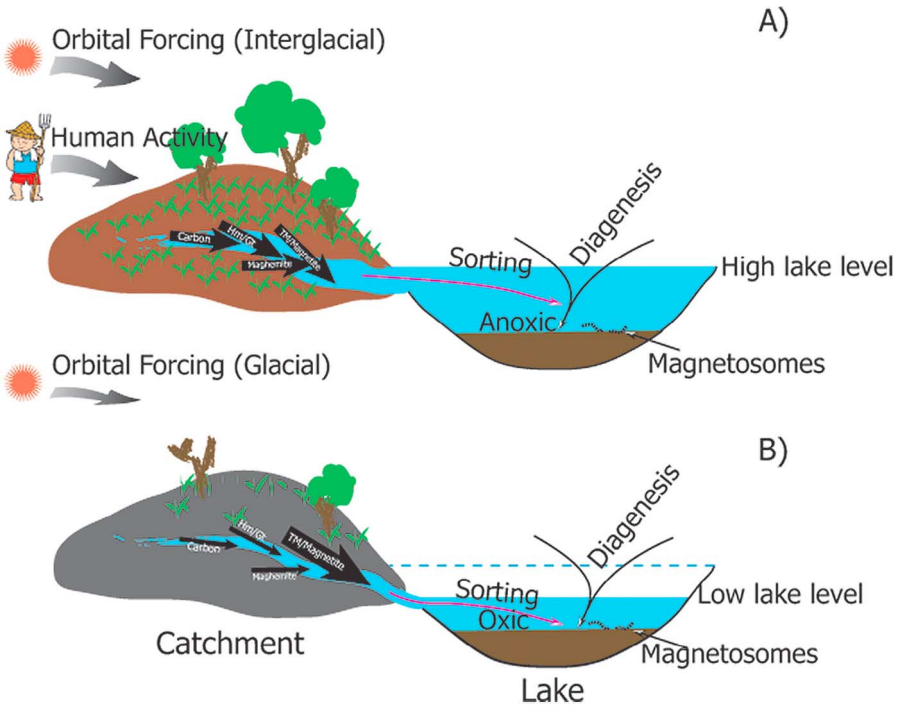

Figure 8. Conceptual model of processes that control the transportation, deposition, and postdepositional alteration of magnetic minerals in lake catchment systems during (a) interglacial and (b) glacial periods. To first order, the global climatic background (orbital forcing) affects the local climate/environment. During the Holocene, human activities have also significantly affected local environments. The more temperate climatic conditions of the Holocene are illustrated as favoring expansion of vegetation within a catchment, which increases the input of carbon and hematite/goethite and dissolved nutrients but reduces erosion and lithogenic inputs. This situation would favor diagenetic processes that can dissolve magnetic minerals within the lake. An inverse process is indicated for cold periods. The thickness of arrows in the figure indicates changes in the amount of the relevant material released into the lake. These scenarios are for illustration: Many alternative scenarios are possible.

dominated by the global climatic background, for recent deposits, human activities (e.g., extractive industries, land clearance, fire, overgrazing, changes in nutrient budget, heavy construction in the catchment, etc.) can also significantly modulate the local environment [*Dearing et al.*, 1981; *Higgitt et al.*, 1991; *van der Post et al.*, 1997; *Lanci et al.*, 1999; *Gedye et al.*, 2000; *Hirt et al.*, 2003; *Oldfield et al.*, 2003]. When postdepositional effects are limited, the concentration of magnetic minerals can be used to semiquantitatively estimate sediment influxes within a lake catchment [*Dearing et al.*, 1981; *Dearing and Flower*, 1982]. However, bulk magnetic properties reflect variable, potentially interacting, processes, including climatic factors. For example, a change from periglacial to temperate conditions will favor expansion of vegetation within a catchment. This, in turn, increases the input of carbon and dissolved nutrients, but reduces erosion by reducing freeze-thaw activity, and increasing surface cohesion, thereby reducing lithogenic inputs. Therefore, it is necessary to determine the different origins of the magnetic assemblage in lake sediments to enable robust environmental interpretation. Usually, magnetic particles produced by erosion have relatively coarser (PSD/MD) grain sizes. However, pedogenic transformation of primary iron oxides (e.g., from titanomagnetite to magnetite) in catchments can lead to complex magnetic signals. Pedogenesis produces fine-grained (SP/SD) maghemite and pigmentary hematite. Thus, changes in magnetic mineral grain size and the relative abundance of magnetite and hematite in lake sediments can potentially be used to trace the potential weathering history of the source region. For example, in Klamath Lake (Oregon, USA), decreased S ratios correspond to increased weathering of parent materials [*Rosenbaum and Reynolds*, 2004]. Moreover, before lithogenic components accumulate in lakes, catchment-derived magnetic minerals can be altered through hydrodynamic sorting by removal of coarser particles along sediment transportation pathways [*Rosenbaum and Reynolds*, 2004].

[56] Variations in the properties of magnetic minerals can be strongly influenced by many processes, e.g., erosion history, soil and slope processes, and land use changes in the catchment. What is often important is the balance between surface erosion by rainsplash and rill development (which acts on the most weathered horizons) and incised gully erosion, which removes proportionally much more unweathered substrate [*Oldfield et al.*, 1979; *Walling et al.*,

TABLE 1. Global Estimates of the Total Mass of Terrigenous Input to the World's Oceans

Source	Total Sediment Load (Tg/yr)	Estuarine and Coastal Areas (Tg/yr)	Shelf and Slope (<1000 mwd) (Tg/yr)	Deep Sea (>1000 mwd) (Tg/yr)
Ice[a]	2,900		1,400	1,500
Rivers[b]	20,000	18,000	1,700	300
Eolian dust[c]	1,100		1,000	100
Coastal erosion[a]	200	200	0	0
Cosmic particles[d]	0.002		0.0002	0.0018
Volcanic material[e]	375		40	335
Total	24,575		22,340	2,235

[a]*Raiswell et al.* [2006].
[b]*Milliman and Syvitski* [1992].
[c]Calculated after values reported by *Maher et al.* [2010].
[d]Calculated after *Love and Brownlee* [1993].
[e]Calculated after extrapolating estimates for the Pacific Ocean [*Straub and Schmincke*, 1998] to the world's oceans. Estimates of the fraction of terrigenous sources that accumulated in different settings have been made, when possible, following *Raiswell et al.* [2006].

1979]. Therefore, to interpret accurately the paleoenvironmental significance of magnetic properties of lake sediments, we need to know the linkage between lake sediments and the corresponding catchment. There are three major components of the lake catchment system: catchment source materials (bedrocks, soils, etc.), material along the pathway (floodplain sediments, river bed load sediments, river suspensions), and lake sediments. In practice, lake deposits and catchment materials are often studied together. *Oldfield et al.* [1979] demonstrated that magnetic parameters are useful for distinguishing different types of catchment magnetic minerals. The systematic study of the source-lake linkage by *Dearing et al.* [2001] provides a model for such work. These authors analyzed lake sediments from the central plain of Petit Lac d'Annecy, France, two floodplain cores, river bed load sediments and several hundred soil samples from the catchment. Lake sediments also often have isolated peaks in magnetic mineral concentrations. Such peaks are often related to tephra-rich horizons, microturbidite horizons (sediments transported and deposited by density flows) [*Ryves et al.*, 1996] or to greigite formation due to rapid redox changes [*Snowball and Thompson*, 1990; *Snowball*, 1991; *Roberts et al.*, 1996], although other mechanisms are also possible. Overall, while individual events (e.g., floods, landslides, volcanic eruptions, etc.) and diagenesis can have a large impact on the magnetic record of lake sediments, these archives remain an important source of information concerning terrestrial environmental change.

4.1.4. Other Continental Materials

[57] Other materials, in addition to sediments and soils, can provide environmental magnetic records of continental paleoenvironmental variability. These include polar ice sheets, mountain glaciers, and speleothems. Environmental studies of ice samples from a Greenland (NGRIP) ice core have shown a close correlation between eolian dust contents and the concentration of magnetic minerals, which are paced by glacial-interglacial climate variability [*Lanci et al.*, 2004; *Lanci and Kent*, 2006; *Lanci et al.*, 2012]. The magnetic mineralogy of the NGRIP samples consists of mixtures of magnetite/maghemite and hematite and does not change through time; this similarity to Chinese loess samples [cf. *Biscaye et al.*, 1997] also points to an East Asian origin [*Lanci et al.*, 2004; *Lanci and Kent*, 2006]. Magnetic properties of Antarctic ice indicate no clear link between magnetic particle concentration and climate variability; instead, changes in coercivity, and hence in mineralogy and thus provenance, are evident at glacial-interglacial time scales [*Lanci et al.*, 2008, 2012]. Preliminary rock magnetic studies of an ice cap located between the Taklimakan desert and the CLP also indicate changes in the flux and provenance of eolian dust at glacial-interglacial time scales, which further illustrates the potential of rock magnetic properties to record changes in concentration, grain size and provenance of dust in ice records [*Maher*, 2011].

[58] Speleothems have been reported to host magnetic minerals whose concentrations are readily measurable using standard rock magnetic techniques [*Perkins*, 1996; *Openshaw et al.*, 1997; *Lascu and Feinberg*, 2011]. Although the main interest of rock magnetic studies of speleothems has been constraining the reliability of records of geomagnetic field behavior (mainly paleosecular variation and geomagnetic reversals), the common occurrence of detrital natural magnetizations indicates that environmental magnetic studies of speleothems can potentially provide useful records of climate variability with U-Th chronologies that are much more accurate compared to other methods [e.g., *Perkins*, 1996; *Lascu and Feinberg*, 2011].

4.2. Depositional Signals in Marine Records

[59] Magnetic minerals are delivered to the oceans as detrital grains carried mostly by wind, water and ice [*Henshaw and Merrill*, 1980; *Evans and Heller*, 2003]. At present, riverine supply is the main contributor of sediment load to the oceans, with global estimates of about 20,000 Tg/yr (Table 1). Ice and wind transportation account for smaller sediment loads of about 2,900 and 1,100 Tg/yr, respectively (Table 1). Other suppliers of sediment load are coastal erosion and cosmic particles. Coastal erosion delivers small sediment loads of about 200 Tg/yr. Coastal sediments are mainly characterized by coarse grain sizes, with deposition in proximal locations with discontinuous sedimentation, so they are seldom the focus of environmental magnetic studies. Cosmic particles contribute a much smaller load of 0.002 Tg/yr (Table 1) and generally have negligible significance for environmental

magnetic studies [*Itambi at al.*, 2010a], although the low terrigenous mineral content of ice means that cosmic flux is measurable in ice [e.g., *Lanci et al.*, 2012]. Volcanoes intermittently deliver significant amounts (about 375 Tg/yr, Table 1) of ash to marine sediments. Ash layers can be useful for correlation and dating, but typically lack any paleoclimatic signal.

[60] At present, ice occupies less than 10% of the Earth's surface and is mainly restricted to high (>60°) latitudes. Rivers are found at virtually all latitudes, although they are less important in polar regions and dominate temperate regions and low-latitude monsoon-dominated continental areas. Dust is transported mainly from midlatitude, large continental areas (i.e., Asia) and also from zonal and shadow deserts (i.e., Sahara, Arabia, Australia, Namibia, Atacama) that are characterized by little or no present-day fluvial activity [*Maher et al.*, 2010]. Because of the lower-carrying capacity of air and water, only 10% and 2% of the total dust and riverine sediment load, respectively, reach deep marine depositional environments. In contrast, ice delivers about 50% of its sediment load to distal deep marine settings (Table 1). Several mechanisms can alter depositional signals of terrigenous sedimentation. The first is reworking of sediments by bottom currents linked either to geostrophic flows or to the occurrence of marine gateways. Such processes involve physical alteration of the sediment, and might result in a depositional signal with a specific magnetic signature and environmental significance. The second, and much more widespread, process that can alter the depositional signal of terrigenous sedimentation is postdepositional diagenesis, which is driven by the bacterially mediated degradation of organic matter (see section 4.3.2). Below, we discuss how magnetic properties have contributed to extracting environmental information encoded in the marine sedimentary record, both as depositional signals of terrigenous sedimentation and reworking.

4.2.1. Terrigenous Sediment Supply by Ice

[61] About half of the sediment load eroded by ice and transported to marine environments (1400 Tg/yr, Table 1) accumulates in proximal settings within the continental shelf and slope when ice meets water and melts [*Raiswell et al.*, 2006]. Once there, these particles, which range in size from boulders to clays, are often affected by gravitational flows or are reworked by bottom currents. The other 1500 Tg/yr of particles transported by ice (1500 Tg/yr) is carried much further away from glacial margins by icebergs [*Raiswell et al.*, 2006]. When icebergs melt, these ice rafted debris (IRD) particles, which usually range in size from coarse sands to clays, sink and accumulate on the seafloor. IRD layers are typified by a large fraction of coarse-grained (often defined as >150 μm) sediment particles, and are interbedded with biogenic carbonate-poor and finer-grained sediments (typically clays). IRD layers are known from both hemispheres and for periods beyond the Quaternary "ice house," while IRD layers wasted from the Laurentide ice sheet (LIS) into the North Atlantic Ocean during the so-called Heinrich events (HE) [*Heinrich*, 1988; *Hemming*, 2004; *Stanford et al.*, 2011] are well studied. These events correspond to centennial-scale warming periods at the end of glacial intervals, which witnessed the sudden discharge of massive amounts of icebergs. Since the LIS catchment is dominated by strongly magnetic crystalline and volcanic rocks rich in (titano)magnetite, IRD layers have magnetic susceptibility values that are much higher than those of the background sediments [*Stoner and Andrews*, 1999]. This has made magnetic susceptibility a powerful tool for delineating not only the extent and thickness of IRD layers within the North Atlantic, but also for inferring their source regions and contemporaneous climatic patterns [*Robinson*, 1986; *Grousset at al.*, 1993; *Dowdeswell et al.*, 1995; *Robinson et al.*, 1995; *Lebreiro et al.*, 1996]. Concentration- and grain size–dependent magnetic parameters have been further used to validate conclusions based on magnetic susceptibility and to map the extent of IRD as far south as offshore of the Iberian Peninsula [*Robinson*, 1986; *Stoner et al.*, 1996, 1998; *Thouveny et al.*, 2000]. However, the distinctive magnetic signature of different horizons within and below some IRD layers [*Thouveny et al.*, 2000; *Scourse et al.*, 2000; *Walden et al.*, 2007; *Peters et al.*, 2008], along with the presence of some IRD layers that do not correlate to HE [*Stoner et al.*, 1998], are increasingly suggesting a prominent role of other ice sheets (i.e., East Greenland, British, Icelandic, Fennoscandian) as a source of IRD layers, thereby corroborating previous inferences based on the isotopic signature of IRD material [*Grousset et al.*, 2000]. Magnetic properties of older North Atlantic sediments have also contributed to tracking ice-rafting back to the late Eocene [*Eldrett et al.*, 2007], which illustrates the potential of rock magnetism for studying terrigenous material transported by ice into the oceans and, hence, to better constrain past climate evolution.

[62] Despite the potential for rock magnetic techniques to identify IRD, we are aware of only a handful of studies where environmental magnetic parameters (especially χ) have been used to study Antarctic IRD [e.g., *Hou et al.*, 1998; *Brachfeld et al.*, 2002; *Kanfoush et al.*, 2002; *Pirrung et al.*, 2002; *Venuti et al.*, 2011]. Warm waters surrounded Antarctica throughout most of the Paleogene [*Ehrmann and Mackensen*, 1992], which prevented long-distance transport of IRD at those times, while the strong influence of currents complicates interpretation of Quaternary IRD layers [*Pirrung et al.*, 2002]. Regardless, in many cases, Antarctic IRD layers are characterized, like Quaternary North Atlantic IRD layers, by high χ values [*Kanfoush et al.*, 2002; *Pirrung et al.*, 2002; *Venuti et al.*, 2011] due to enhanced concentrations of magnetic minerals with respect to background sediments [*Hou et al.*, 1998].

4.2.2. Terrigenous Sediment Supply by Wind

[63] Generally, eolian dust is more strongly magnetic than background, biogenic-dominated sediments that accumulate at distal open marine sites when contributions from volcanic sources and submarine hydrothermal mineralization [*Dekov et al.*, 2009, 2010] are insignificant. For this reason, magnetic susceptibility has been one of the most widely used rock magnetic parameters to identify changes in eolian dust, sourced from zonal and shadow deserts (i.e., Sahara, Arabia, Australia, Patagonia) and continental interiors (i.e., Asia), deposited in neighboring marine basins such as the Red Sea

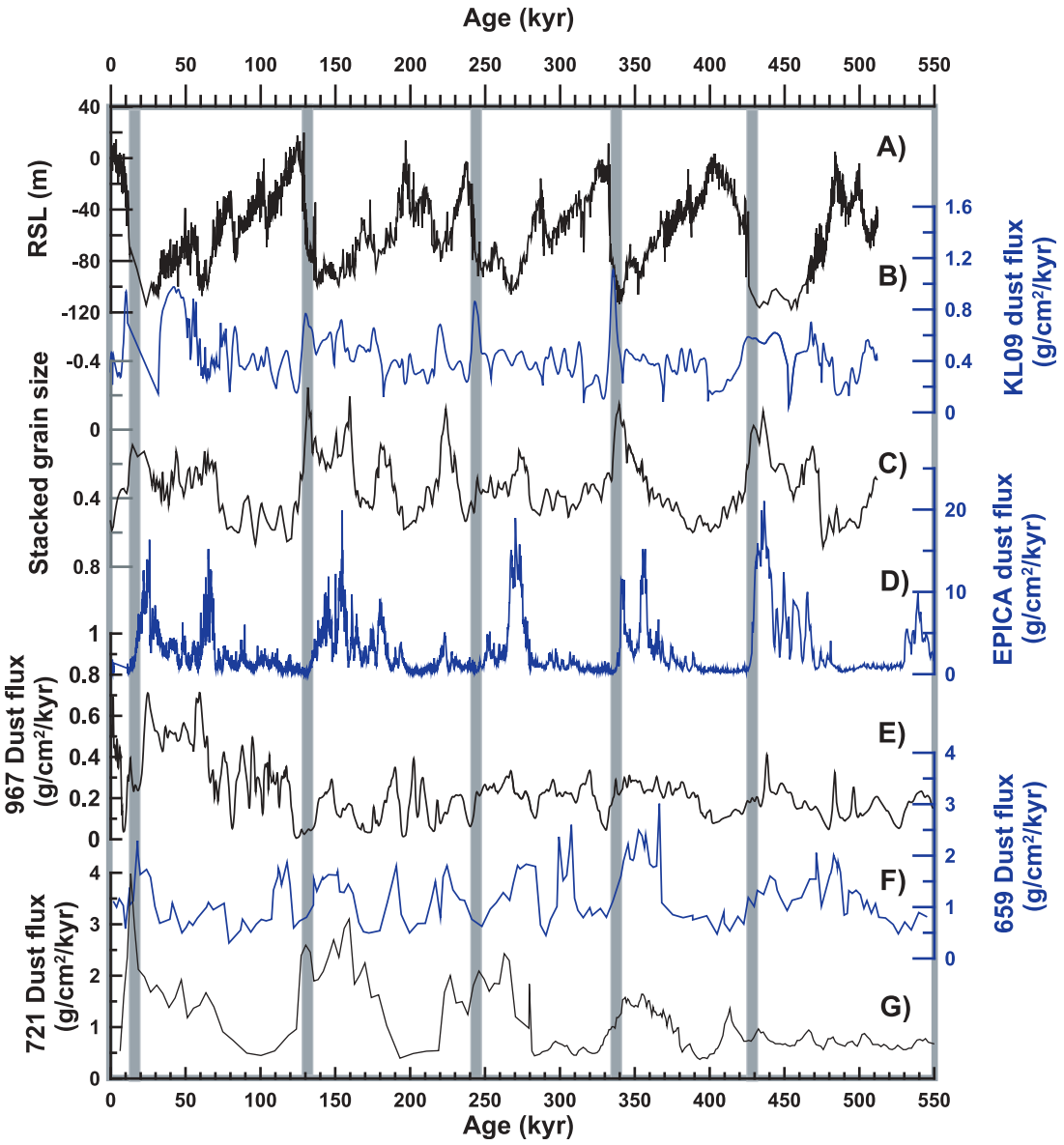

Figure 9. Comparison of sea level and dust records from the Red Sea with those from Antarctica and North Africa [after *Roberts et al.*, 2011c]. The vertical gray bars indicate the positions of the last 5 glacial terminations. (a) Sea level [*Rohling et al.*, 2009]. (b) Dust record for Red Sea core KL09 [*Roberts et al.*, 2011c]. (c) Stacked grain size from the Zhaojiachuan and Lingtai sections and Chinese Loess Plateau [*Sun et al.*, 2006b]. (d–g) Dust records from EPICA Dome C, Antarctica [*Lambert et al.*, 2008]; and ODP sites 967 [*Larrasoaña et al.*, 2003a], 659 [*Tiedemann et al.*, 1994], and 721 [*deMenocal et al.*, 1991], respectively.

[*Rohling et al.*, 2008], the Indian Ocean [*Bloemendal and deMenocal*, 1989], the Pacific Ocean [*Doh et al.*, 1988; *Yamazaki*, 2009] and the North Atlantic [*Bloemendal and deMenocal*, 1989; *Itambi et al.*, 2009, 2010a, 2010b]. These studies have made important contributions mainly to understanding the influence and interaction of high- and low-latitude climatic forcing on the evolution of monsoonal climates. However, combination of magnetic susceptibility data with other environmental magnetic parameters and auxiliary proxies for eolian dust supply have shown that, with the exception of some well documented cases [*Rohling et al.*, 2008], the appealing link between eolian dust and magnetic susceptibility is not straightforward given the role of other terrigenous sources and reductive diagenesis on magnetic mineral assemblages [*Bloemendal et al.*, 1988, 1993; *Hounslow and Maher*, 1999; *Larrasoaña et al.*, 2008; *Itambi et al.*, 2009]. These and other studies [*Doh et al.*, 1988; *Yamazaki and Ioka*, 1997b; *Maher and Dennis*, 2001; *Dinarès-Turell et al.*, 2003; *Larrasoaña et al.*, 2003a; *Köhler et al.*, 2008; *Maher*, 2011; *Roberts et al.*, 2011c] collectively demonstrate that other magnetic parameters, especially those indicative of the relative (e.g., S ratio) or absolute (HIRM and similar parameters) concentration of high-coercivity minerals, constitute better proxies for the supply of eolian dust (Figure 9). The oxidizing and dehydrating environments of deserts means that hematite is abundant in eolian dust

from such source areas and is easily detected using environmental magnetic measurements [*Robinson*, 1986; *Doh et al.*, 1988; *Bloemendal et al.*, 1988, 1993; *Balsam et al.*, 1995; *Yamazaki and Ioka*, 1997b; *Hounslow and Maher*, 1999; *Maher and Hounslow*, 1999; *Maher and Dennis*, 2001; *Dinarès-Turell et al.*, 2003; *Larrasoaña et al.*, 2003a, 2008; *Köhler et al.*, 2008; *Itambi et al.*, 2009; *Maher*, 2011; *Roberts et al.*, 2011c]. It should be noted, however, that the equipment available in most laboratories for imparting an IRM, on which the S ratio and HIRM are based, do not typically exceed 1 T, and at this field any goethite that might be present is barely magnetized. Therefore, virtually all magnetic parameters used to determine the concentration of high-coercivity minerals record hematite abundances despite geochemical or DRS evidence that often indicates the presence of goethite [*Robinson*, 1986; *Köhler et al.*, 2008]. A benefit of this circumstance is that these hematite-biased parameters can be useful for identifying dust source areas in regions with hot and arid climates, which favor hematite rather than goethite formation [e.g., *Maher*, 1986]. For example, *Larrasoaña et al.* [2003a] used meteorological, satellite and geochemical data to identify the source area for dust that accumulated in the eastern Mediterranean from the eastern Sahara north of the central Saharan watershed (at ~21°N). Precise identification of the dust source area enabled identification of the role of regional aridity changes, which dominate over changes in wind speed or atmospheric circulation patterns as drivers of eolian dust supply. Separation of these factors is often neglected in studies of eolian dust supply despite their importance [*Rea*, 1994; *Trauth et al.*, 2009].

4.2.3. Terrigenous Sediment Supply by Rivers

[64] Despite the fact that rivers are the main contributors of sediment to the ocean (Table 1), fluvially derived marine sediments have seldom been a focus of environmental magnetic studies. This is probably due to the characteristics of fluvial sedimentation into marine settings, which are often governed by autocyclic (i.e., channel avulsion) and allocyclic (i.e., tides and tectonic/eustatic control of accommodation space) factors other than climate. In consequence, there are few examples, most of which have focused on application of magnetic susceptibility, that report enhanced χ values as the concentration and/or grain size of detrital particles increases in response to enhanced terrigenous supply [*Weber et al.*, 2003; *Stein et al.*, 2004; *Alt-Epping et al.*, 2009; *De Vleeschouwer et al.*, 2011] whose ultimate driving mechanism might range from monsoonal [*De Vleeschouwer et al.*, 2011] to high-latitude-dominated (i.e., North Atlantic Oscillation related [*Stein et al.*, 2004; *Alt-Epping et al.*, 2009]) precipitation or to an interplay between both mechanisms [*Weber et al.*, 2003]. Changes in terrigenous supply or source area have also been inferred for large rivers such as the Amazon [*Maslin et al.*, 2000] and Ganges-Brahmaputra [*Prakash Babu et al.*, 2010] by using additional concentration- and grain size–dependent magnetic parameters, although in these cases storage of terrigenous material in the delta during periods of sea level rise might have dominated the sedimentary record compared to climatically modulated riverine supply.

[65] In other cases, the climatic signal encoded in fluvially derived marine sediments is not linked to variations in fluvial discharge but rather to aridity changes in the source area [*Zhang et al.*, 2008]. Thus, the hematite/goethite ratio in large tropical rivers has been linked to aridity changes in source areas because hematite typically forms under drier conditions compared to goethite [e.g., *Maher*, 1986]. The ratio between these minerals as determined by rock magnetic records has been used by *Abrajevitch et al.* [2009] to infer cyclic changes in monsoon-derived fluvial discharge of the Ganges-Brahmaputra rivers, although diagenesis has also distorted the initial depositional signal. *Colin et al.* [1998] also suggested that aridity changes in the source area of the Ganges-Brahmaputra and Irrawaddy rivers conditioned the concentration and grain size of (titano)magnetite grains delivered by these rivers.

4.2.4. Reworking of Sediments by Bottom Currents

[66] Once deposited, marine sediments can be affected by bottom currents that alter both their primary physical characteristics and depositional signal. This results in formation of so-called contourites or drift deposits, whose characteristics and distribution are independent of latitude [*Faugères and Stow*, 1993]. Concentration- and grain size–dependent magnetic parameters from Quaternary drift sediments have been used to detect changes in the strength of bottom currents, mainly in the North Atlantic [*Kissel et al.*, 1997, 1998, 1999, 2009; *Andrews et al.*, 2003a, 2003b; *Hassold et al.*, 2006; *Rousse et al.*, 2006; *Stanford et al.*, 2006] and around Antarctica [*Mazaud et al.*, 2007, 2010], although the specific link between bottom current activity and climate variability is not always fully understood [*Andrews et al.*, 2003a, 2003b; *Rousse et al.*, 2006]. Bottom currents affect not only the sorting of particles in drift sediments, but also their spatial arrangement. This typically results in enhancement of the initial sedimentary fabric; important insights on bottom current dynamics have also therefore been inferred from both the directional properties of the magnetic fabric (anisotropy of magnetic susceptibility, AMS) [*Parés et al.*, 2007] as well as its shape and degree of anisotropy [*Kissel et al.*, 1997, 1998; *Hassold et al.*, 2006, 2009a, 2009b]. Most if not all rock magnetic and AMS studies of drift sediments have focused on bottom current dynamics in high-latitude settings such as the North Atlantic and peri-Antarctic basins.

4.2.5. Mixed Terrigenous Sedimentary Signals

[67] Although different terrigenous sediment sources dominate at specific latitudes, they are often mixed in the diffuse boundaries between such regions. Mixing of eolian dust and fluvially derived terrigenous material has been reported from low-latitude marine sedimentary records in the northeast Atlantic (Figure 10) [*Bloemendal et al.*, 1988; *Itambi et al.*, 2009, 2010b; *Just et al.*, 2012] and the South China Sea [*Kissel et al.*, 2003]. Overall, these studies have consistently indicated an antiphase relationship between dust and riverine supply. A notable case of mixing of different terrigenous signals is provided by identification of eolian hematite sourced from the Sahara in IRD layers off the Iberian Peninsula [*Robinson*, 1986; *Thouveny et al.*, 2000].

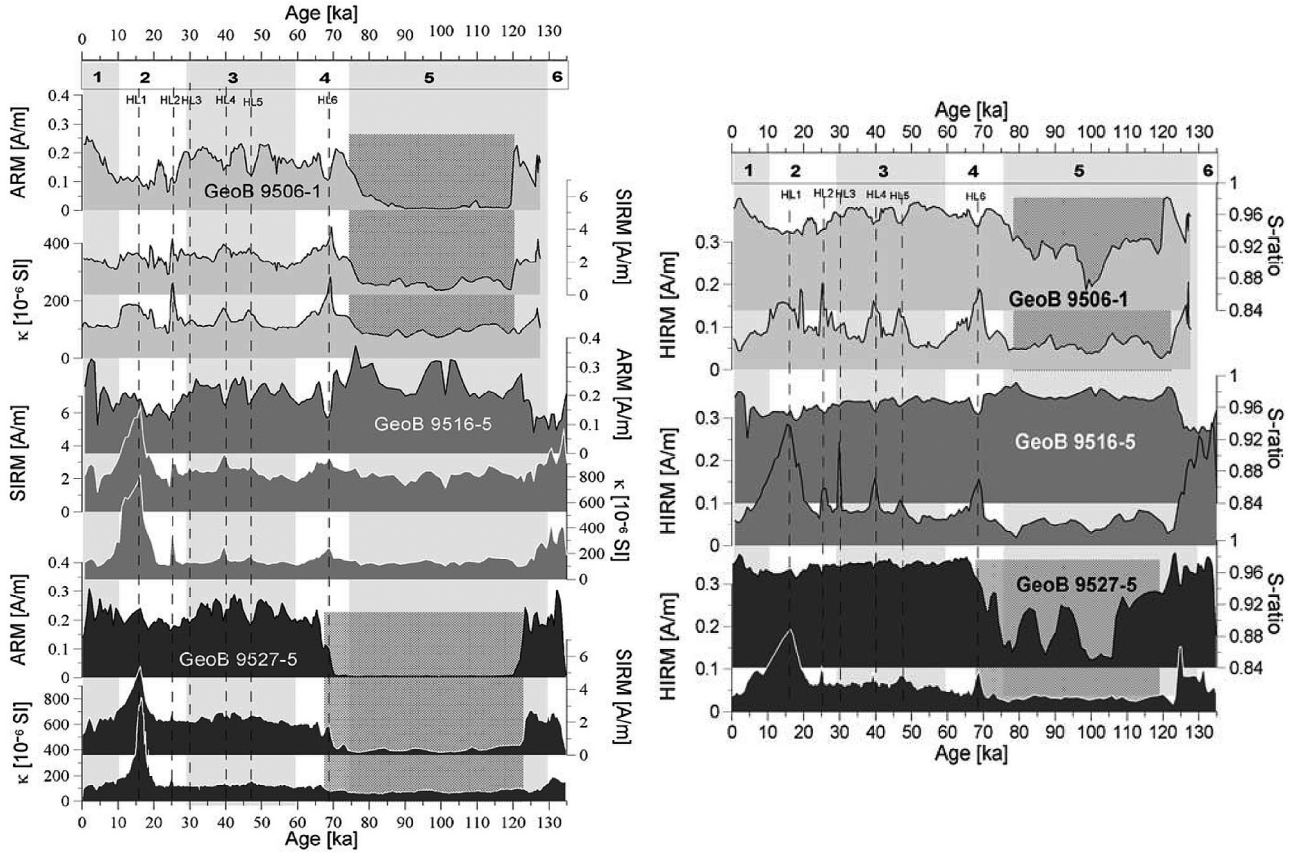

Figure 10. Magnetic parameters for marine sediment cores GeoB 9506-1, GeoB 9516-5, and GeoB 9527-5 recovered from the Senegal continental margin along a N-S transect offshore of environments ranging from desert (15°N) to fluvial drainage from inland savannah (12°N) landscapes [*Itambi et al.*, 2009]. High S ratios during warmer periods (see horizontal bar indicating marine isotopic stages (MIS) 1 to 6) indicate the dominance of fluvial magnetite, whose concentration (depicted by ARM curves) diminishes during Heinrich events HL1 to HL6 in response to colder and drier conditions and hence to decreased runoff. Highest HIRM and κ values during HL1 to HL6, along with lower S ratios, indicate simultaneous enhanced supply of hematite-rich eolian Saharan dust at those times. Moderately decreased HIRM and strikingly low ARM and S ratios between 70 and 120 ka in cores GeoB 9506-1 and GeoB 9527-5 attest to widespread reductive dissolution (cross hatching) of magnetite and only partial dissolution of hematite during MIS 5. Clearly, different parameters reflect different paleoenvironmental processes.

Sediments enriched in eolian material and IRD are typically associated with low- and high-latitude settings, respectively. Coexistence of material from both terrigenous sources illustrates the ability of the climate system to alter the latitudinal distribution of these materials. Mixing of eolian dust and IRD signals can also be deduced for peri-Antarctic marine sediments from magnetic susceptibility records that are strikingly similar to geochemical records of dust deposition in Antarctic ice cores [*Pugh et al.*, 2009]. This suggests that the magnetic susceptibility record is linked to the supply of dust sourced either from Patagonia or/and Australia [*Grousset et al.*, 1992; *De Deckker et al.*, 2010]. This is important because correlation between these marine sediments and ice core records enables establishment of detailed age models for sediments that are otherwise difficult to date [*Pugh et al.*, 2009]. However, the magnetic susceptibility signal of other peri-Antarctic marine sediments has been linked mainly to IRD material [*Hou et al.*, 1998; *Kanfoush et al.*, 2002; *Pirrung et al.*, 2002]. Unmixing IRD and dust signals is further complicated by reworking of peri-Antarctic marine sediments by the Antarctic Circumpolar Current [*Parés et al.*, 2007; *Mazaud et al.*, 2007, 2010; *Hassold et al.*, 2009a, 2009b]. A similarly complicated situation exists in the Northwest Pacific Ocean, where both IRD and eolian dust, in addition to volcanic ash, have been shown to influence the magnetic properties of sediments [*Bailey et al.*, 2011].

4.3. Postdepositional Signals

4.3.1. Pedogenic Processes and Soils

[68] Soils form through chemical-physical alteration (pedogenesis) of parent material that acts [e.g., *Vincent et al.*, 1994] under the integrated effects of the soil-forming factors (climate, organisms, relief, parent material, and time) [*Jenny*, 1941, 1980]. Soils consist of several interrelated horizons (A, B, and C). The A horizon has the highest organic matter content, but soluble and/or mobile components (e.g., silicate clays, iron, aluminum and humic substances) can be transported to the underlying B horizon.

The C horizon represents relatively unaltered parent material. The magnetic properties of the A and B horizons are often enhanced [*Maher*, 1998] due to neoformation of nano-sized ferrimagnets (magnetite and/or maghemite) [*Zhou et al.*, 1990; *Maher*, 1998] with iron-bearing clays and mafic silicates providing the iron source [*Spassov et al.*, 2003]. Soil magnetic properties therefore carry important information about the dynamics of pedogenic processes [*Zhou et al.*, 1990; *Tauxe et al.*, 1990; *Singer et al.*, 1996], and the linkage between magnetic properties and climate [*Maher et al.*, 1994].

[69] Usually, lithogenic eolian materials and their parent materials have relatively uniform and weak magnetic properties. This is true for loess deposits from Europe and Asia, especially the CLP. In contrast, ancient soils that are intercalated with loess in loess/paleosol sequences are strongly magnetic because of magnetic enhancement due to pedogenic magnetite/maghemite formation [e.g., *Kukla et al.*, 1988; *Zhou et al.*, 1990; *Liu et al.*, 2007a]. There are currently two hypothesized alternative major pathways for maghemite formation in soils: a direct precipitation process and a process by which maghemite forms from a transient intermediate mineral, ferrihydrite. For direct precipitation, fermentation is invoked with nanoparticulate magnetite forming directly by reducing Fe^{3+} to Fe^{2+} in the presence of organic matter and/or iron-reducing bacteria [*Mullins*, 1977]. The magnetite is then oxidized into maghemite. The second mechanism calls on formation of strongly magnetic intermediate ferrihydrite by transformation of weakly magnetic ferrihydrite doped with adsorbed ligands (phosphate, citrate) into hematite [*Barrón and Torrent*, 2002; *Barrón et al.*, 2003; *Michel et al.*, 2010]. A major hindrance to understanding transformation processes of magnetic minerals during pedogenesis is that the intermediate phases rarely survive pedogenic processes. Nevertheless, useful hints arise from the concentrations of strongly magnetic maghemite and weakly magnetic hematite and goethite in soils. Only hematite is intrinsically correlated with nanoparticulate maghemite in soils [*Ji et al.*, 2001; *Liu et al.*, 2006b; *Lyons et al.*, 2010]. *Liu et al.* [2010] observed a positive correlation between unblocking temperatures of pedogenically produced maghemite (which is related to magnetic particle volume) and its concentration in samples from a chronosequence in Spain. However, for paleosol horizons from the CLP, the grain size distribution peaks at about 25 nm and is independent of the degree of pedogenesis, and is thus indicative of the second stage of pedogenesis [*Liu et al.*, 2005a, 2007a]. This could indicate that the pedogenic maghemite evolved into a mature state and thus that the grain size of these particles remains relatively constant.

[70] Although the transformation of magnetic minerals during pedogenesis is controlled by a range of factors (e.g., temperature, precipitation, organic carbon content, pH, Eh, etc.), statistical analyses have been taken to indicate that the magnetic properties (especially χ) of modern soils are predominantly determined by the amount of rainfall [*Heller et al.*, 1993; *Maher et al.*, 1994; *Maher and Thompson*, 1995; *Maher*, 1998; *Florindo et al.*, 1999; *Maher et al.*, 2002, 2003; *Maher and Hu*, 2006; *Geiss et al.*, 2004; *Liu et al.*, 2005c]. This makes it possible to reconstruct past temporal and spatial trends in precipitation [*Maher et al.*, 1994; *Maher and Thompson*, 1995]. However, the relationship between magnetic susceptibility and rainfall is nonlinear. When rainfall exceeds a threshold (~550–600 mm/yr), the concentration of ferrimagnetic minerals decreases due to dissolution effects [*Han et al.*, 1996; *Balsam et al.*, 2004]. *Guo et al.* [2001] and *Bloemendal and Liu* [2005] suggested that there is a complex response between magnetic mineral transformation and climate. *Liu et al.* [2007a] suggested a conceptual model in which the ratio of the concentration of hematite to maghemite-magnetite (Hm/Mag) is superior to χ alone for estimating paleoprecipitation because this ratio has a more monotonic correlation with rainfall [*Torrent et al.*, 2006].

[71] *Orgeira and Compagnucci* [2006] suggested that it is the potential water storage (PWS) rather than total precipitation that controls transformation of magnetic minerals during pedogenesis. PWS is a measure of the net annual precipitation surplus and is defined as the difference between the total precipitation (water gain) and evapotranspiration (water loss). When PWS is negative (water loss > water gain), as is the case for the CLP and Russian Steppe, reducing conditions are inhibited and magnetic material of eolian origin can be preserved and magnetic nanoparticle formation is favored during pedogenesis. In contrast, when PWS is positive (e.g., Argentina), magnetic minerals are depleted by dissolution. Magnetic paleoclimate transfer functions have proved useful for semiquantitatively estimating paleoclimate changes on orbital time scales and at regional scales where postdepositional magnetic mineral dissolution has a minor influence and where soil parent material and magnetic mineral content are relatively uniform [*Maher and Thompson*, 1995].

[72] CLP and Russian Steppe soils are consistently characterized by magnetic enhancement. The positive relationship between magnetic susceptibility variations for Chinese loess-paleosol sequences and fluctuations in deep-sea oxygen isotope records demonstrates that local climate (i.e., the East Asian monsoon system) is teleconnected to global paleoclimate signals at orbital [*Liu*, 1985; *Liu and Ding*, 1998], suborbital [*Deng et al.*, 2006] and even at millennial time scales [*Porter and An*, 1995; *Chen et al.*, 1997] (Figure 11). Furthermore, direct comparison of dust variations from Arabia with those from the CLP demonstrates an atmospheric teleconnection over all of these time scales for the last 5 glacial cycles [*Roberts et al.*, 2011c]. *Chen et al.* [1997] investigated three sequences that span the most recent loess unit L1 (<75 ka) from the western CLP and found that magnetic and nonmagnetic parameters have strong similarity to climate signals in ice core records from Greenland and Antarctica. *Deng et al.* [2006] investigated long-term (<2.6 Ma) paleoclimate variations recorded by the loess/paleosol sequence at Jingbian at the northern fringe of the CLP and reported a long-term increase in aridification in the Asian interior driven by global cooling and other related climate factors. *Guo et al.* [2002] demonstrated that Chinese loess-paleosol sequences extend back to ~22 Ma. This indicates that the source(s) of eolian dust in the Asian

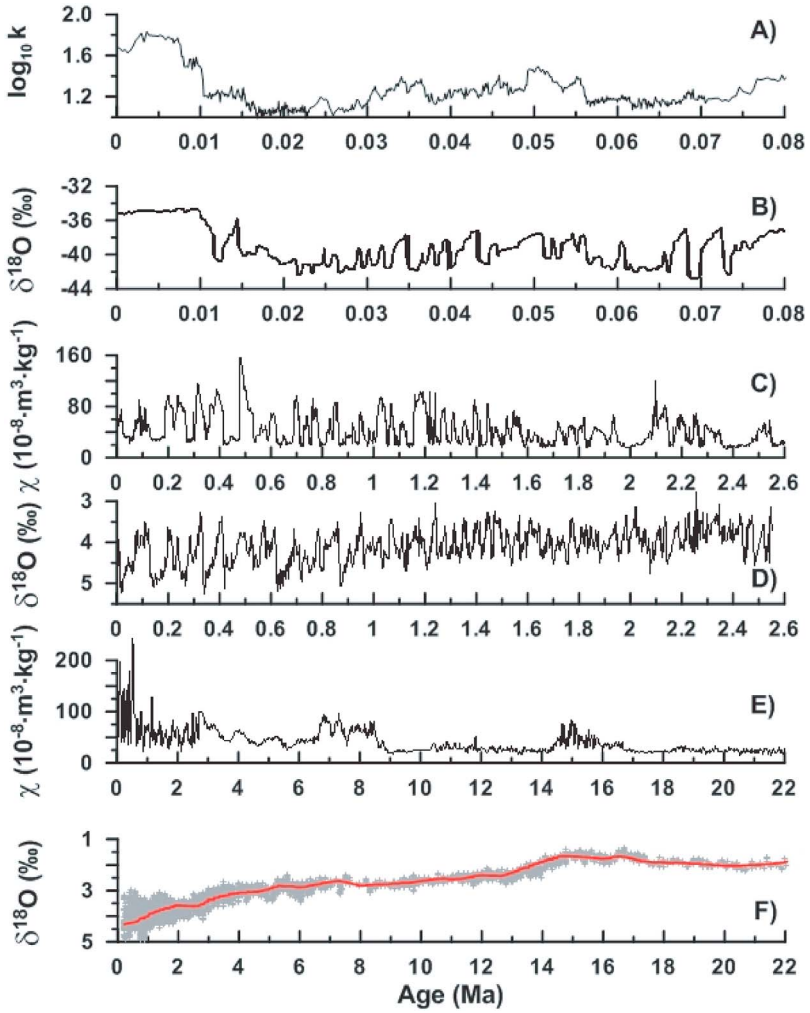

Figure 11. Comparison of magnetic susceptibility for Chinese loess/paleosol sequences and marine oxygen isotope records over different time scales: (a–b) <0.08 Ma, (c–d) <2.6 Ma, and (e–f) <22 Ma. Data in Figures 11a and 11b are from *Chen et al.* [1997], in Figures 11c and 11d are from *Ding et al.* [2005], in Figure 11e are from *Guo et al.* [2002], and in Figure 11f are from *Zachos et al.* [2001].

interior and the Asian winter monsoon have existed since the early Miocene, which probably resulted from aridification associated with progressive uplift of the Tibetan Plateau and global cooling. *Oldfield and Bloemendal* [2011] confirmed that Miocene loess sequences in China are of eolian origin. *Hao et al.* [2008] observed that the magnetic properties of Miocene loess sequences vary on both orbital and supraorbital time scales, but in a more complicated manner than for younger eolian sequences.

[73] Magnetic susceptibility is controlled by many factors and is not a simple paleoclimatic proxy [*Sun and Liu*, 2000; *Guo et al.*, 2001]. In addition to χ, *Banerjee et al.* [1993] used low-temperature techniques to separate local signals from regional paleomonsoon signals on the CLP. Similarly, *Hunt et al.* [1995b] used several magnetic parameters to investigate the concentration, composition and grain size of magnetic minerals in loess. Variations in magnetic parameters are not always directly related to the intensity of the Asian summer monsoons [*Vidic et al.*, 2003; *Sun et al.*, 2006a]. Temporal variations of magnetic signals between different profiles are mainly caused by geographic differences in the timing and amount of local monsoon precipitation. To better understand this question, *Hao and Guo* [2005] constructed maps of spatial variations of magnetic susceptibility for the Chinese loess over the last 600 ka. In these contour maps there are many clusters with low magnetic susceptibilities, termed "bull's eyes," that are strongly linked to local topography. Typically, the effects of the Asian summer monsoons are weak in the western CLP. Therefore, caution must be used when interpreting long-term magnetic variations from a single profile. For example, loess unit L8 on the CLP is characterized by low χ values and abnormally coarser grain sizes. However, the corresponding unit in Tajikistan has regular variations in grain size. This strongly indicates that the abnormal behavior of unit L8 is a local signal, probably related to expansion of the dust source region [*Yang et al.*, 2006]. Overall, however, environmental magnetic studies have proven to be extremely fruitful for monsoon/paleoprecipitation studies through analysis of

paleosols and for studies of eolian processes through analysis of loess and other eolian deposits.

4.3.2. Diagenesis

[74] Chemical reactions that occur during diagenesis, as discussed briefly above, can be an important determinant of the magnetic properties of both marine and lake sediments. The degree to which diagenetic reactions affect sediments depends mainly on the interplay between the supply and type of organic matter and the oxygen content of bottom waters and sediment pore waters. Shelf and slope (<1 km water depth) marine settings are characterized by large supplies of terrigenous material (Table 1) and organic carbon. In these settings, surficial sediments are oxidized through contact with oxygenated bottom waters, while underlying sediments become rapidly anoxic due to intense microbially mediated organic matter degradation and rapid sediment accumulation, which prevents downward diffusion of oxygen from the bottom waters. This results in a zonation that is characterized by an upper oxic layer that preserves the initial detrital magnetic mineral assemblage, a second suboxic layer where magnetite begins to be dissolved, and a third anoxic layer where most remaining detrital magnetic minerals have also been dissolved. These early diagenetic changes are accompanied by authigenic growth of greigite, first as SP particles (intermediate zone) and eventually as SD particles (lower zone) [*Rey et al.*, 2000, 2005; *Emiroglu et al.*, 2004; *Liu et al.*, 2004; *Roberts and Weaver*, 2005; *Kawamura et al.*, 2007; *Rowan et al.*, 2009; *Mohamed et al.*, 2011]. As sedimentation continues, this zonation migrates upward so that sediments through which the anoxic zone has passed are eventually characterized by widespread dissolution of detrital magnetic minerals and occurrence of SP and SD greigite. This is a common situation in shallow marine settings [*Rey et al.*, 2000, 2005; *Emiroglu et al.*, 2004; *Liu et al.*, 2004; *Kawamura et al.*, 2007; *Zheng et al.*, 2010; *Mohamed et al.*, 2011; *Roberts et al.*, 2011a] and in deeper marginal marine sediments characterized by high accumulation rates [e.g., *Leslie et al.*, 1990; *Tric et al.*, 1991; *Roberts and Turner*, 1993; *Florindo and Sagnotti*, 1995; *Horng et al.*, 1998; *Robinson et al.*, 2000; *Jiang et al.*, 2001; *Roberts and Weaver*, 2005; *Dillon and Bleil*, 2006; *Vasiliev et al.*, 2008; *Rowan et al.*, 2009; *Roberts et al.*, 2011a], and is responsible for the widespread lack of genuine depositional paleomagnetic signals often reported in diagenetically reduced marine sediments.

[75] Preservation of authigenic greigite is favored by an excess of iron with respect to dissolved sulfide, so that pyritization reactions are not brought to completion [*Kao et al.*, 2004]. The concentration and mobilization of iron and sulfide are subject to dynamic chemical gradients and are affected by other processes such as sediment texture and variations in organic carbon delivery, therefore, the environmental significance of the presence of greigite in sediments is not linked to variations in its concentration but rather to the fact that it signals anoxic conditions. Good examples of this situation are provided by the formation of greigite in connection with changes in terrigenous sediment supply [*Blanchet et al.*, 2009] and variations in the ventilation of bottom waters [*Vigliotti*, 1997; *Larrasoaña et al.*, 2003b]. Whereas signals of terrigenous sediment supply by ice and of bottom water dynamics associated with sediment drift deposits have seldom been reported to be overprinted by reductive diagenetic processes, such alterations are common for terrigenous signals of riverine and eolian sedimentation. Reductive diagenetic processes have been reported to alter the riverine-related magnetic signal encoded in marine sediments even to the point of compromising the paleoenvironmental record carried by magnetic minerals [*Abrajevitch and Kodama*, 2011]. In the case of eolian dust incorporated within marine sediments, however, it has often been shown that reducing diagenetic conditions did not prevent isolation of the depositional signal typically associated with hematite-rich dust supply, probably because the depositional environments under investigation were more oxic and because hematite is more resistant to reductive dissolution than magnetite [*Bloemendal et al.*, 1993; *Larrasoaña et al.*, 2003a; *Abrajevitch and Kodama*, 2011]. Different mineral surface properties and their influence on sulfide complexation processes, which ultimately drive reductive dissolution, appear to be responsible for the lower reactivity of hematite with respect to magnetite reported typically in marine sediments [*Poulton et al.*, 2004]. Isomorphous Al-for-Fe substitution also decreases the reactivity of hematite and goethite to sulfide [*Liu et al.*, 2004a].

[76] Other processes that result in the release of dissolved sulfide in marine sediments, and that are known to promote authigenic growth of greigite, are anaerobic oxidation of methane [e.g., *Housen and Musgrave*, 1996; *Kasten et al.*, 1998; *Neretin et al.*, 2004; *Garming et al.*, 2005; *Musgrave et al.*, 2006; *van Dongen et al.*, 2007; *Enkin et al.*, 2007; *Larrasoaña et al.*, 2007; *Fu et al.*, 2008; *Chen et al.*, 2009; *Roberts et al.*, 2011a] and degradation of hydrocarbons at seepages [*Reynolds et al.*, 1991]. When these processes affect sediments over prolonged periods of time (i.e., during late early diagenesis), monoclinic pyrrhotite can also form in addition to greigite [*Reynolds et al.*, 1991; *Housen and Musgrave*, 1996; *Musgrave et al.*, 2006; *Larrasoaña et al.*, 2007; *Roberts et al.*, 2010]. The characteristic association of later diagenetic greigite and pyrrhotite with gas hydrate-bearing marine sediments has led to the suggestion that these minerals can be used to detect the past presence of gas hydrates in ancient sediments [*Housen and Musgrave*, 1996; *Larrasoaña et al.*, 2007; *van Dongen et al.*, 2007; *Chen et al.*, 2009; *Roberts et al.*, 2010], which is important because gas hydrates are key elements in the carbon cycle and leave elusive evidence for their former occurrence.

[77] In deeper (>1 km water depth) marine settings characterized by low sediment accumulation rates, both the supply of terrigenous material (Table 1) and organic carbon contents decrease. In these settings, the thickness of the uppermost oxic sediments expands at the expense of the lower anoxic zone, which can occur at depths of tens to hundreds of meters below the sediment/water interface or it might not exist due to the scarcity of fuel (organic matter) and downward diffusion of oxygen from the overlying water

mass due to low sediment accumulation rates. In this case, goethite and hematite might form and coexist with preexisting magnetic minerals, as has been documented in pelagic limestones and marls [*Channell et al.*, 1982; *Freeman*, 1986; *Galbrun et al.*, 1994; *Moreau et al.*, 1994; *Mamet and Preat*, 2006]. The environmental significance of hematite and/or goethite in these rocks is uncertain because they might have grown authigenically between a few thousand [*Channell et al.*, 1982] and millions of years [*Moreau et al.*, 1994] after deposition, but they appear to be linked to oxygenation of bottom waters during sediment accumulation.

[78] Oxic conditions that prevail during slow deposition of deep-sea sediments can be transiently disrupted by increased organic matter supply, decreased bottom water oxygenation, or both. *Tarduno* [1994] argued that enhanced organic carbon supply during glacial periods resulted in reductive dissolution of magnetite at cyclic stratigraphic intervals. Links between nonsteady state diagenetic conditions and oxygenation of bottom waters are well exemplified by the widespread reductive dissolution of magnetite and authigenic growth of greigite in Eastern Mediterranean sediments that result from degradation of orbitally controlled organic-rich layers (sapropels) [*van Santvoort et al.*, 1997; *Roberts et al.*, 1999; *Passier et al.*, 2001; *Kruiver and Passier*, 2001; *Passier and Dekkers*, 2002; *Larrasoaña et al.*, 2003b, 2006]. Downward migration of oxygen into sapropels after their formation led to authigenic magnetite formation at paleooxidation fronts [*Passier et al.*, 2001; *Kruiver and Passier*, 2001; *Passier and Dekkers*, 2002; *Larrasoaña et al.*, 2003b, 2006; *Garming et al.*, 2004]. Comparison of magnetic and geochemical data indicates that diagenetic conditions associated with sapropels and the resulting magnetic signature are linked to both an enhanced supply of organic carbon and a simultaneous decrease of bottom water ventilation, with the latter factor determining the eventual magnetic properties [*Larrasoaña et al.*, 2003b]. Use of whole-core measurement techniques [*Mead et al.*, 1986; *Weeks et al.*, 1993; *Nagy and Valet*, 1993; *Roberts*, 2006] enables time-efficient study of magnetic properties of long sedimentary sequences at high resolution, and has been used to assess long-term climatically modulated ventilation changes in the eastern Mediterranean Sea [*Larrasoaña et al.*, 2003b].

[79] The magnetic properties of lake sediments can also be affected by reductive diagenesis. Organic matter in lakes, especially arising from biologic productivity within the lake, dilutes the concentration of lithogenic magnetic minerals, which can result in a negative correlation between these parameters. In addition, lithogenic magnetic minerals can be partially to completely dissolved in organic-rich, freshwater sediments under anoxic diagenetic conditions through the same microbially mediated reactions that occur in marine sediments [e.g., *Berner*, 1980; *Snowball and Thompson*, 1988, 1990; *Roberts et al.*, 1996; *Williamson et al.*, 1998; *Reynolds et al.*, 1999]. The redox-driven processes are controlled by lake level, sediment accumulation rate, sediment organic matter content, availability of iron and sulfate [*Berner*, 1984], and the grain size and composition of iron-bearing minerals [*Hilton and Lishman*, 1985; *Anderson and Rippey*, 1988; *Canfield et al.*, 1992; *Morse and Wang*, 1997; *Poulton et al.*, 2004]. For example, lake level and stratification strongly affect lake conditions, and thus the preservation of magnetic minerals. *Williamson et al.* [1998] investigated tropical maar lake sediments from Lake Tritrivakely, Madagascar, in which high-coercivity "oxides" were preferentially preserved during dry periods with low lake levels but are absent in siderite-rich laminated sediments associated with permanent and stratified water bodies. In sulfidic/nonsulfidic environments, authigenic siderite can form and it can cooccur with greigite and pyrite in sulfidic environments [*Berner*, 1980; *Oldfield et al.*, 1992; *Roberts and Weaver*, 2005]. This will either increase or decrease the bulk magnetization of sediments depending on whether greigite or a nonferrimagnetic final product forms. *Stockhausen and Thouveny* [1999] examined the magnetic properties of last interglacial sediments from Lac du Bouchet, France, and from two neighboring lakes (Lac St. Front and Ribains maar lake). Even the Lac du Bouchet χ record, which provides an excellent detrital record of paleoclimate variations [*Thouveny et al.*, 1994], is partly attenuated by postdepositional magnetite dissolution. Poor correlation of χ records among the three lakes indicates strong local effects (e.g., dissolution and dilution effects) on the original climatically modulated detrital signal.

4.4. Biogenic Magnetic Minerals

[80] Biogenic magnetic minerals are found in animals [*Kirschvink and Gould*, 1981; *Wiltschko and Wiltschko*, 2005] (e.g., birds [*Beason et al.*, 1995; *Altringham*, 1996], bats [*Tian et al.*, 2010]), bees [*Kirschvink and Kirschvink*, 1991], fish [*Moore et al.*, 1990], termites [*Maher*, 1998; *Alves et al.*, 2004]), and humans [e.g., *Kirschvink et al.*, 1992; *Fuller et al.*, 1995; *Dubiel et al.*, 1999]. Biomagnetic material (e.g., ferritin) can also play an important role in disease [*Dobson and Grassi*, 1996; *Dobson*, 2001; *Brem et al.*, 2006]. In this review, we focus on organisms that are relevant for environmental magnetic studies of sediments.

[81] Biogenic processes can produce magnetic minerals in two major ways within sedimentary environments, namely biologically controlled mineralization (BCM) and biologically induced (BIM) mineralization [*Moskowitz*, 1995; *Bazylinski and Frankel*, 2004; *Faivre and Schüler*, 2008; *Kopp and Kirschvink*, 2008], respectively. BIM produces different iron oxide species (e.g., magnetite, goethite, lepidocrocite, and ferrihydrite) with a wide distribution of grain sizes [*Hesse and Stolz*, 1999; *Egli*, 2004a, 2004b]. Fine-grained greigite can also be produced by BIM processes, which are dominated by SP and a smaller proportion of SD particles [*Watson et al.*, 2000]. The wide distribution of grain sizes produced means that environmental records associated with BIM magnetic minerals are difficult to discern even if they dominate the magnetic assemblage. In contrast, BCM pathways produce stoichiometrically pure and morphologically distinct SD crystals (magnetosomes) of either magnetite [*Blakemore*, 1975; *Stolz et al.*, 1986; *Pósfai et al.*, 2006; *Li et al.*, 2010] (Figure 12) or greigite [*Mann*

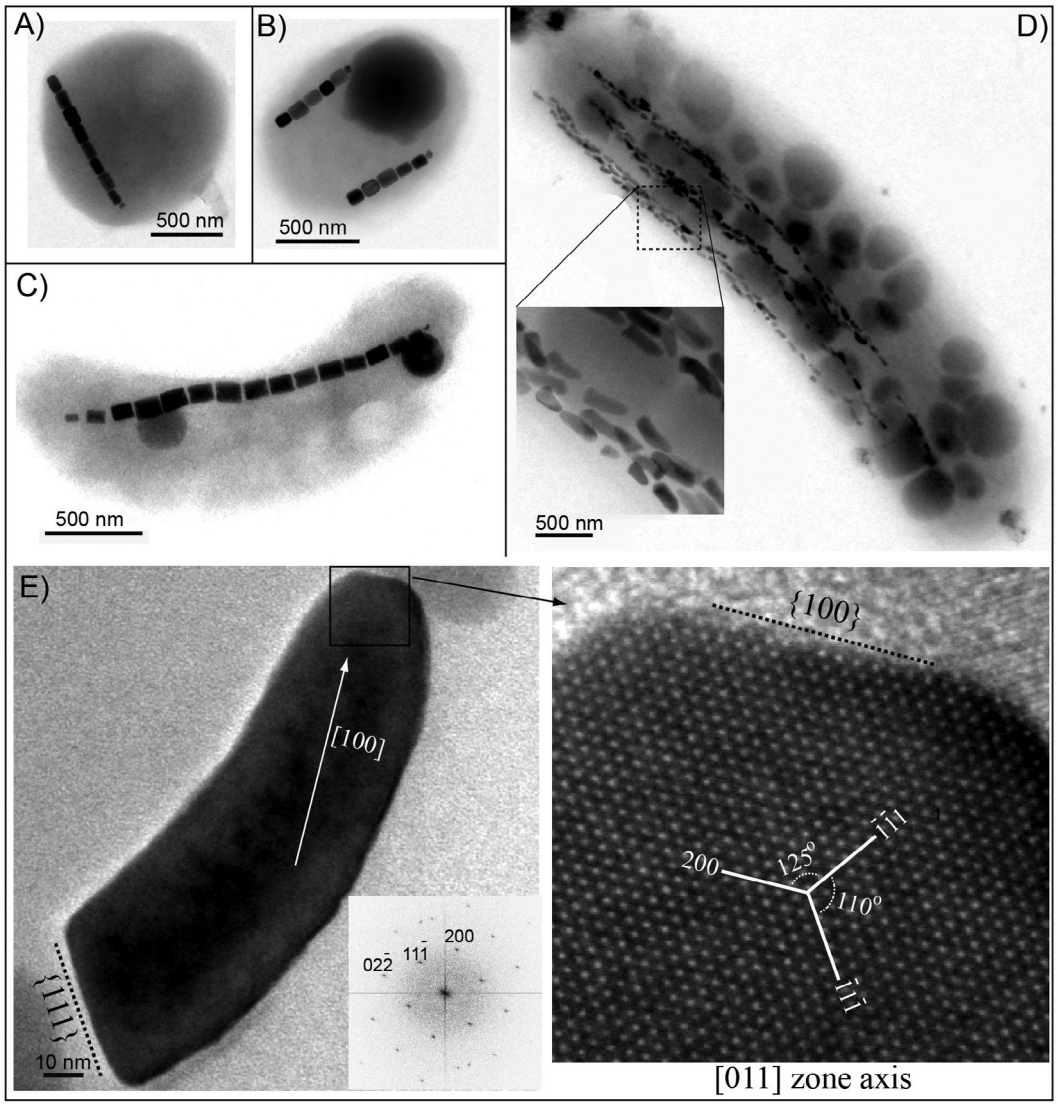

Figure 12. Magnetotactic bacteria detected from Lake Miyun in Beijing and their intracellular magnetite magnetosomes. (a) Magnetotactic coccus with single chain of prismatic magnetosomes. (b) Magnetotactic coccus with double chains. (c) Magnetotactic vibrio with single chain. (d) Rod-shaped magnetotactic bacterium (tentatively named MYR-1) with multiple chains of bullet-shaped magnetosomes. (e) High-resolution TEM image of bullet-shaped magnetosome within MYR-1. Unlike prismatic and cuboctahedral magnetite magnetosomes with [111] elongation and orientation, the bullet-shaped magnetosomes are formed by MYR-1 and are elongated along the [100] crystal direction of magnetite [*Li et al.*, 2010, also unpublished data].

et al., 1990; *Bazylinski et al.*, 1993; *Kasama et al.*, 2006] that are used by magnetotactic bacteria to navigate along geomagnetic field lines in search of appropriate redox boundaries around and below, respectively, the oxic-anoxic transition zone (OATZ) [*Bazylinski et al.*, 1993; *Kopp and Kirschvink*, 2008; *Moskowitz et al.*, 2008]. Much initial interest in magnetotactic bacteria stemmed from the potential role of fossil magnetosomes (magnetofossils) as carriers of the natural remanent magnetization in sediments [*Kirschvink*, 1983; *Stolz et al.*, 1986; *Snowball*, 1994]. Given the link between magnetotactic bacteria and specific redox and environmental conditions, magnetofossils are potential recorders of environmental variability [*Oldfield et al.*, 1992; *Lean and McCave*, 1998; *Yamazaki and Kawahata*, 1998; *Dinarès-Turell et al.*, 2003; *Faivre et al.*, 2008; *Kopp and Kirschvink*, 2008; *Li et al.*, 2010; *Roberts et al.*, 2011b; *Yamazaki*, 2012] and are useful markers of past biologic activity [*Arató et al.*, 2005; *Kopp and Kirschvink*, 2008; *Jiménez-López et al.*, 2010].

[82] In marine sediments, magnetotactic bacteria are found from shallow (coastal) marine settings down to and exceeding water depths of 4,500 m [*Stolz et al.*, 1986; *Petermann and Bleil*, 1993; *Hesse*, 1994; *Hesse and Stolz*, 1999; *Bazylinski and Frankel*, 2004; *Housen and Moskowitz*, 2006; *Faivre and Schüler*, 2008; *Kopp and Kirschvink*, 2008]. Despite the potential abundance of magnetosomes in modern marine sediments, reports of the occurrence of magnetofossils that dominate the magnetic

signal of ancient marine sediments have not been frequent because these fine particles are prone to dissolution upon burial [e.g., *Schwartz et al.*, 1997; *Kopp and Kirschvink*, 2008]. Studies of Quaternary marine sediments have shown that bacterial magnetite can carry a genuine syndepositional signal with changes in concentration and grain size linked to glacial-interglacial variations. Production of biogenic magnetite has been shown to decrease during glacial conditions in some settings in response to decreased oxygen contents in the pore waters, which likely resulted from a decrease in bottom water oxygenation and/or an increase in organic carbon supply [*Hesse*, 1994; *Lean and McCave*, 1998; *Dinarès-Turell et al.*, 2003]. Similarly, production of equidimensional with respect to elongated magnetosomes has been reported to be favored during periods of decreased organic carbon supply [*Hesse*, 1994; *Yamazaki and Kawahata*, 1998; *Yamazaki*, 2012], although other studies have shown the contrary relationship [*Lean and McCave*, 1998]. These studies imply that bacterial magnetite was produced at or above the sediment-water interface. However, some studies have shown that bacterial magnetite can be produced within the sediment column if redox conditions force the OATZ to be buried beneath the sediment-water interface. In this case, magnetofossils can be carriers of a bio(geo)chemical magnetization with an environmental signal that is younger than the host sediments [*Tarduno and Wilkison*, 1996; *Tarduno et al.*, 1998; *Abrajevitch and Kodama*, 2011]. Bacterial magnetite preservation indicates diagenetic conditions that enabled its preservation with ongoing sedimentation. Such environmental signals are typically linked to increased sediment accumulation rates or to changing paleoproductivity during Quaternary glacial-interglacial cycles [*Tarduno et al.*, 1998; *Abrajevitch and Kodama*, 2011]. Nevertheless, a major remaining difficulty in interpreting ancient magnetofossil records is disentangling the competing signals of magnetofossil productivity and preservation [*Hesse and Stolz*, 1999].

[83] A notable exception to the general lack of bacterial magnetite in pre-Quaternary sediments is the Paleocene-Eocene thermal maximum (PETM), which is one of the best ancient analogs for major global warming [*Zachos et al.*, 2001]. Several authors have demonstrated the widespread occurrence of biogenic magnetite in shallow PETM (<200 m water depth) sediments from the mid-Atlantic U.S. continental margin [*Lippert and Zachos*, 2007; *Kopp et al.*, 2007, 2009; *Schumann et al.*, 2008]. *Kopp et al.* [2009] hypothesized that magnetofossils preferentially accumulated near the mouth of a large tropical river in response to enhanced global warmth and humidity, which resulted in increased organic carbon and terrigenous supply to the continental shelf and thereby favored proliferation of magnetotactic bacteria. The striking coincidence of magnetofossils with PETM sediments suggests a preservation effect linked to establishment of a thick zone with suboxic diagenetic conditions, which resulted from a transient increase in sedimentation rates that isolated PETM sediments from underlying sulfidic sediments [*Dickens*, 2008; *Kopp et al.*, 2009]. If this is the case, magnetofossil abundances are unlikely to be reliable proxies of bacterial activity. Rather, they are more likely to be indicative of specific, transient diagenetic conditions in the sedimentary record. In deep marine settings, where iron is an essential limiting micronutrient for phytoplankton, optimal conditions for accumulation and preservation of magnetite magnetofossils have been suggested to be provided by the iron supplied by eolian dust [*Roberts et al.*, 2011b; *Larrasoaña et al.*, 2012]. Such iron fertilization would enhance primary productivity and subsequent export of organic carbon to the seafloor, thereby providing mild iron-reducing conditions that would release iron from the most reactive components of eolian dust to enable both growth and preservation of magnetofossils. The common report of magnetofossils alongside eolian dust [*Bloemendal et al.*, 1992; *Yamazaki and Ioka*, 1997b; *Dinarès-Turell et al.*, 2003; *Yamazaki*, 2009; *Abrajevitch and Kodama*, 2011] suggests a widespread link between magnetotactic bacteria and iron fertilization by eolian dust, although this mechanism will only apply in marine environments that are iron limited [*Roberts et al.*, 2011b].

[84] Greigite magnetosomes have been reported in marine sediments, within anoxic environments below the OATZ [*Bazylinski et al.*, 1993; *Vasiliev et al.*, 2008; *Kopp and Kirschvink*, 2008; *Lefèvre et al.*, 2011], although there have been few reports of greigite magnetofossils in the geological record. Greigite magnetofossils are expected to produce a delayed bio(geo)chemical magnetization, although the delay in recording should be small in rapidly deposited sediments where the OATZ can lie within the water column or at shallow depths within the sediment column.

[85] Magnetotactic bacteria have been reported near the sediment-water interface in lakes and swamps worldwide [*Hawthorne and McKenzie*, 1993; *Peck and King*, 1996; *Hesse and Stolz*, 1999]. In most lakes from temperate or semiarid climate zones, which often have high biologic productivity and sediment accumulation rates, anoxic conditions prevent preservation of magnetofossils upon burial [*Hesse and Stolz*, 1999]. In many high-latitude lakes, a combination of relatively small catchments with low relief, vegetated surfaces and seasonal ice cover limits detrital input and produces optimal conditions for magnetofossil formation and preservation in Late Pleistocene and Holocene sediments [*Snowball*, 1994; *Nolan et al.*, 1999; *Snowball et al.*, 1999, 2002; *Paasche et al.*, 2004; *Paasche and Løvlie*, 2011]. Variations in magnetofossil concentrations in such lakes can carry important paleoenvironmental information at glacial-interglacial to seasonal time scales, although the mechanisms linking climate and magnetofossil abundances remain a matter of discussion [*Paasche and Løvlie*, 2011].

4.5. Anthropogenic Pollution

[86] With development of new techniques during the past two decades, environmental magnetism has become increasingly mature. Relevant applications are not confined to analysis of sediments, but address an array of questions. Environmental magnetic methods have been widely used to investigate the degree, source, scope and temporal evolution of anthropogenic pollution related to industrial and other human activities [*Oldfield et al.*, 1985; *Maher and Thompson*, 1999;

Petrovský and Ellwood, 1999; *Muxworthy et al.*, 2001; *Evans and Heller*, 2003; *Horng et al.*, 2009]. There have been two main phases of pollution studies using magnetic approaches, as discussed below.

[87] The basic principles of the subject were established in the 1980s, including identification of linkages between magnetic properties and heavy metal concentrations, and recognition of the special morphology of anthropogenically produced magnetic particles [*Oldfield et al.*, 1985; *Maher and Thompson*, 1999]. For example, magnetic spherules produced during fossil fuel combustion and during iron or steel production [*Heller et al.*, 1998] are clearly distinguishable from their natural counterparts. Generally, magnetic minerals of industrial origin have larger grain sizes than natural magnetic minerals, and therefore have lower ARM/SIRM ratios. Winnowing of larger particles means that ARM/SIRM systematically increases downwind. For most cases related to fossil fuel combustion, there is a positive correlation between magnetic mineral concentration and that of heavy metals (e.g., Pb, Zn, Cu, Co, Ni) in pollutants [*Heller et al.*, 1998]. Magnetic minerals can act as pollutant carriers through adsorption [*Rose and Bianchi-Mosquera*, 1993], and by structural incorporation of heavy metals into the mineral [*Cornell and Schwertmann*, 2003]. Thus, it is practical to semiquantify the degree of pollution using magnetic parameters at a local (regional) scale.

[88] The last decade has seen rapid progress in magnetic studies of pollution. One reason for progress is the ease of access to materials for such studies. While early studies focused more on lake or river surface sediments [e.g., *Oldfield et al.*, 1985], recent studies have extended their scope to a wide range of materials including tree leaves [*Matzka and Maher*, 1999; *Moreno et al.*, 2003; *Hanesch et al.*, 2003; *Lehndorff et al.*, 2006; *Maher et al.*, 2008; *Szönyi et al.*, 2008], tree rings [*Zhang et al.*, 2008], tree bark [*Huhn et al.*, 1995], tree roots [*Jordanova et al.*, 2003], grass [*Hoffmann et al.*, 1999; *Jordanova et al.*, 2003], air filters [*Muxworthy et al.*, 2001; *Sagnotti et al.*, 2006], roads and roadside dusts [*Hoffmann et al.*, 1999], subway dusts [*Zhang et al.*, 2011], fly ashes [*Blaha et al.*, 2008], soils [*Hanesch and Scholger*, 2002; *Blundell et al.*, 2009a], and other materials. For example, because of their large total surface area and wide distribution, tree leaves are excellent media for particle collection. Tree leaves also provide a nonmagnetic background for collecting particles and leaf wax helps leaves to trap and retain particulate pollutants. Furthermore, consistency can be achieved by using the same deciduous tree species with leaves of the same age [*Maher et al.*, 2010].

[89] Progress in pollution-related environmental magnetic studies has been driven by focus on local (regional) studies [*Blundell et al.*, 2009a] (Figure 13) on seasonal (or yearly) time scales, although large-scale mapping of anthropogenic inputs has also been conducted [*Hay et al.*, 1997; *Hanesch and Scholger*, 2002]. For example, local studies have been carried out around iron and steel plants [e.g., *Strzyszcz et al.*, 1996], or along streets or highways [e.g., *Moreno et al.*, 2003]. Compared to the complications of lake and marine sediments, the provenance of pollution and the transportation pathways are often well defined. The techniques for identifying and quantifying the degree of pollution using magnetic techniques are well established, therefore studies of subnational or national soil data sets [*Boyko et al.*, 2004; *Fialová et al.*, 2006; *Hanesch et al.*, 2007; *Blundell et al.*, 2009a] have focused on determining larger scale pollution patterns using statistical methods [*Blundell et al.*, 2009b]. For these larger-scale studies, regional differences in pedogenic processes must be considered to enable discrimination of pollution signals from the highly magnetic soil background [e.g., *Dearing et al.*, 1996]. A second branch of studies has aimed at constructing time series for environmental monitoring [*Kim et al.*, 2007] to determine spatiotemporal variations in pollution patterns. The largest magnetic anomalies can be easily detected, but the exact nature of pollution needs to be further investigated by other more diagnostic techniques.

[90] The benefits of magnetic detection of pollution are its speed, cost effectiveness and sensitivity to a particle size range of recognized hazard to human health (i.e., particulate matter $\leq$10 μm, known as PM10), while its major weakness is that magnetic properties are not necessarily related to the concentration of any toxins (e.g., Pb). Thus, while environmental magnetism can be used to detect a wide range of pollutants, it is best suited to detecting particulates that represent a respiratory hazard. There is considerable scope for future work in this area. In other situations, magnetic methods can be used to detect pollution "hot spots" that can then be investigated in more detail with more expensive and time consuming, but more immediately diagnostic, techniques for assessing human health or other hazards. To make progress with magnetic monitoring of pollution, it will be important to become more multidisciplinary, with input from toxicology, epidemiology, geographic information systems, environmental statistics, and with involvement of local authorities to develop meaningful strategies to mitigate the effects of pollution.

5. AMBIGUITIES OF MAGNETIC PARAMETERS AND INTERPRETATIONS

[91] As summarized above, magnetic parameters have been widely used to address environmental questions. *Dekkers* [1997] briefly listed several drawbacks of using magnetic parameters (e.g., the nonuniqueness of some parameters and the complexities of mixed magnetic mineral assemblages). Nevertheless, nonuniqueness in interpretation of magnetic parameters in terms of environmental processes is often neglected. Linking magnetic parameters to natural processes requires detailed consideration of such ambiguities.

5.1. Inherent Complexities of Magnetic Parameters in Monomineralic Magnetic Assemblages

[92] Even when magnetic properties are dominated by a single magnetic phase, multiple factors, including domain state, measurement frequency, magnetic interactions, impurities, etc., will affect the magnetic properties. We consider such variables below.

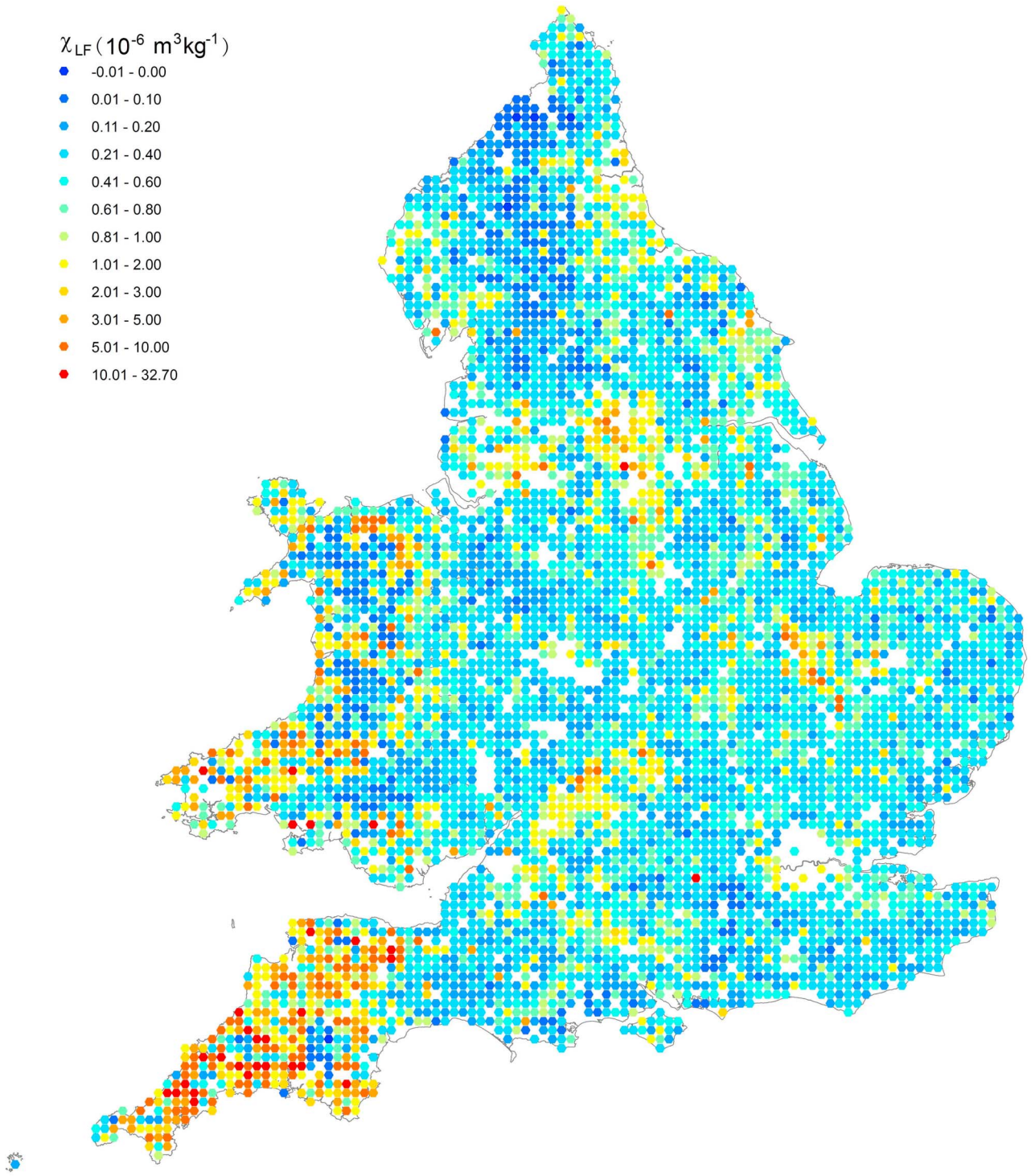

Figure 13. Distribution of magnetic susceptibility values for soils from England and Wales. Spatial variations in χ values indicate potential variations in geological setting. (Reprinted from *Blundell et al.* [2009a], with permission from Elsevier.)

5.1.1. Domain State

[93] As mentioned earlier, mineral magnetic properties systematically change with respect to domain state. Many magnetic properties of SP and MD particles are frustratingly similar. For example, both SP and MD particles have higher χ values than SD and fine-grained PSD particles, although the intrinsic magnetic behavior of SP and MD particles is different. If the magnetic mineral concentration of a sample is constant, a χ enhancement could be due to either the presence of more SP particles (e.g., paleosols from the CLP, which are dominated by pedogenic processes) or to a coarsening of grain size to PSD or MD particles (e.g., paleosols from Siberia, which are controlled by wind dynamics). A solution to this problem is to determine the grain size distribution of

the magnetic mineral assemblage. If the fine-grained particles have a relatively broad grain size distribution spanning both SP and SD particles, χ_{fd}% is useful for detecting viscous SP particles near the SP/SD threshold size (~20–25 nm for magnetite) (Figure 6). A positive correlation between χ_{fd} and bulk χ indicates that the bulk χ is controlled by the concentration of these fine particles rather than by variations in grain size. However, χ_{fd} (or χ_{fd}%) is not sensitive to extremely fine particles (e.g., <10 nm) because the χ of these SP particles is independent of measurement frequency. Low-temperature (<300 K) χ_{fd} measurements are needed to detect such grains [*Worm and Jackson*, 1999; *Liu et al.*, 2005a; *Jackson et al.*, 2006; *Egli*, 2009]. However, such sophisticated rock magnetic measurements are not widely accessible. In this case, combined measurement of χ_{fd}, χ/M_s, correlation between ARM and χ, and the timed viscous decay of IRM are suggested to deduce the possible presence of SP particles.

[94] Coarse PSD and MD particles often have a χ_{fd} peak at ~50 K due to relaxation of domain walls in magnetite or titanomagnetite [*Šimša et al.*, 1985; *Radhakrishnamurty and Likhite*, 1993; *Moskowitz et al.*, 1998; *Skumryev et al.*, 1999; *Kosterov*, 2003; *Lagroix et al.*, 2004], which can be confused with signatures due to SP particles with sizes of several nm. Such a peak has been observed for soil samples from Argentina. *Liu et al.* [2010] found that this peak is resistant to the CBD reagent, which dissolves submicron pedogenic ferrimagnets. This strongly indicates that the 50 K χ_{fd} peak in Argentinian soils is not caused by extremely fine SP particles, and thus excludes a special formation mechanism for such unusual pedogenic particles, which are not observed elsewhere. Instead, it appeared to be associated with coarse lithogenic material.

[95] ARM also depends strongly on domain state. By definition, SP particles cannot carry a remanence. However, natural samples almost always have a grain size distribution (e.g., a lognormal distribution), thus ARM does not respond uniformly to changes in average magnetic grain size. SD particles have the highest ARM per unit mass. Therefore, ARM has been widely used as a proxy for the SD particle concentration. However, when the concentration of PSD/MD particles is also significant, their contributions to the ARM of bulk samples cannot be neglected. In this case, the ARM remaining after AF demagnetization at 20 mT can efficiently eliminate the effects of PSD/MD particles. Equally, a partial ARM (pARM) imparted with an AF >20 mT is superior to the ARM alone for semiquantifying the concentration of SD particles [*Liu et al.*, 2005d].

[96] Beside concentration-dependent magnetic parameters, bivariate ratios are designed to cancel the effects of magnetic mineral concentration, and enhance the signal due to variations in grain size. The most popular ratios are χ_{ARM}/χ, ARM/SIRM, χ/M_s, M_{rs}/M_s, and χ_{fd}/χ. Ambiguities in interpreting these ratios arise in two ways. First, inherent ambiguities for a single parameter (e.g., χ and ARM) can be inherited by the ratio. Second, the ratio can be modulated by the denominator. Bivariate plots can help to unravel such effects and identify magnetic grain size variations. For example, linear correlation between two magnetic parameters, say χ_{ARM} and χ, indicates that the grain size distribution is constant for the magnetic particles that contribute to χ_{ARM} and χ. In contrast, changes in χ_{ARM}/χ can indicate variations in the grain size of magnetic minerals.

[97] Similarly, χ_{fd}/χ (or χ_{fd}%) is inherently related more to the grain size distribution than to the magnetic mineral concentration [*Worm*, 1998]. For example, pedogenically produced ferrimagnetic nanoparticles in paleosols from the CLP have a fixed grain size distribution with peak grain size of 20–25 nm, which coincides with the SP/SD boundary for maghemite [*Liu et al.*, 2004c, 2005a, 2007a]. This can be clearly demonstrated by linear correlation between χ_{fd} and χ for samples across a loess to paleosol transition. However, χ_{fd}% also gradually increases with increasing pedogenesis in incipient soils. Assuming that χ_{fd}% for a bulk sample is caused only by changes in the grain size distribution can lead to the faulty conclusion that the grain size distribution of the pedogenic maghemite is narrower for more mature paleosols. Such an apparent contradiction results also from neglecting the effects of the lithogenic background signal [*Liu et al.*, 2004c].

5.1.2. Isomorphous Substitution

[98] Fe in magnetic minerals is often isomorphously substituted (e.g., by Ti or Al within the crystal lattice). Titanomagnetites are practically regarded as a new class of mineral rather than as Ti-substituted magnetite. Thus, confusion between magnetite and titanomagnetite has been well resolved. However, ambiguities remain for hematite and goethite. These minerals are treated as high-coercivity minerals, but in reality both have a wide range of coercivities [e.g., *Roberts et al.*, 2006]. The coercivity of stoichiometric goethite can be higher than several tens of Tesla [*Rochette et al.*, 2005]. However, because of its low T_N (~120°C), T_N sharply decreases with increasing Al content, and the coercivity decreases accordingly. When T_N approaches room temperature, Al-goethite is paramagnetic, and by definition, the coercivity will be zero. *Liu et al.* [2007b] found that when the Al content is >~13–15 mol% (a reasonable value for Al-goethite in soils), the room temperature coercivity of Al-goethite is <100 mT, which is comparable to that of magnetite. Hematite also has a complicated response to Al substitution. The T_N of hematite is 680°C, therefore effects associated with the reduced T_N due to Al substitution are less important. Nevertheless, Al substitution still affects the coercivity in two ways: by changing internal stress and the size of the unit cell. Initial substitution of Al increases the internal stress of Al hematite, which enhances coercivity. However, with further Al substitution, the unit cell size decreases and the grain size of Al-hematite systematically shrinks, which results in reduced coercivity. As the grain size decreases below 20–30 nm, the SP/SD threshold size for pure hematite [*Banerjee*, 1971], the coercivity of Al hematite approaches zero (i.e., it becomes superparamagnetic).

[99] The large coercivity range of Al-hematite with respect to Al content also strongly affects parameters such as HIRM and S ratio, which have been widely used to trace the "absolute" and "relative" concentration of hematite and goethite, respectively. Clearly, these two parameters cannot detect either pure goethite (extremely high coercivity) or Al-goethite with Al content >13–15 mol% (low coercivity,

<100 mT). HIRM for Al-hematite and goethite correlates positively with bulk coercivity [*Liu et al.*, 2007b]. Thus, these two parameters can only be interpreted in a conventional way when the hardness parameter (L ratio) remains constant. Combined interpretation of HIRM (S ratio) with the L ratio is highly recommended.

5.1.3. Magnetic Interactions

[100] In most environmental magnetic studies, magnetic parameters are interpreted by assuming a negligible influence from magnetostatic interactions among magnetic particles. However, magnetostatic interactions can have an important influence on the magnetic properties of SP/SD grains. *Sugiura* [1979] demonstrated that ARM/SIRM decreases with increased magnetite concentration. *Yamazaki and Ioka* [1997a] found that ARM/χ is related to magnetic mineral concentration in Pacific Ocean sediments. This strongly indicates that the effects of magnetic interactions on ARM/χ should be considered to enable accurate interpretation of this ratio as a grain size proxy and to use ARM as a reliable magnetic concentration-dependent parameter for estimating relative geomagnetic paleointensities [*Yamazaki*, 2008].

[101] On the basis of numerical simulations, *Muxworthy et al.* [2004] confirmed that interacting SD particles exhibit more MD-like behavior, which indicates that the SD particles become magnetically softer than their noninteracting counterparts. In contrast, interactions among SP particles efficiently increase their magnetic anisotropy and they become more SD-like, resulting in a sharp drop in χ_{fd} values [*Muxworthy*, 2001]. Similarly, PSD magnetite particles with grain sizes >100 nm also become more magnetically stable under the effect of magnetic interactions, e.g., shifting hysteresis parameters from PSD to SD values [*Muxworthy et al.*, 2003].

[102] To detect the effects of magnetic interactions, there are three main approaches: (1) determination of the Wohlfarth *R* value of *Cisowski* [1981], (2) investigating the interaction field distribution parallel to the *y* axis of a FORC diagram [*Pike et al.*, 1999; *Roberts et al.*, 2000; *Muxworthy et al.*, 2004], and (3) assessing any correlation between ARM/χ (or ARM/SIRM) and magnetic mineral concentration [*Yamazaki and Ioka*, 1997a; *Yamazaki*, 2008]. Noninteracting SD particles have an *R* value of 0.5; magnetic interactions reduce the *R* value [*Cisowski*, 1981]. However, interpretation of *R* values <0.5 becomes ambiguous because such values can be produced by non-SD behavior as well as by magnetic interactions. The effects of magnetic interactions can also be expressed by a broadened distribution along the *y* axis in FORC diagrams. For example, such a pattern is indicated by strongly interacting greigite particles in natural samples [*Roberts et al.*, 2006]. *Pike et al.* [1999] demonstrated that FORC diagrams are quantitatively much more sensitive to detection of magnetic interactions than approaches similar to those of *Cisowski* [1981]. Finally, negative correlation between ARM/χ and magnetic mineral concentration has been used to detect magnetic interactions [*Yamazaki and Ioka*, 1997a; *Yamazaki*, 2008]. However, the North Pacific sediments on which these parameters have been used contain mixed magnetic mineral assemblages and it is not clear that the magnetically interacting component is the same as the strongly magnetic component in these sediments. Such possibilities are much more clearly discerned using FORC diagrams. Each of these lines of evidence can potentially be used to indicate magnetic interactions, although caution is needed to avoid misinterpretation of the presence or absence of interactions in environmental studies. FORC diagrams provide the most robust means of estimating magnetic interactions [*Pike et al.*, 1999].

5.2. Resolving Ambiguities Associated With Environmental Processes

[103] Ambiguities inherent to magnetic parameters can be resolved using sophisticated magnetic measurement and data analysis techniques. For mixed magnetic mineral assemblages, separation of magnetic signals (section 2.2) is crucially important. However, there remain additional barriers to uniquely linking magnetic parameters to environmental processes. Unlike climatic proxies that can be quantitatively linked to environmental processes (e.g., oxygen isotopes), magnetic parameters often provide only semiquantitative information in terms of shifts in the balance between two contrasting climatic states. In most contexts, magnetic properties are related to climate through a range of potentially interacting environmental processes. From source to deposition, magnetic minerals released from rocks by weathering experience tectonic, environmental, and climatic processes that transport and alter the minerals. For example, grain size variations in eolian PSD/MD magnetite from the CLP can be related either to changes in the distance from source or wind strength, or both. More detailed information is needed to distinguish between such processes. Furthermore, magnetic minerals in natural samples can have multiple origins that are related to different processes. For example, the χ signal of marine sediments from ODP Site 882 in the North Pacific Ocean was initially interpreted as an IRD signal [e.g., *Haug et al.*, 1995]. However, recent work has demonstrated that the χ variations are caused more by eolian and volcanic inputs [*Bailey et al.*, 2011]. Finally, postdepositional processes can alter lithogenic magnetic minerals to different extents, thereby obscuring the original environmental signals.

[104] Interpretation of rock magnetic data in many contexts requires evaluation of possible links between sources and deposited materials. Several processes may make this unreliable if measurements are only performed on bulk samples [*Oldfield et al.*, 2009]. These processes include hydrodynamic sorting and winnowing during transportation, postdepositional alteration and pedogenesis, and contributions from biogenic magnetic minerals. While care is needed to resolve such ambiguities, the techniques outlined above can assist researchers to reach robust environmental conclusions.

6. FUTURE OF ENVIRONMENTAL MAGNETIC STUDIES

6.1. General Environmental Magnetism

[105] All materials exhibit a magnetic response to an applied field, so magnetic parameters can be used to investigate many natural materials and processes (climatic and

environmental change, and a wide range of geological processes). However, as discussed above, interpretation of magnetic parameters is often complicated. Contributions of magnetism to climatic and environmental studies vary with context, site, and research focus. For example, in studies of Chinese loess and paleosol sequences, magnetic parameters have played a leading role in understanding the spatial-temporal evolution of the Asian Monsoon. To improve the significance and objectivity of environmental magnetic studies, it is important to differentiate between contexts in which magnetic properties provide useful proxies of environmental processes, and those in which magnetic measurements are complementary to and help to qualify, refine or reinforce evidence from other methods. In many contexts, it is more appropriate to base reconstructions of climate forcing on the best available proxies (e.g., stable isotopes, fauna, flora, etc.), and to use magnetic properties to help quantify the effects of climate change, although in complex environmental systems, separation between cause and effect is not always straightforward.

[106] When new environments, applications, time scales and archives are under investigation, magnetic parameters need to be studied alongside a wider range of environmental or climatic parameters. Such an interdisciplinary approach involves not only a combination of magnetic and nonmagnetic proxies, but also thorough discussion among different specialists. For example, it took more than a decade to determine the exact mechanism of the χ enhancement for CLP paleosols [*Zhou et al.*, 1990; *Liu et al.*, 2007a]. Such efforts are equally important for lake sediments because of the complex magnetic mineral assemblages and the wide range of processes that can affect magnetic parameters. Therefore, the main benefits of environmental magnetism in the near future are likely to come from applications in interdisciplinary contexts. For example, when tracing eolian inputs into marine sediments, the hard fraction of magnetic remanences, DRS, geochemical parameters (e.g., Ti/Al), and mineralogical studies of nonmagnetic constituents (e.g., clay minerals, quartz) can combine powerfully to detect eolian materials and identify their sources. It will be essential to continue to develop additional analytical and statistical techniques. Further studies of hematite and goethite are needed. Unless the provenance and intrinsic magnetic properties of these minerals are invariant, proxies for the "hard" magnetic mineral concentration can be variable. The DRS technique seems to have potential for characterizing and quantifying the concentration of these minerals, particularly when using quantitative spectral unmixing techniques [e.g., *Heslop et al.*, 2007]. Nevertheless, DRS spectra are also strongly affected by Al substitution [*Liu et al.*, 2011], so more robust understanding is needed of such effects to enable conversion of DRS measurements into hematite and goethite concentrations.

[107] Future studies are likely to involve transitional locations between different bioclimatic zones. In order to provide more robust environmental interpretations, and to avoid misinterpretations, adopting a source-to-sink approach (e.g., for lake and marine sediments) will be especially important. By doing so, site locations can be more accurately selected to minimize environmental variables in the source area and therefore to understand environmental signals in terms of climate variability.

[108] The power of environmental magnetism lies in the advantages it confers over other methods. Magnetic measurements are generally rapid and, therefore, large, high-resolution data sets can be obtained relatively easily, especially for bulk samples. Environmental magnetism is therefore well suited to rapid pollution monitoring at local or national scales, and to large-scale monitoring of other processes, e.g., dust transportation [*Maher et al.*, 2010]. Magnetic properties also vary significantly even for nano-sized particles. Therefore, magnetic parameters have the power to characterize magnetic mineral assemblages in ways that provide important insights into environmental sources and processes. Moreover, magnetic measurements have the power to do this at concentrations that lie well below the measurement threshold for conventional mineralogical (e.g., XRD) and geochemical techniques. Finally, subtle relationships between ferrimagnetic and antiferromagnetic minerals in low concentrations can be investigated quantitatively, which cannot be easily achieved with other methods.

6.2. Future Studies of Loess and Soils

[109] Future environmental magnetic studies of loess and paleosol sequences need to resolve two important issues. First, the formation and transformation mechanisms of magnetic minerals during pedogenesis need further study. Second, detailed exploration of the paleoclimatic implications of loess magnetism, especially in the context of global climate change and its regional expression, is needed. Concerning the first issue, the fundamental question is why so little magnetite/maghemite is produced in soils that dry seasonally but that remain moist long enough to produce Fe^{2+}. Mediterranean soils that are imperfectly drained (so that Fe^{2+} is produced in winter) contain goethite but little hematite and maghemite. Therefore, magnetic mineral transformations during pedogenesis need further study. Another complexity arises from the fact that in some environments, magnetic properties may (partially) reflect conditions that prevailed under previous climatic regimes (e.g., terra rossa soils in Mediterranean climates). Intermediate magnetic phases produced during pedogenesis may not exist, therefore, analysis of combined mineralogical and/or magnetic data with respect to climatic factors (e.g., Hm/Gt and Hm/Mag versus temperature and precipitation) provide practical tests of proposed magnetic mineral formation mechanisms either from laboratory or model simulations. Concerning the second issue, comparison of loess and other eolian records from around the world will not only help to distinguish between global and local driving mechanisms, but it will also contribute to improving our understanding of atmospheric changes on a global scale [e.g., *Roberts et al.*, 2011c]. Finally, provenance studies of loess are essential to generate comprehensive models for transport and postdepositional alteration.

6.3. Future Studies of Other Continental Sediments

[110] Lakes have advantages in recording local signals that can be put into historical context in relation to human activities. Continued emphasis is expected on paleoenvironmental and paleomagnetic studies. We consider that studies of fluvial and alluvial sediments will also become increasingly important because they have the potential to provide records of environmental variability in continental regions (e.g., the semiarid climatic belt) and periods (e.g., Neogene and Quaternary) that typically demand a multiproxy approach. They will also be relevant for source-to-sink studies aimed at interpreting sedimentary records in marine and lacustrine environments. Loose surface sediments located in deflated areas and ice from ice caps and mountain glaciers also have potential for eolian source-to-sink studies. Environmental magnetism of speleothems is also likely to be a growth area in the near future.

6.4. Future Studies of Marine Sediments

[111] Riverine supply has been under-studied compared to other terrigenous sediment sources despite the important role of rivers in the cycling of iron and carbon [*Raiswell et al.*, 2006]. Environmental magnetic studies of sediment drifts can provide important insights into the evolution of thermohaline circulation and the configuration and functioning of ocean gateways. For both riverine supply and sediment reworking by bottom currents, careful selection of study sites and an accurate knowledge of source areas are especially relevant. In the case of terrigenous material supplied by ice, it is expected that future environmental magnetic studies will provide new insights into the extent and dynamics of ice caps not only during the Neogene and Quaternary but also during previous "ice house" periods and to assess the presence of smaller ice bodies during greenhouse periods [e.g., *Eldrett et al.*, 2007]. Most current knowledge on past "ice house" periods, especially prior to the Paleogene, is based on studies of coarse-grained, diamicton-type sediments [*Eyles*, 1993]. By studying coeval, and much more volumetrically important, fine-grained, IRD-bearing sediments, environmental magnetic studies should be able to provide new insights into the extent and dynamics of ancient ice caps. Antarctica has been permanently glaciated since the earliest Oligocene [e.g., *Zachos et al.*, 2001], as demonstrated by IRD layers in peri-Antarctic marine sediments that accumulated at those times [*Ehrmann and Mackensen*, 1992; *Williams et al.*, 2010]. Records of IRD deposition are expected to exist just south of the present polar front (around 50°S), therefore environmental magnetic studies of circum-Antarctic marine sediments might provide important information on Antarctic ice sheet dynamics [*Kanfoush et al.*, 2002].

[112] Atmospheric dust is an important driver and indicator of climate change, yet knowledge of its global role during the Quaternary (let alone older periods) remains poor [*Maher et al.*, 2010]. It is, therefore, expected that environmental magnetic studies of eolian dust in marine sediments will increase in frequency, especially considering the usefulness of magnetic minerals in identifying eolian dust and assessing the environmental variables that drive its formation. Additionally, eolian dust has often been reported to occur alongside biogenic magnetite [*Bloemendal et al.*, 1992; *Yamazaki and Ioka*, 1997b; *Dinarès-Turell et al.*, 2003; *Yamazaki*, 2009; *Abrajevitch and Kodama*, 2011; *Roberts et al.*, 2011b; *Larrasoaña et al.*, 2012]. Although potential links between dust and magnetotactic bacteria have not been studied in detail, their frequent cooccurrence suggests a causal link via dust as a provider of reactive iron for biomineralization [*Roberts et al.*, 2011b; *Larrasoaña et al.*, 2012]. Given the common link between bacterial magnetite and transient changes in redox conditions, better understanding of factors that control formation and preservation of bacterial magnetite in the marine sedimentary record is likely to be obtained by studying transient warming periods such as Paleogene hyperthermal (e.g., the PETM) and Mesozoic oceanic anoxic events (OAEs).

[113] Concerning postdepositional diagenetic changes, reductive dissolution of magnetic minerals and authigenic formation and preservation of greigite is expected to be increasingly used to signal variations between anoxic and oxic conditions, whether they are related to changes in sea ice cover (at high latitudes), ventilation of bottom waters (especially in semienclosed basins), in transient accumulations of organic-rich (e.g., sapropel-like) sediments, or to variations in the supply of riverine input, among many other cases. An additional prospective application of environmental magnetism is the signaling of the past presence of gas hydrates in ancient marine sediments by the cooccurrence of late diagenetic pyrrhotite and greigite [e.g., *Housen and Musgrave*, 1996; *Larrasoaña et al.*, 2007; *Enkin et al.*, 2007; *Roberts et al.*, 2010]. Such studies could shed new light on events where gas hydrate stability has played a major role in driving or responding to climate change. One such event is the PETM, when an inferred sudden dissociation of gas hydrates resulted in a massive carbon cycle perturbation that drove a period of global warming [*Zachos et al.*, 2001].

[114] Potential targets for environmental magnetic studies of oxic postdepositional diagenesis are the so-called Cretaceous oceanic red beds, which are marine sedimentary rocks that occur between OAEs. These sediments record most of the climate variability during the progressive Middle to Late Cretaceous global cooling, but they have not been well studied until recently [*Wang et al.*, 2011]. Cretaceous oceanic red beds have been reported to host early diagenetic hematite and goethite in response to changes in the supply of organic carbon to the seafloor and bottom water oxygenation [*Li et al.*, 2011]; they therefore appear to be highly suitable for environmental magnetic analysis.

6.5. Future Studies of Biogenic Magnetic Minerals

[115] Future studies of biomagnetism are likely to focus on fundamental issues: reliable identification of biogenic magnetic minerals, biomineralization processes, and determination of environmental information from biogenic magnetic minerals. Magnetic criteria for identification of biogenic magnetite have been proposed, e.g., the low-temperature

Moskowitz test [*Moskowitz et al.*, 1993] and the typical noninteracting SD pattern in FORC diagrams [*Egli et al.*, 2010], but these may not guarantee correct identification, in part because magnetosome chains can collapse or oxidize [*Li et al.*, 2010; *Kind et al.*, 2011]. To help constrain biotic or abiotic origins of magnetic minerals, measurement of iron isotopes [*Anbar et al.*, 2000] could prove useful by helping to determine the iron isotopic values associated with the two processes. To understand dynamic biomineralization processes, it is necessary to determine how environmental factors control magnetosome formation. Likewise, the ability to use magnetofossils with different morphologies to interpret paleoenvironmental records will require detailed understanding of modern environments and the locations of the habitats of different magnetotactic bacteria species within local redox gradients. A positive side benefit of research on magnetic biomineralization is the potential for contributing to basic rock magnetism. For example, *Cao et al.* [2010] synthesized ideal noninteracting nano-sized magnetoferritin with a narrow grain size distribution using the recombinant human H chain ferritin. Such materials can provide a better understanding of superparamagnetic systems, which are important for environmental magnetic studies.

7. CONCLUSIONS

[116] Environmental magnetism has developed considerably over the past 30 years so that it is now a sophisticated, quantitative discipline. With maturation of the subject, increasingly advanced measurement and data analysis techniques, and better understanding of the magnetic properties of an increasingly wide range of materials, environmental magnetism is well positioned to continue to address many important questions. Challenges remain in resolving ambiguities when interpreting magnetic properties, and in addressing complex environmental questions, but the armory of tools available to address such issues is large and expanding. Overall, we foresee a highly promising future for environmental magnetism within an interdisciplinary context that is likely to lead to the growing importance of magnetism in the environmental sciences.

NOTATION

Summary of the acronyms of major terms used in this paper.

χ (κ)	magnetic susceptibility, mass-specific (volume-specific)
χ_{para}	χ of paramagnetic minerals within a sample
χ_{high}	high-field χ taken from the high-field slope of a hysteresis loop
χ_{ferri}	χ of ferrimagnetic minerals within a sample $\chi_{ferri} = \chi - \chi_{high}$
χ_{fd}	frequency-dependent susceptibility, χ_{fd} (= $\chi_{lf} - \chi_{hf}$), where χ_{lf} and χ_{hf} are χ measured at low- and high-frequency, respectively
$\chi_{fd}\%$	$\chi_{fd}/\chi_{ferri} \times 100\%$
AF	alternating field
DC	direct current
H, B	magnetic field, *H* in A/m, and *B* in T
ARM	anhysteretic remanent magnetization
χ_{ARM}	ARM normalized by the magnitude of the DC field used during ARM acquisition
IRM	isothermal remanent magnetization
SIRM (M_{rs})	saturation isothermal remanent magnetization (M_{rs} is equivalent and is obtained from hysteresis measurements)
HIRM	the "hard" (or high-field) IRM calculated as HIRM = (SIRM + $IRM_{-0.3\ T}$)/2, where $IRM_{-0.3T}$ is the IRM remaining after exposure to a reversed field of −0.3 T following acquisition of a SIRM
NRM	natural remanent magnetization
S ratio	S = ($-IRM_{-0.3\ T}$/SIRM)
L ratio	L ratio (= (SIRM + $IRM_{-0.3\ T}$)/(SIRM + $IRM_{-0.1\ T}$))
Hm/Mag	the ratio of the concentration of hematite to maghemite/magnetite
SD	single domain
SP	superparamagnetic
PSD	pseudo single domain
MD	multidomain
Coercive force	H_c in A/m, and B_c in T
Coercivity of remanence	H_{cr} in A/m, and B_{cr} in T
M_s	saturation magnetization
T_C	Curie temperature
T_N	Néel temperature
T_b	blocking temperature
T_V	Verwey transition temperature (∼120–122 K) for magnetite
T_M	Morin transition temperature (∼250 K) for hematite
BCM	biologically controlled mineralization
BIM	biologically induced mineralization
CBD	citrate-bicarbonate-dithionite
CLP	Chinese Loess Plateau
DRS	diffuse reflectance spectroscopy
FORC	first-order reversal curve
HE	Heinrich event
IRD	ice-rafted debris
OATZ	oxic-anoxic transition zone
OAE	oceanic anoxic event
PETM	Paleocene-Eocene thermal maximum

XMCD	X-ray magnetic circular dichroïsm
XAS	X-ray absorption spectrum

[117] **ACKNOWLEDGMENTS.** We are grateful for instructive discussions with J. Dearing, J. Torrent, D. Heslop, C. Zhang, X. Zhao, Z. Jiang, Z. Duan, K. Ge, C. Kissel, and C. Laj. This study was supported by the National Natural Science Foundation of China (grants 41025013, 40974036, and 40821091), by the Australian Research Council (grant DP110105419), and by the U.S. National Science Foundation (grant EAR1013192).

[118] Mark Moldwin thanks the reviewers for their assistance in evaluating this paper.

REFERENCES

Abrajevitch, A., and K. Kodama (2011), Diagenetic sensitivity of paleoenvironmental proxies: A rock magnetic study of Australian continental margin sediments, *Geochem. Geophys. Geosyst.*, *12*, Q05Z24, doi:10.1029/2010GC003481.

Abrajevitch, A., R. Van der Voo, and D. K. Rea (2009), Variations in relative abundances of goethite and hematite in Bengal Fan sediments: Climatic vs. diagenetic signals, *Mar. Geol.*, *267*, 191–206, doi:10.1016/j.margeo.2009.10.010.

Akimoto, S. (1962), Magnetic properties of FeO-Fe_2O_3-TiO_2 system as a basis of rock magnetism, *J. Phys. Soc.*, *17*, 706–710.

Alt-Epping, U., J. B. W. Stuut, D. Hebbeln, and R. Schneider (2009), Variations in sediment provenance during the past 3000 years off the Tagus River, Portugal, *Mar. Geol.*, *261*, 82–91, doi:10.1016/j.margeo.2008.11.008.

Altringham, J. D. (1996), *Bats: Biology and Behaviour*, Oxford Univ. Press, Oxford, U. K.

Alves, O. C., E. Wajnberg, J. F. de Oliveira, and D. M. S. Esquivel (2004), Magnetic material arrangement in oriented termites: A magnetic resonance study, *J. Magn. Reson.*, *168*, 246–251.

An, Z. S., and S. C. Porter (1997), Millennial-scale climatic oscillations during the last interglaciation in central China, *Geology*, *25*, 603–606, doi:10.1130/0091-7613(1997)025<0603:MSCODT>2.3.CO;2.

Anbar, A. D., J. E. Roe, J. Barling, and K. H. Nealson (2000), Nonbiological fractionation of iron isotopes, *Science*, *288*, 126–128, doi:10.1126/science.288.5463.126.

Anderson, N. J., and B. Rippey (1988), Diagenesis of magnetic minerals in the recent sediments of a eutrophic lake, *Limnol. Oceanogr.*, *33*, 1476–1492, doi:10.4319/lo.1988.33.6_part_2.1476.

Andrews, J. T., J. Hardardóttir, G. B. Kristjansdóttir, K. Grönvold, and J. S. Stoner (2003a), A high-resolution Holocene sediment record from Hunafloaall, N Iceland margin: Century to millennial-scale variability since the Vedde tephra, *Holocene*, *13*, 625–638, doi:10.1191/0959683603hl651ft.

Andrews, J. T., J. Hardadottir, J. S. Stoner, M. E. Mann, G. B. Kristjansdottir, and N. Koc (2003b), Decadal to millennial-scale periodicities in North Iceland shelf sediments over the last 12,000 cal yr: Long-term North Atlantic oceanographic variability and solar forcing, *Earth Planet. Sci. Lett.*, *210*, 453–465, doi:10.1016/S0012-821X(03)00139-0.

Arató, B., Z. Szányi, C. Flies, D. Schüler, R. B. Frankel, P. R. Buseck, and M. Pósfai (2005), Crystal-size and shape distributions of magnetite from uncultured magnetotactic bacteria as a potential biomarker, *Am. Mineral.*, *90*, 1233–1240, doi:10.2138/am.2005.1778.

Ayyub, P., M. Multani, M. Barma, V. R. Palkar, and R. Vijayaraghavan (1988), Size-induced structural phase transitions and hyperfine properties of microcrystalline Fe_2O_3, *J. Phys. C Solid State Phys.*, *21*, 2229–2245, doi:10.1088/0022-3719/21/11/014.

Bailey, I., Q. S. Liu, G. E. A. Swann, Z. X. Jiang, Y. B. Sun, X. Zhao, and A. P. Roberts (2011), Iron fertilisation and biogeochemical cycles in the sub-Arctic northwest Pacific during the late Pliocene intensification of northern hemisphere glaciation, *Earth Planet. Sci. Lett.*, *307*, 253–265, doi:10.1016/j.epsl.2011.05.029.

Bajt, S., S. R. Sutton, and J. S. Delaney (1994), X-ray microprobe analysis of iron oxidation states in silicates and oxides using X-ray absorption near edge structure (XANES), *Geochim. Cosmochim. Acta*, *58*, 5209–5214, doi:10.1016/0016-7037(94)90305-0.

Balsam, W. L., B. L. Otto-Bliesner, and B. C. Deaton (1995), Modern and Last Glacial Maximum eolian sedimentation patterns in the Atlantic Ocean interpreted from sediment iron oxide content, *Paleoceanography*, *10*(3), 493–507, doi:10.1029/95PA00421.

Balsam, W., J. F. Ji, and J. Chen (2004), Climatic interpretation of the Luochuan and Lingtai loess sections, China, based on changing iron oxide mineralogy and magnetic susceptibility, *Earth Planet. Sci. Lett.*, *223*, 335–348, doi:10.1016/j.epsl.2004.04.023.

Bando, M., Y. Kiyama, N. Yamamoto, T. Takada, T. Shinjo, and H. Takaki (1965), Magnetic properties of α-Fe_2O_3 fine particles, *J. Phys. Soc. Jpn.*, *20*, 2086, doi:10.1143/JPSJ.20.2086.

Banerjee, S. K. (1971), New grain size limits for palaeomagnetic stability in haematite, *Nature*, *232*, 15–16.

Banerjee, S. K., J. King, and J. Marvin (1981), A rapid method for magnetic granulometry with applications to environmental studies, *Geophys. Res. Lett.*, *8*, 333–336, doi:10.1029/GL008i004p00333.

Banerjee, S. K., C. P. Hunt, and X. Liu (1993), Separation of local signals from the regional paleomonsoon record of the Chinese Loess Plateau: A rock-magnetic approach, *Geophys. Res. Lett.*, *20*, 843–846, doi:10.1029/93GL00908.

Barrón, V., and J. Torrent (2002), Evidence for a simple pathway to maghemite in Earth and Mars soil, *Geochim. Cosmochim. Acta*, *66*, 2801–2806, doi:10.1016/S0016-7037(02)00876-1.

Barrón, V., J. Torrent, and E. de Grave (2003), Hydromaghemite, an intermediate in the hydrothermal transformation of 2-line ferrihydrite into hematite, *Am. Mineral.*, *88*, 1679–1688.

Bazylinski, D. A., and R. B. Frankel (2004), Magnetosome formation in prokaryotes, *Nat. Rev. Microbiol.*, *2*, 217–230, doi:10.1038/nrmicro842.

Bazylinski, D. A., B. R. Heywood, S. Mann, and R. B. Frankel (1993), Fe_3O_4 and Fe_3S_4 in a bacterium, *Nature*, *366*, 218, doi:10.1038/366218a0.

Beason, R., N. Dussourd, and M. Deutschlander (1995), Behavioural evidence for the use of magnetic material in magnetoreception by a migratory bird, *J. Exp. Biol.*, *198*, 141–146.

Begét, J. E., D. B. Stone, and D. B. Hawkins (1990), Paleoclimatic forcing of magnetic susceptibility variations in Alaskan loess during the late Quaternary, *Geology*, *18*, 40–43, doi:10.1130/0091-7613(1990)018<0040:PFOMSV>2.3.CO;2.

Berner, R. A. (1980), *Early Diagenesis: A Theoretical Approach*, Princeton Univ. Press, Princeton, N. J.

Berner, R. A. (1981), A new geochemical classification of sedimentary environments, *J. Sediment. Petrol.*, *51*, 359–365.

Berner, R. A. (1984), Sedimentary pyrite formation: An update, *Geochim. Cosmochim. Acta*, *48*, 605–615, doi:10.1016/0016-7037(84)90089-9.

Bidegain, J. C., Y. Rico, A. Bartel, M. Chaparro, and S. Jurado (2009), Magnetic parameters reflecting pedogenesis in Pleistocene loess deposits of Argentina, *Quat. Int.*, *209*, 175–186, doi:10.1016/j.quaint.2009.06.024.

Biscaye, P. E., F. E. Grousset, M. Revel, S. van der Gaast, G. A. Zielinski, A. Vaars, and G. Kukla (1997), Asian provenance of glacial dust (stage 2) in the Greenland Ice Sheet Project 2 Ice Core, Summit, Greenland, *J. Geophys. Res.*, *102*, 26,765–26,781, doi:10.1029/97JC01249.

Blaha, U., B. Sapkota, E. Appel, H. Stanjek, and W. Rösler (2008), Micro-scale grain-size analysis and magnetic properties of coal-fired power plant fly ash and its relevance for environmental

magnetic pollution studies, *Atmos. Environ.*, *42*, 8359–8370, doi:10.1016/j.atmosenv.2008.07.051.

Blakemore, R. (1975), Magnetotactic bacteria, *Science*, *190*, 377–379, doi:10.1126/science.170679.

Blanchet, C. L., N. Thouveny, and L. Vidal (2009), Formation and preservation of greigite (Fe_3S_4) in sediments from the Santa Barbara basin: Implications for paleoenvironmental changes during the past 35 ka, *Paleoceanography*, *24*, PA2224, doi:10.1029/2008PA001719.

Bloemendal, J., and P. B. deMenocal (1989), Evidence for a change in the periodicity of tropical climate cycles at 2.4 Myr from whole-core magnetic susceptibility measurements, *Nature*, *342*, 897–900, doi:10.1038/342897a0.

Bloemendal, J., and X. M. Liu (2005), Rock magnetism and geochemistry of two Plio-Pleistocene Chinese loess-palaeosol sequences: Implications for quantitative palaeoprecipitation reconstruction, *Palaeogeogr. Palaeoclimatol. Palaeoecol.*, *226*, 149–166, doi:10.1016/j.palaeo.2005.05.008.

Bloemendal, J., B. Lamb, and J. King (1988), Paleoenvironmental implications of rock-magnetic properties of Late Quaternary sediment cores from the eastern equatorial Atlantic, *Paleoceanography*, *3*, 61–87, doi:10.1029/PA003i001p00061.

Bloemendal, J., J. W. King, F. R. Hall, and S.-J. Doh (1992), Rock magnetism of late Neogene and Pleistocene deep-sea sediments: Relationship to sediment source, diagenetic processes, and sediment lithology, *J. Geophys. Res.*, *97*, 4361–4375, doi:10.1029/91JB03068.

Bloemendal, J., J. W. King, A. Hunt, P. B. deMenocal, and A. Hayashida (1993), Origin of the sedimentary magnetic record at the Ocean Drilling Program sites on the Owen Ridge, *J. Geophys. Res.*, *98*, 4199–4219, doi:10.1029/92JB02914.

Blundell, A., J. A. Hannam, J. A. Dearing, and J. F. Boyle (2009a), Detecting atmospheric pollution in surface soils using magnetic measurements: A reappraisal using an England and Wales database, *Environ. Pollut.*, *157*, 2878–2890, doi:10.1016/j.envpol.2009.02.031.

Blundell, A., J. A. Dearing, J. F. Boyle, and J. A. Hannam (2009b), Controlling factors for the spatial variability of soil magnetic susceptibility across England and Wales, *Earth Sci. Rev.*, *95*, 158–188, doi:10.1016/j.earscirev.2009.05.001.

Bógalo, M. F., F. Heller, and M. L. Osete (2001), Isothermal remanence experiments at room and at liquid nitrogen temperature: Application to soil studies, *Geophys. Res. Lett.*, *28*, 419–422, doi:10.1029/2000GL012032.

Boily, J. F., J. Lutzenkirchen, O. Balmes, J. Beattie, and S. Sjoberg (2001), Modeling proton binding at the goethite (α-FeOOH)-water interface, *Colloids Surf. A*, *179*, 11–27, doi:10.1016/S0927-7757(00)00712-3.

Boyko, T., R. Scholger, and H. Stanjek (2004), Topsoil magnetic susceptibility mapping as a tool for pollution monitoring: Repeatability of in situ measurements, *J. Appl. Geophys.*, *55*, 249–259, doi:10.1016/j.jappgeo.2004.01.002.

Brachfeld, S. A., S. K. Banerjee, Y. Guyodo, and G. D. Acton (2002), A 13,200 year history of century to millennial-scale paleoenvironmental change magnetically recorded in the Palmer Deep, western Antarctic Peninsula, *Earth Planet. Sci. Lett.*, *194*, 311–326, doi:10.1016/S0012-821X(01)00567-2.

Brem, F., A. M. Hirt, M. Winklhofer, K. Frei, Y. Yonekawa, H.-G. Wieser, and J. Dobson (2006), Magnetic iron compounds in the human brain: A comparison of tumour and hippocampal tissue, *J. R. Soc. Interface*, *3*, 833–841, doi:10.1098/rsif.2006.0133.

Brice-Profeta, S., M. A. Arrio, E. Tronc, N. Menguy, I. Letard, C. C. D. Moulin, M. Nogues, C. Chanéac, J. P. Jolivet, and P. Sainctavit (2005), Magnetic order in γ-Fe_2O_3 nanoparticles: A XMCD study, *J. Magn. Magn. Mater.*, *288*, 354–365, doi:10.1016/j.jmmm.2004.09.120.

Canfield, D. E., and R. A. Berner (1987), Dissolution and pyritization of magnetite in anoxic marine sediments, *Geochim. Cosmochim. Acta*, *51*, 645–659, doi:10.1016/0016-7037(87)90076-7.

Canfield, D. E., R. Raiswell, and S. Bottrell (1992), The reactivity of sedimentary iron minerals toward sulfide, *Am. J. Sci.*, *292*, 659–683, doi:10.2475/ajs.292.9.659.

Cao, C. Q., L. X. Tian, Q. S. Liu, W. F. Liu, G. J. Chen, and Y. X. Pan (2010), Magnetic characterization of noninteracting, randomly oriented, nanometer-scale ferrimagnetic particles, *J. Geophys. Res.*, *115*, B07103, doi:10.1029/2009JB006855.

Carter-Stiglitz, B., S. K. Banerjee, A. Gourlan, and E. Oches (2006), A multi-proxy study of Argentina loess: Marine oxygen isotope stage 4 and 5 environmental record from pedogenic hematite, *Palaeogeogr. Palaeoclimatol. Palaeoecol.*, *239*, 45–62, doi:10.1016/j.palaeo.2006.01.008.

Carvallo, C., P. Sainctavit, M. A. Arrio, N. Menguy, Y. H. Wang, G. Ona-Nguema, and S. Brice-Profeta (2008), Biogenic vs. abiogenic magnetite nanoparticles: A XMCD study, *Am. Mineral.*, *93*, 880–885, doi:10.2138/am.2008.2713.

Casey, W. H., and J. R. Rustad (2007), Reaction dynamics, molecular clusters, and aqueous geochemistry, *Annu. Rev. Earth Planet. Sci.*, *35*, 21–46, doi:10.1146/annurev.earth.35.031306.140117.

Chang, L., A. P. Roberts, Y. Tang, B. D. Rainford, A. R. Muxworthy, and Q. Chen (2008), Fundamental magnetic parameters from pure synthetic greigite (Fe_3S_4), *J. Geophys. Res.*, *113*, B06104, doi:10.1029/2007JB005502.

Chang, L., A. P. Roberts, C. J. Rowan, Y. Tang, P. Pruner, Q. Chen, and C.-S. Horng (2009), Low-temperature magnetic properties of greigite (Fe_3S_4), *Geochem. Geophys. Geosyst.*, *10*, Q01Y04, doi:10.1029/2008GC002276.

Channell, J. E. T., and T. Hawthorne (1990), Progressive dissolution of titanomagnetites at ODP Site 653 (Tyrrhenian Sea), *Earth Planet. Sci. Lett.*, *96*, 469–480, doi:10.1016/0012-821X(90)90021-O.

Channell, J. E. T., R. Freeman, F. Heller, and W. Lowrie (1982), Timing of diagenetic hematite growth in red pelagic limestones from Gubbio (Italy), *Earth Planet. Sci. Lett.*, *58*, 189–201, doi:10.1016/0012-821X(82)90193-5.

Chen, F. H., J. Bloemendal, J. M. Wang, J. J. Li, and F. Oldfield (1997), High-resolution multi-proxy climate records from Chinese loess: Evidence for rapid climatic changes over the last 75 kyr, *Palaeogeogr. Palaeoclimatol. Palaeoecol.*, *130*, 323–335, doi:10.1016/S0031-0182(96)00149-6.

Chen, Z., W. Yan, X. Z. Tang, J. G. Liu, M. H. Chen, and H. P. Yang (2009), Magnetic susceptibility in surface sediments in the southern China Sea and its implications for sub-sea methane venting, *J. Earth Sci.*, *20*, 193–204, doi:10.1007/s12583-009-0019-y.

Cisowski, S. (1981), Interacting vs. non-interacting single domain behavior in natural and synthetic samples, *Phys. Earth Planet. Inter.*, *26*, 56–62, doi:10.1016/0031-9201(81)90097-2.

Colin, C., C. Kissel, D. Blamart, and L. Turpin (1998), Magnetic properties of sediments in the Bay of Bengal and the Andaman Sea: Impact of rapid North Atlantic Ocean climatic events on the strength of the Indian Monsoon, *Earth Planet. Sci. Lett.*, *160*, 623–635, doi:10.1016/S0012-821X(98)00116-2.

Colman, S. M., J. A. Peck, E. B. Karabanov, S. J. Carter, J. P. Bradbury, J. W. King, and D. F. Williams (1995), Continental climate response to orbital forcing from biogenic silica records in Lake Baikal, *Nature*, *378*, 769–771, doi:10.1038/378769a0.

Cornell, R. M., and U. Schwertmann (2003), *The Iron Oxides: Structure, Properties, Reactions, Occurrences and Uses*, Wiley, New York.

Cui, Y. L., K. L. Verosub, and A. P. Roberts (1994), The effect of maghemitization on large multi-domain magnetite, *Geophys. Res. Lett.*, *21*, 757–760, doi:10.1029/94GL00639.

Day, R., M. Fuller, and V. A. Schmidt (1977), Hysteresis properties of titanomagnetites: Grain-size and compositional dependence, *Phys. Earth Planet. Inter.*, *13*, 260–267, doi:10.1016/0031-9201(77)90108-X.

Dearing, J., Y. Q. Hu, P. Doody, P. A. James, and A. Brauer (2001), Preliminary reconstruction of sediment-source linkages for the past 6000 yr at the Petit Lac d'Annecy, France, based on mineral

magnetic data, *J. Paleolimnol.*, *25*, 245–258, doi:10.1023/A:1008186501993.

Dearing, J. A., and R. J. Flower (1982), The magnetic susceptibility of sedimenting material trapped in Lough Neagh, northern Ireland, and its erosional significance, *Limnol. Oceanogr.*, *27*, 969–975, doi:10.4319/lo.1982.27.5.0969.

Dearing, J. A., J. K. Elner, and C. M. Happey-Wood (1981), Recent sediment flux and erosional processes in a Welsh upland lake catchment based on magnetic susceptibility measurements, *Quat. Res.*, *16*, 356–372, doi:10.1016/0033-5894(81)90016-8.

Dearing, J. A., K. Hay, S. Baban, A. S. Huddleston, E. M. H. Wellington, and P. J. Loveland (1996), Magnetic susceptibility of topsoils: A test of conflicting theories using a national database, *Geophys. J. Int.*, *127*, 728–734, doi:10.1111/j.1365-246X.1996.tb04051.x.

De Deckker, P., M. Norman, I. D. Goodwin, A. Wain, and F. X. Gingele (2010), Lead isotopic evidence for an Australian source of aeolian dust to Antarctica at times over the last 170,000 years, *Palaeogeogr. Palaeoclimatol. Palaeoecol.*, *285*, 205–223, doi:10.1016/j.palaeo.2009.11.013.

Dekkers, M. J. (1989a), Magnetic properties of natural pyrrhotite. II. High- and low-temperature behaviour of J_{rs} and TRM as function of grain-size, *Phys. Earth Planet. Inter.*, *57*, 266–283, doi:10.1016/0031-9201(89)90116-7.

Dekkers, M. J. (1989b), Magnetic properties of natural goethite-II. TRM behaviour during thermal and alternating field demagnetization and low-temperature treatment, *Geophys. J.*, *97*, 341–355, doi:10.1111/j.1365-246X.1989.tb00505.x.

Dekkers, M. J. (1997), Environmental magnetism: An introduction, *Geol. Mijnbouw*, *76*, 163–182, doi:10.1023/A:1003122305503.

Dekkers, M. J., H. F. Passier, and M. A. A. Schoonen (2000), Magnetic properties of hydrothermally synthesized greigite (Fe_3S_4)—II. High- and low-temperature characteristics, *Geophys. J. Int.*, *141*, 809–819, doi:10.1046/j.1365-246x.2000.00129.x.

Dekov, V. M., et al. (2009), Metalliferous sediments from Eolo Seamount (Tyrrhenian Sea): Hydrothermal deposition and re-deposition in a zone of oxygen depletion, *Chem. Geol.*, *264*, 347–363, doi:10.1016/j.chemgeo.2009.03.023.

Dekov, V. M., S. Petersen, C.-D. Garbe-Schönberg, G. D. Kamenov, M. Perner, E. Kuzmann, and M. Schmidt (2010), Fe–Si-oxyhydroxide deposits at a slow-spreading centre with thickened oceanic crust: The Lilliput hydrothermal field (9°33′S, Mid-Atlantic Ridge), *Chem. Geol.*, *278*, 186–200, doi:10.1016/j.chemgeo.2010.09.012.

deMenocal, P., J. Bloemendal, and J. King (1991), A rock-magnetic record of monsoonal dust deposition to the Arabian Sea: Evidence for a shift in the mode of deposition at 2.4 Ma, *Proc. Ocean Drill. Program Sci. Results*, *177*, 389–407.

Deng, C., R. Zhu, M. J. Jackson, K. L. Verosub, and M. J. Singer (2001), Variability of the temperature-dependent susceptibility of the Holocene eolian deposits in the Chinese loess plateau: A pedogenesis indicator, *Phys. Chem. Earth*, *26*, 873–878, doi:10.1016/S1464-1895(01)00135-1.

Deng, C. L., J. Shaw, Q. S. Liu, Y. X. Pan, and R. X. Zhu (2006), Mineral magnetic variation of the Jingbian loess/paleosol sequence in the northern Loess Plateau of China: Implications for Quaternary development of Asian aridification and cooling, *Earth Planet. Sci. Lett.*, *241*, 248–259, doi:10.1016/j.epsl.2005.10.020.

De Vleeschouwer, D., A. C. da Silva, F. Boulvain, M. Crucifix, and P. Claeys (2011), Precessional and half-precessional climate forcing of mid-Devonian monsoon-like dynamics, *Clim. Past Discuss.*, *7*, 1427–1455, doi:10.5194/cpd-7-1427-2011.

Dickens, G. R. (2008), The riddle of the clays, *Nat. Geosci.*, *1*, 86–88, doi:10.1038/ngeo118.

Dillon, M., and U. Bleil (2006), Rock magnetic signatures of diagenetically altered sediments from the Niger deep-sea fan, *J. Geophys. Res.*, *111*, B03105, doi:10.1029/2004JB003540.

Dinarès-Turell, J., B. A. A. Hoogakker, A. P. Roberts, E. J. Rohling, and L. Sagnotti (2003), Quaternary climatic control of biogenic magnetite production and eolian dust input in cores from the Mediterranean Sea, *Palaeogeogr. Palaeoclimatol. Palaeoecol.*, *64*, 221–240.

Ding, Z. L., E. Derbyshire, S. L. Yang, Z. W. Yu, S. F. Xiong, and T. S. Liu (2002), Stacked 2.6-Ma grain size record from the Chinese loess based on five sections and correlation with the deep-sea $\delta^{18}O$ record, *Paleoceanography*, *17*(3), 1033, doi:10.1029/2001PA000725.

Ding, Z. L., E. Derbyshire, J. M. Sun, and T. S. Liu (2005), Stepwise expansion of desert environment across northern China in the past 3.5 Ma and implications for monsoon evolution, *Earth Planet. Sci. Lett.*, *237*, 45–55, doi:10.1016/j.epsl.2005.06.036.

Dobson, J. (2001), Nanoscale biogenic iron oxides and neurodegerative disease, *FEBS Lett.*, *496*, 1–5, doi:10.1016/S0014-5793(01)02386-9.

Dobson, J., and P. Grassi (1996), Magnetic properties of human hippocampal tissue-evolution of artifact and contamination sources, *Brain Res. Bull.*, *39*, 255–259, doi:10.1016/0361-9230(95)02132-9.

Doh, S. J., J. King, and M. Leinen (1988), A rock-magnetic study of giant piston core LL44–GPC3 from the central North Pacific and its paleoceanographic implications, *Paleoceanography*, *3*, 89–111, doi:10.1029/PA003i001p00089.

Dowdeswell, J. A., M. A. Maslin, J. T. Andrews, and I. N. McCave (1995), Iceberg production, debris rafting, and the extent and thickness of Heinrich layers (H-1, H-2) in North Atlantic sediments, *Geology*, *23*, 301–304, doi:10.1130/0091-7613(1995)023<0297:IPDRAT>2.3.CO;2.

Dräger, G., R. Frahm, G. Materlik, and O. Brummer (1988), On the multipole character of the X-ray transitions in the pre-edge structure of Fe K absorption spectra: An experimental study, *Phys. Status Solidi B*, *146*, 287–294, doi:10.1002/pssb.2221460130.

Drits, V. A., B. A. Sakharov, A. L. Salyn, and A. Manceau (1993), A structural model for ferrihydrite, *Clay Miner.*, *28*, 185–207, doi:10.1180/claymin.1993.028.2.02.

Dubiel, S. M., B. Zablotna-Rypien, J. B. Mackey, and J. M. Williams (1999), Magnetic properties of human liver and brain ferritin, *Eur. Biophys. J.*, *28*, 263–267, doi:10.1007/s002490050208.

Duce, R. A., et al. (1991), The atmospheric input of trace species to the world ocean, *Global Biogeochem. Cycles*, *5*, 193–259, doi:10.1029/91GB01778.

Dunlop, D. J. (1973), Superparamagnetic and single-domain threshold sizes in magnetite, *J. Geophys. Res.*, *78*, 1780–1793, doi:10.1029/JB078i011p01780.

Dunlop, D. J. (2002a), Theory and application of the Day plot (M_{rs}/M_s versus H_{cr}/H_c): 1. Theoretical curves and tests using titanomagnetite data, *J. Geophys. Res.*, *107*(B3), 2056, doi:10.1029/2001JB000486.

Dunlop, D. J. (2002b), Theory and application of the Day plot (M_{rs}/M_s versus H_{cr}/H_c): 2. Application to data for rocks, sediments, and soils, *J. Geophys. Res.*, *107*(B3), 2057, doi:10.1029/2001JB000487.

Dunlop, D. J., and Ö. Özdemir (1997), *Rock Magnetism, Fundamentals and Frontiers*, Cambridge Univ. Press, Cambridge, U. K., doi:10.1017/CBO9780511612794.

Egli, R. (2004a), Characterization of individual rock magnetic components by analysis of remanence curves: 1. Unmixing natural sediments, *Stud. Geophys. Geod.*, *48*, 391–446, doi:10.1023/B:SGEG.0000020839.45304.6d.

Egli, R. (2004b), Characterization of individual rock magnetic components by analysis of remanence curves: 2. Fundamental properties of coercivity distributions, *Phys. Chem. Earth*, *29*, 851–867, doi:10.1016/S1474-7065(04)00129-9.

Egli, R. (2004c), Characterization of individual rock magnetic components by analysis of remanence curves: 3. Bacterial magnetite and natural processes in lakes, *Phys. Chem. Earth*, *29*, 869–884, doi:10.1016/j.pce.2004.03.010.

Egli, R. (2009), Magnetic susceptibility measurements as a function of temperature and frequency I: Inversion theory, *Geophys. J. Int.*, *177*, 395–420, doi:10.1111/j.1365-246X.2009.04081.x.

Egli, R., A. P. Chen, M. Winklhofer, K. P. Kodama, and C.-S. Horng (2010), Detection of noninteracting single domain particles using first-order reversal curve diagrams, *Geochem. Geophys. Geosyst.*, *11*, Q01Z11, doi:10.1029/2009GC002916.

Ehrmann, W. U., and A. Mackensen (1992), Sedimentological evidence for the formation of an East Antarctic ice sheet in Eocene/Oligocene time, *Palaeogeogr. Palaeoclimatol. Palaeoecol.*, *93*, 85–112, doi:10.1016/0031-0182(92)90185-8.

Eldrett, J. S., I. C. Harding, P. A. Wilson, E. Butler, and A. P. Roberts (2007), Continental ice in Greenland during the Eocene and Oligocene, *Nature*, *446*, 176–179, doi:10.1038/nature05591.

Emiroglu, S., D. Rey, and N. Petersen (2004), Magnetic properties of sediments in the Ria de Arousa (Spain): Dissolution of iron oxides and formation of iron sulfides, *Phys. Chem. Earth*, *29*, 947–959, doi:10.1016/j.pce.2004.03.012.

Enkin, R. J., J. Baker, D. Nourgaliev, P. Iassonov, and T. S. Hamilton (2007), Magnetic hysteresis parameters and Day plot analysis to characterize diagenetic alteration in gas-hydrate-bearing sediments, *J. Geophys. Res.*, *112*, B06S90, doi:10.1029/2006JB004638.

Evans, M. E., and F. Heller (2001), Magnetism of loess/paleosol sequences: Recent developments, *Earth Sci. Rev.*, *54*, 129–144, doi:10.1016/S0012-8252(01)00044-7.

Evans, M. E., and F. Heller (2003), *Environmental Magnetism: Principles and Applications of Enviromagnetics*, Academic, San Diego, Calif.

Eyles, N. (1993), Earth's glacial record and its tectonic setting, *Earth Sci. Rev.*, *35*, 1–248, doi:10.1016/0012-8252(93)90002-O.

Faivre, D., and D. Schüler (2008), Magnetotactic bacteria and magnetosomes, *Chem. Rev.*, *108*, 4875–4898, doi:10.1021/cr078258w.

Faivre, D., N. Menguy, M. Posfai, and D. Schüler (2008), Environmental parameters affect the physical properties of fast-growing magnetosomes, *Am. Mineral.*, *93*, 463–469, doi:10.2138/am.2008.2678.

Faugères, J. C., and D. A. V. Stow (1993), Bottom-current-controlled sedimentation–a synthesis of the contourite problem, *Sediment. Geol.*, *82*, 287–297, doi:10.1016/0037-0738(93)90127-Q.

Fialová, H., G. Maier, E. Petrovsky, A. Kapicka, T. Boyko, and R. Scholger, and the MAGPROX Team (2006), Magnetic properties of soils from sites with different geological and environmental settings, *J. Appl. Geophys.*, *59*, 273–283, doi:10.1016/j.jappgeo.2005.10.006.

Flies, C. B., H. M. Jonkers, D. de Beer, K. Bosselmann, M. E. Böttcher, and D. Schüler (2005), Diversity and vertical distribution of magnetotactic bacteria along chemical gradients in freshwater microcosms, *FEMS Microbiol. Ecol.*, *52*, 185–195, doi:10.1016/j.femsec.2004.11.006.

Florindo, F., and L. Sagnotti (1995), Palaeomagnetism and rock magnetism at the upper Pliocene Valle Ricca (Rome, Italy) section, *Geophys. J. Int.*, *123*, 340–354, doi:10.1111/j.1365-246X.1995.tb06858.x.

Florindo, F., R. X. Zhu, and B. Guo (1999), Low-field susceptibility and palaeorainfall estimates: New data along a N-S transect of the Chinese Loess Plateau, *Phys. Chem. Earth A*, *24*, 817–821, doi:10.1016/S1464-1895(99)00120-9.

France, D. E., and F. Oldfield (2000), Identifying goethite and hematite from rock magnetic measurements of soils and sediments, *J. Geophys. Res.*, *105*, 2781–2795, doi:10.1029/1999JB900304.

Franke, C., T. Frederichs, and M. J. Dekkers (2007), Efficiency of heavy liquid separation to concentrate magnetic particles, *Geophys. J. Int.*, *170*, 1053–1066, doi:10.1111/j.1365-246X.2007.03489.x.

Franke, C., C. Kissel, E. Robin, P. Bonte, and F. Lagroix (2009), Magnetic particle characterization in the Seine river system: Implications for the determination of natural versus anthropogenic input, *Geochem. Geophys. Geosyst.*, *10*, Q08Z05, doi:10.1029/2009GC002544.

Fredrickson, J. K., J. M. Zachara, D. W. Kennedy, M. C. Duff, Y. A. Gorby, S. M. Li, and K. M. Krupka (2000), Reduction of U(VI) in goethite (α-FeOOH) suspensions by a dissimilatory metal-reducing bacterium, *Geochim. Cosmochim. Acta*, *64*, 3085–3098, doi:10.1016/S0016-7037(00)00397-5.

Freeman, R. (1986), Magnetic mineralogy of pelagic limestones, *Geophys. J. R. Astron. Soc.*, *85*, 433–452, doi:10.1111/j.1365-246X.1986.tb04522.x.

Froelich, P. N., G. P. Klinkhammer, M. L. Bender, N. A. Luedtke, G. R. Heath, D. Cullen, O. Dauphin, D. Hammond, B. Hartman, and V. Maynard (1979), Early oxidation of organic matter in pelagic sediments of the eastern equatorial Atlantic–suboxic diagenesis, *Geochim. Cosmochim. Acta*, *43*, 1075–1090, doi:10.1016/0016-7037(79)90095-4.

Fu, Y., T. von Dobeneck, C. Franke, D. Heslop, and S. Kasten (2008), Rock magnetic identification and geochemical process models of greigite formation in Quaternary marine sediments from the Gulf of Mexico (IODP Hole U1319A), *Earth Planet. Sci. Lett.*, *275*, 233–245, doi:10.1016/j.epsl.2008.07.034.

Fuller, M., J. Dobson, H. G. Wieser, and S. Moser (1995), On the sensitivity of the human brain to magnetic fields: Evocation of epileptiform activity, *Brain Res. Bull.*, *36*, 155–159, doi:10.1016/0361-9230(94)00183-2.

Galbrun, B., R. Mouterde, F. Baudin, T. Deliant, and J. Dercourt (1994), Magnetostratigraphy and biostratigraphy of the Toarcian Ammonitico-Rosso Formation from the Ionian Zone (Epirus, Greece), *Eclogae Geol. Helv.*, *87*, 91–111.

Garming, J. F. L., G. J. de Lange, M. J. Dekkers, and H. F. Passier (2004), Changes in magnetic parameters after sequential iron phase extraction of eastern Mediterranean sapropel S1 sediments, *Stud. Geophys. Geod.*, *48*, 345–362, doi:10.1023/B:SGEG.0000020837.18450.76.

Garming, J. F. L., U. Bleil, and N. Riedinger (2005), Alteration of magnetic mineralogy at the sulfate-methane transition: Analysis of sediments from the Argentine continental slope, *Phys. Earth Planet. Inter.*, *151*, 290–308, doi:10.1016/j.pepi.2005.04.001.

Gedye, S. J., R. T. Jones, W. Tinner, B. Ammann, and F. Oldfield (2000), The use of mineral magnetism in the reconstruction of fire history: A case study from Lago di Origlio, Swiss Alps, *Palaeogeogr. Palaeoclimatol. Palaeoecol.*, *164*, 101–110, doi:10.1016/S0031-0182(00)00178-4.

Geiss, C. E., C. W. Zanner, S. K. Banerjee, and M. Joanna (2004), Signature of magnetic enhancement in a loessic soil in Nebraska, United States of America, *Earth Planet. Sci. Lett.*, *228*, 355–367, doi:10.1016/j.epsl.2004.10.011.

Gómez-Paccard, M., J. C. Larrasoaña, C. Sancho, A. Muñoz, E. McDonald, E. J. Rhodes, M. C. Osácar, E. Costa, and E. Beamud (2012), Environmental response of a fragile, semiarid landscape (Bardenas Reales Natural Park, NE Spain) to Early Holocene climate variability: A paleo- and environmental-magnetic approach, *Catena*, doi:10.1016/j.catena.2011.05013, in press.

Grousset, F. E., P. E. Biscaye, M. Revel, J. R. Petit, K. Pye, S. Jossaume, and J. Jouzel (1992), Antarctic (Dome C) ice-core dust at 18 k.y. B.P.: Isotopic constraints on origins, *Earth Planet. Sci. Lett.*, *111*, 175–182, doi:10.1016/0012-821X(92)90177-W.

Grousset, F. E., L. Labeyrie, J. A. Sinko, M. Cremer, G. Bond, J. Duprat, E. Cortijo, and S. Huon (1993), Patterns of ice-rafted detritus in the glacial North Atlantic (40–55°N), *Paleoceanography*, *8*, 175–192, doi:10.1029/92PA02923.

Grousset, F. E., C. Pujol, L. Labeyrie, G. Auffret, and A. Boelaert (2000), Were the North Atlantic Heinrich events triggered by the behavior of the European ice sheets?, *Geology*, *28*, 123–126, doi:10.1130/0091-7613(2000)28<123:WTNAHE>2.0.CO;2.

Guo, B., R. X. Zhu, A. P. Roberts, and F. Florindo (2001), Lack of correlation between paleoprecipitation and magnetic susceptibility of Chinese loess/paleosol sequences, *Geophys. Res. Lett.*, *28*, 4259–4262, doi:10.1029/2001GL013290.

Guo, Z. T., W. F. Ruddiman, Q. Z. Hao, H. B. Wu, Y. S. Qiao, R. X. Zhu, S. Z. Peng, J. J. Wei, B. Y. Yuan, and T. S. Liu (2002), Onset of Asian desertification by 22 Myr ago inferred from loess deposits in China, *Nature*, *416*, 159–163, doi:10.1038/416159a.

Guyodo, Y., T. M. LaPara, A. J. Anschutz, R. L. Penn, S. K. Banerjee, C. E. Geiss, and W. Zanner (2006a), Rock magnetic, chemical and bacterial community analysis of a modern soil from Nebraska, *Earth Planet. Sci. Lett.*, *251*, 168–178, doi:10.1016/j.epsl.2006.09.005.

Guyodo, Y., S. K. Banerjee, R. L. Penn, D. Burleson, T. S. Berquo, T. Seda, and P. Solheid (2006b), Magnetic properties of synthetic 6-line ferrihydrite nanoparticles, *Phys. Earth Planet. Inter.*, *154*, 222–233, doi:10.1016/j.pepi.2005.05.009.

Guyodo, Y., et al. (2012), X-ray magnetic circular dichroïsm provides strong evidence for tetrahedral iron in ferrihydrite, *Geochem. Geophys. Geosyst.*, *13*, Q06Z44, doi:10.1029/2012GC004182.

Han, J., H. Lu, N. Wu, and Z. Guo (1996), Magnetic susceptibility of modern soils in China and climate conditions, *Stud. Geophys. Geod.*, *40*, 262–275.

Hanesch, M., and R. Scholger (2002), Mapping of heavy metal loadings in soils by means of magnetic susceptibility measurements, *Environ. Geol.*, *42*, 857–870.

Hanesch, M., R. Scholger, and D. Rey (2003), Mapping dust distribution around an industrial site by measuring magnetic parameters of tree leaves, *Atmos. Environ.*, *37*, 5125–5133, doi:10.1016/j.atmosenv.2003.07.013.

Hanesch, M., G. Rantitsch, S. Hemetsberger, and R. Scholger (2007), Lithological and pedological influences on the magnetic susceptibility of soil: Their consideration in magnetic pollution mapping, *Sci. Total Environ.*, *382*, 351–363, doi:10.1016/j.scitotenv.2007.04.007.

Hao, Q., and Z. Guo (2005), Spatial variations of magnetic susceptibility of Chinese loess for the last 600 ka: Implications for monsoon evolution, *J. Geophys. Res.*, *110*, B12101, doi:10.1029/2005JB003765.

Hao, Q., F. Oldfield, J. Bloemendal, and Z. Guo (2008), The magnetic properties of loess and paleosol samples from the Chinese Loess Plateau spanning the last 22 million years, *Palaeogeogr. Palaeoclimatol. Palaeoecol.*, *260*, 389–404, doi:10.1016/j.palaeo.2007.11.010.

Hassold, N. J. C., D. K. Rea, B. A. van der Pluijm, J. M. Parés, J. D. Gleason, and A. C. Ravelo (2006), Late Miocene to Pleistocene paleogeographic records from the Feni and Gardar Drifts: Pliocene reduction in abyssal flow, *Palaeogeogr. Palaeoclimatol. Palaeoecol.*, *236*, 290–301, doi:10.1016/j.palaeo.2005.11.011.

Hassold, N. J. C., D. K. Rea, B. A. van der Pluijm, and J. M. Parés (2009a), A physical record of the Antarctic Circumpolar Current: Late Miocene to recent slowing of abyssal circulation, *Palaeogeogr. Palaeoclimatol. Palaeoecol.*, *275*, 28–36, doi:10.1016/j.palaeo.2009.01.011.

Hassold, N. J. C., D. K. Rea, B. A. van der Pluijm, and J. M. Parés (2009b), Mid-Pliocene to Recent abyssal current flow along the Antarctic Peninsula: Results from ODP Leg 178, Site 1101, *Palaeogeogr. Palaeoclimatol. Palaeoecol.*, *284*, 120–128, doi:10.1016/j.palaeo.2009.09.011.

Hatfield, R. G., and B. A. Maher (2009), Fingerprinting upland sediment sources: Particle size-specific magnetic linkages between soils, lake sediments and suspended sediments, *Earth Surf. Processes Landforms*, *34*, 1359–1373, doi:10.1002/esp.1824.

Haug, G. H., M. A. Maslin, M. Sarnthein, R. Stax, and R. Tiedemann (1995), Evolution of northwest Pacific sedimentation patterns since 6 Ma (Site 882), *Proc. Ocean Drill. Program Sci. Results*, *145*, 293–314.

Hawthorne, T. B., and J. A. McKenzie (1993), Biogenic magnetite: Authigenesis and diagenesis with changing redox conditions in Lake Greifen, Switzerland, *Appl. Paleomagnetism Sediment. Geol.*, *49*, 3–15.

Hay, K. L., J. A. Dearing, S. M. J. Baban, and P. J. Loveland (1997), A preliminary attempt to identify atmospherically derived pollution particles in English topsoils from magnetic susceptibility measurements, *Phys. Chem. Earth*, *22*, 207–210, doi:10.1016/S0079-1946(97)00104-3.

Heider, F., A. Zitzelsberger, and K. Fabian (1996), Magnetic susceptibility and remanent coercive force in grown magnetite crystals from 0.1 μm to 6 mm, *Phys. Earth Planet. Inter.*, *93*, 239–256, doi:10.1016/0031-9201(95)03071-9.

Heinrich, H. (1988), Origin and consequences of cyclic ice rafting in the northeast Atlantic Ocean during the past 130,000 years, *Quat. Res.*, *29*, 142–152, doi:10.1016/0033-5894(88)90057-9.

Heller, F., and M. E. Evans (1995), Loess magnetism, *Rev. Geophys.*, *33*, 211–240, doi:10.1029/95RG00579.

Heller, F., and T. S. Liu (1982), Magnetostratigraphical dating of loess deposits in China, *Nature*, *300*, 431–433, doi:10.1038/300431a0.

Heller, F., and T. S. Liu (1984), Magnetism of Chinese loess deposits, *Geophys. J. R. Astron. Soc.*, *77*, 125–141, doi:10.1111/j.1365-246X.1984.tb01928.x.

Heller, F., and T. S. Liu (1986), Palaeoclimatic and sedimentary history from magnetic susceptibility of loess in China, *Geophys. Res. Lett.*, *13*, 1169–1172, doi:10.1029/GL013i011p01169.

Heller, F., C. D. Shen, J. Beer, X. M. Liu, T. S. Liu, A. Bronger, M. Suter, and B. Bonani (1993), Quantitative estimates of pedogenic ferromagnetic mineral formation in Chinese loess and paleoclimatic implications, *Earth Planet. Sci. Lett.*, *114*, 385–390, doi:10.1016/0012-821X(93)90038-B.

Heller, F., Z. Strzyszcz, and T. Magiera (1998), Magnetic record of industrial pollution in forest soils of Upper Silesia, Poland, *J. Geophys. Res.*, *103*, 17,767–17,774, doi:10.1029/98JB01667.

Hemming, S. R. (2004), Heinrich events: Massive Late Pleistocene detritus layers of the North Atlantic and their global climate imprint, *Rev. Geophys.*, *42*, RG1005, doi:10.1029/2003RG000128.

Henshaw, P. C., and R. T. Merrill (1980), Magnetic and chemical change in marine sediments, *Rev. Geophys.*, *18*, 483–504, doi:10.1029/RG018i002p00483.

Heslop, D. (2009), On the statistical analysis of the rock magnetic S-ratio, *Geophys. J. Int.*, *178*, 159–161, doi:10.1111/j.1365-246X.2009.04175.x.

Heslop, D., and M. Dillon (2007), Unmixing magnetic remanence curves without *a priori* knowledge, *Geophys. J. Int.*, *170*, 556–566, doi:10.1111/j.1365-246X.2007.03432.x.

Heslop, D., and A. P. Roberts (2012a), Estimating best-fit binary mixing lines in the Day plot, *J. Geophys. Res.*, *117*, B01101, doi:10.1029/2011JB008787.

Heslop, D., and A. P. Roberts (2012b), A method for unmixing magnetic hysteresis loops, *J. Geophys. Res.*, *117*, B03103, doi:10.1029/2011JB008859.

Heslop, D., M. J. Dekkers, P. P. Kruiver, and I. H. M. Van Oorschot (2002), Analysis of isothermal remanent magnetisation acquisition curves using the expectation-maximisation algorithm, *Geophys. J. Int.*, *148*, 58–64, doi:10.1046/j.0956-540x.2001.01558.x.

Heslop, D., T. von Dobeneck, and M. Hoecker (2007), Using non-negative matrix factorization in the "unmixing" of diffuse reflectance spectra, *Mar. Geol.*, *241*, 63–78, doi:10.1016/j.margeo.2007.03.004.

Hesse, P. P. (1994), Evidence for bacterial paleoecological origin of mineral magnetic cycles in oxic and sub-oxic Tasman sea sediments, *Mar. Geol.*, *117*, 1–17, doi:10.1016/0025-3227(94)90003-5.

Hesse, P., and J. F. Stolz (1999), Bacterial magnetite and the Quaternary climate record, in *Quaternary Climates, Environments, and Magnetism*, edited by B. A. Maher and R. Thompson, pp. 163–198, Cambridge Univ. Press, Cambridge, U. K., doi:10.1017/CBO9780511535635.006

Higgitt, S. R., F. Oldfield, and P. G. Appleby (1991), The record of land use change and soil erosion in the late Holocene sediments of the Petit Lac d'Annecy, *Holocene*, *1*, 14–28, doi:10.1177/095968369100100104.

Hilton, J., and J. P. Lishman (1985), The effect of redox changes on the magnetic susceptibility of sediments from a seasonally anoxic lake, *Limnol. Oceanogr.*, *30*, 907–909, doi:10.4319/lo.1985.30.4.0907.

Hirt, A. M., L. Lanci, and K. Koinig (2003), Mineral magnetic record of Holocene environmental changes in Sagistalsee, Switzerland, *J. Paleolimnol.*, *30*, 321–331, doi:10.1023/A:1026028728241.

Hoffmann, V., M. Knab, and E. Appel (1999), Magnetic susceptibility mapping of roadside pollution, *J. Geochem. Explor.*, *66*, 313–326, doi:10.1016/S0375-6742(99)00014-X.

Horng, C. S., and C. A. Huh (2011), Magnetic properties as tracers for source-to-sink dispersal of sediments: A case study in the Taiwan Strait, *Earth Planet. Sci. Lett.*, *309*, 141–152.

Horng, C. S., and A. P. Roberts (2006), Authigenic or detrital origin of pyrrhotite in sediments?: Resolving a paleomagnetic conundrum, *Earth Planet. Sci. Lett.*, *241*, 750–762, doi:10.1016/j.epsl.2005.11.008.

Horng, C. S., M. Torii, K. S. Shea, and S. J. Kao (1998), Inconsistent magnetic polarities between greigite- and pyrrhotite/magnetite-bearing marine sediments from the Tsailiao-chi section, southwestern Taiwan, *Earth Planet. Sci. Lett.*, *164*, 467–481, doi:10.1016/S0012-821X(98)00239-8.

Horng, C. S., C. A. Huh, K. H. Chen, P. R. Huang, K. H. Hsiung, and H. L. Lin (2009), Air pollution history elucidated from anthropogenic spherules and their magnetic signatures in marine sediments offshore of Southwestern Taiwan, *J. Mar. Syst.*, *76*, 468–478, doi:10.1016/j.jmarsys.2007.09.014.

Hou, H., Y. Luo, H. Zheng, B. Wang, and X. Tang (1998), Heinrich layer in Antarctic marine sediments and its significance to global changes, *Chin. Sci. Bull.*, *43*, 1830–1834, doi:10.1007/BF02883383.

Hounslow, M. W., and B. A. Maher (1996), Quantitative extraction and analysis of carriers of magnetization in sediments, *Geophys. J. Int.*, *124*, 57–74, doi:10.1111/j.1365-246X.1996.tb06352.x.

Hounslow, M. W., and B. A. Maher (1999), Source of the climate signal recorded by magnetic susceptibility variations in Indian Ocean deep-sea sediments, *J. Geophys. Res.*, *104*, 5047–5061, doi:10.1029/1998JB900085.

Housen, B. A., and B. M. Moskowitz (2006), Depth distribution of magnetofossils in near-surface sediments from the Blake/Bahama Outer Ridge, western North Atlantic Ocean, determined by low-temperature magnetism, *J. Geophys. Res.*, *111*, G01005, doi:10.1029/2005JG000068.

Housen, B. A., and R. J. Musgrave (1996), Rock-magnetic signature of gas hydrates in accretionary prism sediments, *Earth Planet. Sci. Lett.*, *139*, 509–519, doi:10.1016/0012-821X(95)00245-8.

Huhn, G., H. Schulz, H.-J. Stark, R. Tolle, and G. Schuurmann (1995), Evaluation of regional heavy metal deposition by multivariate analysis of element contents in pine tree barks, *Water Air Soil Pollut.*, *84*, 367–383, doi:10.1007/BF00475349.

Hunt, C. P., B. M. Moskowitz, and S. K. Banerjee (1995a), Magnetic properties of rocks and minerals, in *Rock Physics and Phase Relations: A Handbook of Physical Constants*, edited by T. J. Ahrens, pp. 189–204, AGU, Washington, D. C., doi:10.1029/RF003p0189

Hunt, C. P., S. K. Banerjee, J. M. Han, P. A. Solheid, E. Oches, W. W. Sun, and T. S. Liu (1995b), Rock-magnetic proxies of climate change in the loess-palaeosol sequences of the western Loess Plateau of China, *Geophys. J. Int.*, *123*, 232–244, doi:10.1111/j.1365-246X.1995.tb06672.x.

Hunt, C. P., M. J. Singer, G. Kletetschka, J. Tenpas, and K. L. Verosub (1995c), Effect of citrate-bicarbonate-dithionite treatment on fine-grained magnetite and maghemite, *Earth Planet. Sci. Lett.*, *130*, 87–94, doi:10.1016/0012-821X(94)00256-X.

Insam, H., and K. H. Domsch (1988), Relationship between soil organic carbon and microbial biomass on chronosequences of reclamation sites, *Microb. Ecol.*, *15*, 177–188, doi:10.1007/BF02011711.

Ising, G. (1943), *On the Magnetic Properties of Varved Clay: Line of Investigation: Measurements on a Varve Series From Viby in Southern Sweden*, 37 pp., Almqvist and Wiksell, Stockholm.

Itambi, A. C., T. von Dobeneck, S. Mulitza, T. Bickert, and D. Heslop (2009), Millennial-scale northwest African droughts related to Heinrich events and Dansgaard-Oeschger cycles: Evidence in marine sediments from offshore Senegal, *Paleoceanography*, *24*, PA1205, doi:10.1029/2007PA001570.

Itambi, A. C., T. von Dobeneck, M. J. Dekkers, and T. Frederichs (2010a), Magnetic mineral inventory of equatorial Atlantic Ocean marine sediments off Senegal–glacial and interglacial contrast, *Geophys. J. Int.*, *183*, 163–177, doi:10.1111/j.1365-246X.2010.04736.x.

Itambi, A. C., T. von Dobeneck, M. J. Dekkers, and T. Frederichs (2010b), Millennial-scale precipitation changes over central Africa during the Late Quaternary and Holocene: Evidence in sediments from the Gulf of Guinea, *J. Quat. Sci.*, *25*, 267–279, doi:10.1002/jqs.1306.

Jackson, M., B. Carter-Stiglitz, R. Egli, and P. Solheid (2006), Characterizing the superparamagnetic grain distribution $f(V, H_k)$ by thermal fluctuation tomography, *J. Geophys. Res.*, *111*, B12S07, doi:10.1029/2006JB004514.

Jambor, J. L., and J. E. Dutrizac (1998), Occurrence and constitution of natural and synthetic ferrihydrite, a widespread iron oxyhydroxide, *Chem. Rev.*, *98*, 2549–2586, doi:10.1021/cr970105t.

Jenny, H. (1941), *Factors of Soil Formation*, McGraw-Hill, New York.

Jenny, H. (1980), *The Soil Resource—Origin and Behavior*, Springer, New York.

Ji, J., W. Balsam, and J. Chen (2001), Mineralogic and climatic interpretations of the Luochuan loess section (China) based on diffuse reflectance spectrophotometry, *Quat. Res.*, *56*, 23–30, doi:10.1006/qres.2001.2238.

Jiang, W. T., C. S. Horng, A. P. Roberts, and D. R. Peacor (2001), Contradictory magnetic polarities in sediments and variable timing of neoformation of authigenic greigite, *Earth Planet. Sci. Lett.*, *193*, 1–12, doi:10.1016/S0012-821X(01)00497-6.

Jickells, T. D., et al. (2005), Global iron connections between desert dust, ocean biogeochemistry, and climate, *Science*, *308*, 67–71, doi:10.1126/science.1105959.

Jiménez-López, C., C. S. Romanek, and D. A. Bazylinski (2010), Magnetite as a prokaryotic biomarker: A review, *J. Geophys. Res.*, *115*, G00G03, doi:10.1029/2009JG001152.

Jordanova, N. V., D. V. Jordanova, L. Veneva, K. Yorova, and E. Petrovsky (2003), Magnetic response of soils and vegetation to heavy metal pollution—A case study, *Environ. Sci. Technol.*, *37*, 4417–4424, doi:10.1021/es0200645.

Just, J., M. J. Dekkers, T. von Dobeneck, A. van Hoesel, and T. Bickert (2012), Signatures and significance of aeolian, fluvial, bacterial and diagenetic magnetic mineral fractions in Late Quaternary marine sediments off Gambia, NW Africa, *Geochem. Geophys. Geosyst.*, *13*, Q0AO02, doi:10.1029/2012GC004146.

Kanfoush, S. L., D. A. Hodell, C. D. Charles, T. R. Janecek, and F. R. Rack (2002), Comparison of ice-rafted debris and physical properties in ODP Site 1094 (South Atlantic) with the Vostok ice core over the last four climatic cycles, *Palaeogeogr. Palaeoclimatol. Palaeoecol.*, *182*, 329–349, doi:10.1016/S0031-0182(01)00502-8.

Kao, S. J., C. S. Horng, A. P. Roberts, and K. K. Liu (2004), Carbon-sulfur-iron relationships in sedimentary rocks from southwestern Taiwan: Influence of geochemical environment on greigite and pyrrhotite formation, *Chem. Geol.*, *203*, 153–168, doi:10.1016/j.chemgeo.2003.09.007.

Karlin, R. (1990a), Magnetite diagenesis in marine sediments from the Oregon continental margin, *J. Geophys. Res.*, *95*, 4405–4419, doi:10.1029/JB095iB04p04405.

Karlin, R. (1990b), Magnetic mineral diagenesis in suboxic sediments at Bettis Site W-N, NE Pacific Ocean, *J. Geophys. Res.*, *95*, 4421–4436, doi:10.1029/JB095iB04p04421.

Karlin, R., and S. Levi (1983), Diagenesis of magnetic minerals in recent haemipelagic sediments, *Nature*, *303*, 327–330, doi:10.1038/303327a0.

Karlin, R., and S. Levi (1985), Geochemical and sedimentological control of the magnetic properties of hemipelagic sediments, *J. Geophys. Res.*, *90*, 10,373–10,392, doi:10.1029/JB090iB12p10373.

Karlin, R., M. Lyle, and G. R. Heath (1987), Authigenic magnetite formation in suboxic marine sediments, *Nature*, *326*, 490–493, doi:10.1038/326490a0.

Kasama, T., M. Pósfai, R. K. K. Chong, A. P. Finlayson, P. R. Buseck, R. B. Frankel, and R. E. Dunin-Borkowski (2006), Magnetic properties, microstructure, composition, and morphology of greigite nanocrystals in magnetotactic bacteria from electron holography and tomography, *Am. Mineral.*, *91*, 1216–1229, doi:10.2138/am.2006.2227.

Kasten, S., T. Freudenthal, F. X. Gingele, and H. D. Schulz (1998), Simultaneous formation of iron-rich layers at different redox boundaries in sediments of the Amazon deep-sea fan, *Geochim. Cosmochim. Acta*, *62*, 2253–2264, doi:10.1016/S0016-7037(98)00093-3.

Kawamura, N., H. Oda, K. Ikehara, T. Yamazaki, K. Shioi, S. Taga, S. Hatakeyama, and M. Torii (2007), Diagenetic effect on magnetic properties of marine core sediments from the southern Okhotsk Sea, *Earth Planets Space*, *59*, 83–93.

Kim, W., S. J. Doh, Y. H. Park, and S. T. Yun (2007), Two-year magnetic monitoring in conjunction with geochemical and electron microscopic data of roadside dust in Seoul, Korea, *Atmos. Environ.*, *41*, 7627–7641, doi:10.1016/j.atmosenv.2007.05.050.

Kind, J., A. U. Gehring, M. Winklhofer, and A. M. Hirt (2011), Combined use of magnetometry and spectroscopy for identifying magnetofossils in sediments, *Geochem. Geophys. Geosyst.*, *12*, Q08008, doi:10.1029/2011GC003633.

King, J., and J. E. T. Channell (1991), Sedimentary magnetism, environmental magnetism, and magnetostratigraphy, in *U.S. National Report to the International Union of Geodesy and Geophysics*, vol. 29, pp. 358–370, AGU, Washington, D. C.

King, J., S. K. Banerjee, and J. Marvin (1982), A comparison of different magnetic methods for determining the relative grain size of magnetite in natural materials: Some results from lake sediments, *Earth Planet. Sci. Lett.*, *59*, 404–419, doi:10.1016/0012-821X(82)90142-X.

Kirschvink, J. L. (1983), Biomagnetic geomagnetism, *Rev. Geophys.*, *21*, 672–675, doi:10.1029/RG021i003p00672.

Kirschvink, J. L., and J. L. Gould (1981), Biogenic magnetite as a basis for magnetic field detection in animals, *Biosystems*, *13*, 181–201, doi:10.1016/0303-2647(81)90060-5.

Kirschvink, J. L., and A. K. Kirschvink (1991), Is geomagnetic sensitivity real? Replication of the Walker-Bitterman magnetic conditioning experiment in honey bees, *Am. Zool.*, *31*, 169–186.

Kirschvink, J. L., A. Kobayashi-Kirschvink, and B. J. Woodford (1992), Magnetite biomineralization in the human brain, *Proc. Natl. Acad. Sci. U. S. A.*, *89*, 7683–7687, doi:10.1073/pnas.89.16.7683.

Kissel, C., C. Laj, B. Lehman, L. Labeyrie, and V. Bout-Boumazelles (1997), Changes in the strength of the Iceland-Scotland Overflow Water in the last 200,000 years: Evidence from magnetic anisotropy analysis of core SU90–33, *Earth Planet. Sci. Lett.*, *152*, 25–36, doi:10.1016/S0012-821X(97)00146-5.

Kissel, C., C. Laj, A. Mazaud, and T. Dokken (1998), Magnetic anisotropy and environmental changes in two sedimentary cores from the Norwegian Sea and the North Atlantic, *Earth Planet. Sci. Lett.*, *164*, 617–626, doi:10.1016/S0040-1951(98)00223-6.

Kissel, C., C. Laj, L. Labeyrie, T. Dokken, A. Voelker, and D. Blamart (1999), Rapid climatic variations during marine isotopic stage 3: Magnetic analysis of sediments from Nordic Seas and North Atlantic, *Earth Planet. Sci. Lett.*, *171*, 489–502, doi:10.1016/S0012-821X(99)00162-4.

Kissel, C., C. Laj, S. Clemens, and P. Solheid (2003), Magnetic signature of environmental changes in the last 1.2 Myr at ODP Site 1146, South China Sea, *Mar. Geol.*, *201*, 119–132, doi:10.1016/S0025-3227(03)00212-3.

Kissel, C., C. Laj, T. Mulder, C. Wandres, and M. Cremer (2009), The magnetic fraction: A tracer of deep water circulation in the North Atlantic, *Earth Planet. Sci. Lett.*, *288*, 444–454, doi:10.1016/j.epsl.2009.10.005.

Köhler, C. M., D. Heslop, M. J. Dekkers, W. Krijgsman, D. J. J. van Hinsbergen, and T. von Dobeneck (2008), Tracking provenance change during the late Miocene in the eastern Mediterranean using geochemical and environmental magnetic parameters, *Geochem. Geophys. Geosyst.*, *9*, Q12018, doi:10.1029/2008GC002127.

Kopp, R. E., and J. L. Kirschvink (2008), The identification and biogeochemical interpretation of fossil magnetotactic bacteria, *Earth Sci. Rev.*, *86*, 42–61, doi:10.1016/j.earscirev.2007.08.001.

Kopp, R. E., T. D. Raub, D. Schumann, H. Vali, A. V. Smirnov, and J. L. Kirschvink (2007), Magnetofossil spike during the Paleocene-Eocene thermal maximum: Ferromagnetic resonance, rock magnetic, and electron microscopy evidence from Ancora, New Jersey, United States, *Paleoceanography*, *22*, PA4103, doi:10.1029/2007PA001473.

Kopp, R. E., D. Schumann, T. D. Raub, D. S. Powars, L. V. Godfrey, N. L. Swanson-Hysell, A. C. Maloof, and H. Vali (2009), An Appalachian Amazon? Magnetofossil evidence for the development of a tropical river-like system in the mid-Atlantic United States during the Paleocene-Eocene Thermal Maximum, *Paleoceanography*, *24*, PA4211, doi:10.1029/2009PA001783.

Kosterov, A. (2003), Low-temperature magnetization and AC susceptibility of magnetite: Effect of thermomagnetic history, *Geophys. J. Int.*, *154*, 58–71, doi:10.1046/j.1365-246X.2003.01938.x.

Krs, M., F. Novák, M. Krsová, P. Pruner, L. Kouklíková, and J. Jansa (1992), Magnetic properties and metastability of greigite-smythite mineralization in brown-coal basins of the Krusné hory Piedmont, Bohemia, *Phys. Earth Planet. Inter.*, *70*, 273–287, doi:10.1016/0031-9201(92)90194-Z.

Kruiver, P. P., and H. F. Passier (2001), Coercivity analysis of magnetic phases in sapropel S1 related to variations in redox conditions, including an investigation of the *S* ratio, *Geochem. Geophys. Geosyst.*, *2*(12), 1063, doi:10.1029/2001GC000181.

Kruiver, P. P., M. J. Dekkers, and D. Heslop (2001), Quantification of magnetic coercivity components by the analysis of acquisition curves of isothermal remanent magnetization, *Earth Planet. Sci. Lett.*, *189*, 269–276, doi:10.1016/S0012-821X(01)00367-3.

Kukla, G., F. Heller, X. M. Liu, T. C. Xu, T. S. Liu, and Z. S. An (1988), Pleistocene climates in China dated by magnetic susceptibility, *Geology*, *16*, 811–814, doi:10.1130/0091-7613(1988)016<0811:PCICDB>2.3.CO;2.

Kumaravel, V., S. J. Sangode, N. Siva Siddaiah, and R. Kumar (2005), Rock magnetic characterization of pedogenesis under high-energy depositional conditions: A case study from the Mio-Pliocene Siwalik fluvial sequence near Dehra Dun, NW Himalaya, India, *Sediment. Geol.*, *177*, 229–252, doi:10.1016/j.sedgeo.2005.03.006.

Lagroix, F., and S. K. Banerjee (2004), The regional and temporal significance of primary aeolian magnetic fabrics preserved in Alaskan loess, *Earth Planet. Sci. Lett.*, *225*, 379–395, doi:10.1016/j.epsl.2004.07.003.

Lagroix, F., S. K. Banerjee, and M. J. Jackson (2004), Magnetic properties of the Old Crow tephra: Identification of a complex iron titanium oxide mineralogy, *J. Geophys. Res.*, *109*, B01104, doi:10.1029/2003JB002678.

Lam, K. P., et al. (2010), Characterizing magnetism of individual magnetosomes by X-ray magnetic circular dichroism in a scanning transmission X-ray microscope, *Chem. Geol.*, *270*, 110–116, doi:10.1016/j.chemgeo.2009.11.009.

Lambert, F., B. Delmonte, J. R. Petit, M. Bigler, P. R. Kaufmann, M. A. Hutterli, T. F. Stocker, U. Ruth, J. P. Steffensen, and V. Maggi (2008), Dust-climate couplings over the past

800,000 years from the EPICA Dome C ice core, *Nature*, *452*, 616–619, doi:10.1038/nature06763.

Lanci, L., and D. V. Kent (2006), Meteoric smoke fallout revealed by superparamagnetism in Greenland ice, *Geophys. Res. Lett.*, *33*, L13308, doi:10.1029/2006GL026480.

Lanci, L., A. M. Hirt, W. Lowrie, A. F. Lotter, G. Lemcke, and M. Sturm (1999), Mineral-magnetic record of Late Quaternary climatic changes in a high Alpine lake, *Earth Planet. Sci. Lett.*, *170*, 49–59, doi:10.1016/S0012-821X(99)00098-9.

Lanci, L., D. V. Kent, P. E. Biscaye, and J. P. Steffensen (2004), Magnetization of Greenland ice and its relationship with dust content, *J. Geophys. Res.*, *109*, D09104, doi:10.1029/2003JD004433.

Lanci, L., B. Delmote, V. Maggi, J. R. Petit, and D. V. Kent (2008), Ice magnetization in the EPICA-Dome C ice core: Implications for dust sources during glacial and interglacial periods, *J. Geophys. Res.*, *113*, D14207, doi:10.1029/2007JD009678.

Lanci, L., B. Delmote, D. V. Kent, V. Maggi, P. E. Biscaye, and J. R. Petit (2012), Magnetization of polar ice: A measurement of terrestrial dust and extraterrestrial fallout, *Quat. Sci. Rev.*, *33*, 20–31, doi:10.1016/j.quascirev.2011.11.023.

Larrasoaña, J. C., A. P. Roberts, E. J. Rohling, M. Winklhofer, and R. Wehausen (2003a), Three million years of monsoon variability over the northern Sahara, *Clim. Dyn.*, *21*, 689–698, doi:10.1007/s00382-003-0355-z.

Larrasoaña, J. C., A. P. Roberts, J. S. Stoner, C. Richter, and R. Wehausen (2003b), A new proxy for bottom-water ventilation in the eastern Mediterranean based on diagenetically controlled magnetic properties of sapropel-bearing sediments, *Palaeogeogr. Palaeoclimatol. Palaeoecol.*, *190*, 221–242, doi:10.1016/S0031-0182(02)00607-7.

Larrasoaña, J. C., A. P. Roberts, A. Hayes, R. Wehausen, and E. J. Rohling (2006), Detecting missing beats in the Mediterranean climate rhythm from magnetic identification of oxidized sapropels (Ocean Drilling Program Leg 160), *Phys. Earth Planet. Inter.*, *156*, 283–293, doi:10.1016/j.pepi.2005.04.017.

Larrasoaña, J. C., A. P. Roberts, R. J. Musgrave, E. Gràcia, E. Piñero, M. Vega, and F. Martínez-Ruiz (2007), Diagenetic formation of greigite and pyrrhotite in marine sedimentary systems containing gas hydrates, *Earth Planet. Sci. Lett.*, *261*, 350–366, doi:10.1016/j.epsl.2007.06.032.

Larrasoaña, J. C., A. P. Roberts, and E. J. Rohling (2008), Magnetic susceptibility of eastern Mediterranean marine sediments as a proxy for Saharan dust supply?, *Mar. Geol.*, *254*, 224–229, doi:10.1016/j.margeo.2008.06.003.

Larrasoaña, J. C., M. Ortuño, H. H. Birks, B. Valero-Garcés, J. M. Parés, R. Copons, L. Camarero, and J. Bordonau (2010), Palaeoenvironmental and palaeoseismic implications of a 3700-year sedimentary record from proglacial Lake Barrancs (Maladeta Massif, Central Pyrenees, Spain), *Palaeogeogr. Palaeoclimatol. Palaeoecol.*, *294*, 83–93, doi:10.1016/j.palaeo.2009.04.003.

Larrasoaña, J. C., A. P. Roberts, L. Chang, S. A. Schellenberg, J. D. Fitz Gerald, R. D. Norris, and J. C. Zachos (2012), Magnetotactic bacterial response to Antarctic dust supply during the Palaeocene-Eocene thermal maximum, *Earth Planet. Sci. Lett.*, *333–334*, 122–133, doi:10.1016/j.epsl.2012.04.003.

Lascu, I., and J. M. Feinberg (2011), Speleothem magnetism, *Quat. Sci. Rev.*, *30*, 3306–3320, doi:10.1016/j.quascirev.2011.08.004.

Lean, C. M. B., and I. N. McCave (1998), Glacial to interglacial mineral magnetic and palaeoceanographic changes at Chatham Rise, SW Pacific Ocean, *Earth Planet. Sci. Lett.*, *163*, 247–260, doi:10.1016/S0012-821X(98)00191-5.

Lebreiro, S. M., J. C. Moreno, I. N. McCave, and P. P. E. Weaver (1996), Evidence for Heinrich layers off Portugal (Tore Seamount: 39°N, 12°W), *Mar. Geol.*, *131*, 47–56, doi:10.1016/0025-3227(95)00142-5.

Lefèvre, C. T., N. Menguy, F. Abreu, U. Lins, M. Pósfai, T. Prozorov, D. Pignol, R. B. Frankel, and D. Bazylinski (2011), A cultured greigite-producing magnetotactic bacterium in a novel group of sulfate-reducing bacteria, *Science*, *334*, 1720–1723, doi:10.1126/science.1212596.

Lehndorff, E., M. Urbat, and L. Schwark (2006), Accumulation histories of magnetic particles on pine needles as function of air quality, *Atmos. Environ.*, *40*, 7082–7096, doi:10.1016/j.atmosenv.2006.06.008.

Leslie, B. W., S. P. Lund, and D. E. Hammond (1990), Rock magnetic evidence for the dissolution and authigenic growth of magnetic minerals within anoxic sediments of the California continental borderland, *J. Geophys. Res.*, *95*, 4437–4452, doi:10.1029/JB095iB04p04437.

Li, J. H., Y. X. Pan, Q. S. Liu, and H. F. Qin (2009a), A comparative study of magnetic properties between whole cells and isolated magnetosomes of *Magnetospirillum Magneticum* AMB-1: Implications for magnetostatic interaction, *Chin. Sci. Bull.*, *54*, 3345–3351.

Li, J. H., Y. X. Pan, G. J. Chen, Q. S. Liu, L. X. Tian, and W. Lin (2009b), Rock magnetic observations of magnetosome growth and fragmental chain formation of *Magnetospirillum magneticum* AMB-1, *Geophys. J. Int.*, *177*, 33–42, doi:10.1111/j.1365-246X.2009.04043.x.

Li, J. H., et al. (2010), Biomineralization, crystallography and magnetic properties of bullet-shaped magnetite magnetosomes in giant rod magnetotactic bacteria, *Earth Planet. Sci. Lett.*, *293*, 368–376, doi:10.1016/j.epsl.2010.03.007.

Li, X., X. Hu, Y. Cai, and Z. Han (2011), Quantitative analysis of iron oxide concentrations within Aptian-Albian cyclic oceanic red beds in ODP Hole 1049C, North Atlantic, *Sediment. Geol.*, *235*, 91–99, doi:10.1016/j.sedgeo.2010.06.024.

Lie, O., S. O. Dahl, A. Nesje, J. A. Matthews, and S. Sandvold (2004), Holocene fluctuations of a polythermal glacier in high-alpine eastern Jotunheim, central-southern Norway, *Quat. Sci. Rev.*, *23*, 1925–1945, doi:10.1016/j.quascirev.2004.03.012.

Lippert, P. C., and J. C. Zachos (2007), A biogenic origin for anomalous fine-grained magnetic material at the Paleocene-Eocene boundary at Wilson Lake, New Jersey, *Paleoceanography*, *22*, PA4104, doi:10.1029/2007PA001471.

Liu, J., R. X. Zhu, A. P. Roberts, S. Q. Li, and J. H. Chang (2004), High-resolution analysis of early diagenetic effects on magnetic minerals in post-middle-Holocene continental shelf sediments from the Korea Strait, *J. Geophys. Res.*, *109*, B03103, doi:10.1029/2003JB002813.

Liu, Q. S., S. K. Banerjee, M. J. Jackson, R. X. Zhu, and Y. X. Pan (2002), A new method in mineral magnetism for the separation of weak antiferromagnetic signal from a strong ferrimagnetic background, *Geophys. Res. Lett.*, *29*(12), 1565, doi:10.1029/2002GL014699.

Liu, Q. S., S. K. Banerjee, M. J. Jackson, F. H. Chen, Y. X. Pan, and R. X. Zhu (2003), An integrated study of the grain-size-dependent magnetic mineralogy of the Chinese loess/paleosol and its environmental significance, *J. Geophys. Res.*, *108*(B9), 2437, doi:10.1029/2002JB002264.

Liu, Q. S., J. Torrent, Y. J. Yu, and C. L. Deng (2004a), Mechanism of the parasitic remanence of aluminous goethite, [α-(Fe, Al) OOH], *J. Geophys. Res.*, *109*, B12106, doi:10.1029/2004JB003352.

Liu, Q. S., M. J. Jackson, S. K. Banerjee, B. A. Maher, C. L. Deng, Y. X. Pan, and R. X. Zhu (2004b), Mechanism of the magnetic susceptibility enhancements of the Chinese loess, *J. Geophys. Res.*, *109*, B12107, doi:10.1029/2004JB003249.

Liu, Q. S., M. J. Jackson, Y. J. Yu, F. H. Chen, C. L. Deng, and R. X. Zhu (2004c), Grain size distribution of pedogenic magnetic particles in Chinese loess/paleosols, *Geophys. Res. Lett.*, *31*, L22603, doi:10.1029/2004GL021090.

Liu, Q. S., S. K. Banerjee, M. J. Jackson, F. H. Chen, Y. X. Pan, and R. X. Zhu (2004d), Determining the climatic boundary between the Chinese loess and palaeosol: Evidence from aeolian coarse-grained magnetite, *Geophys. J. Int.*, *156*, 267–274, doi:10.1111/j.1365-246X.2003.02148.x.

Liu, Q. S., J. Torrent, B. A. Maher, Y. J. Yu, C. L. Deng, R. X. Zhu, and X. X. Zhao (2005a), Quantifying grain size distribution of pedogenic magnetic particles in Chinese loess and its significance for pedogenesis, *J. Geophys. Res.*, *110*, B11102, doi:10.1029/2005JB003726.

Liu, Q. S., C. L. Deng, Y. J. Yu, J. Torrent, M. J. Jackson, S. K. Banerjee, and R. X. Zhu (2005b), Temperature dependence of magnetic susceptibility in an argon environment: Implications for pedogenesis of Chinese loess/palaeosols, *Geophys. J. Int.*, *161*, 102–112, doi:10.1111/j.1365-246X.2005.02564.x.

Liu, Q. S., S. K. Banerjee, M. J. Jackson, C. L. Deng, Y. X. Pan, and R. X. Zhu (2005c), Inter-profile correlation of the Chinese loess/paleosol sequences during Marine Oxygen Isotope Stage 5 and indications of pedogenesis, *Quat. Sci. Rev.*, *24*, 195–210, doi:10.1016/j.quascirev.2004.07.021.

Liu, Q. S., Y. J. Yu, Y. X. Pan, R. X. Zhu, and X. X. Zhao (2005d), Partial anhysteretic remanent magnetization (pARM) of synthetic single- and multi-domain magnetites and its paleoenvironmental significance, *Chin. Sci. Bull.*, *50*, 2381–2384, doi:10.1007/BF03183751.

Liu, Q. S., Y. J. Yu, J. Torrent, A. P. Roberts, Y. X. Pan, and R. X. Zhu (2006a), Characteristic low-temperature magnetic properties of aluminous goethite [α-(Fe, Al) OOH] explained, *J. Geophys. Res.*, *111*, B12S34, doi:10.1029/2006JB004560.

Liu, Q. S., J. Bloemendal, J. Torrent, and C. L. Deng (2006b), Contrasting behavior of hematite and goethite within paleosol S5 of the Luochuan profile, Chinese Loess Plateau, *Geophys. Res. Lett.*, *33*, L20301, doi:10.1029/2006GL027172.

Liu, Q. S., C. L. Deng, J. Torrent, and R. X. Zhu (2007a), Review of recent developments in mineral magnetism of the Chinese loess, *Quat. Sci. Rev.*, *26*, 368–385, doi:10.1016/j.quascirev.2006.08.004.

Liu, Q. S., A. P. Roberts, J. Torrent, C. S. Horng, and J. C. Larrasoaña (2007b), What do the HIRM and S-ratio really measure in environmental magnetism?, *Geochem. Geophys. Geosyst.*, *8*, Q09011, doi:10.1029/2007GC001717.

Liu, Q. S., J. Torrent, H. Morrás, H. Ao, Z. X. Jiang, and Y. L. Su (2010), Superparamagnetism of two modern soils from the northeastern Pampean region, Argentina, and its paleoclimatic indications, *Geophys. J. Int.*, *183*, 695–705, doi:10.1111/j.1365-246X.2010.04786.x.

Liu, Q. S., J. Torrent, V. Barrón, Z. Q. Duan, and J. Bloemendal (2011), Quantification of hematite from the visible diffuse reflectance spectrum: Effects of aluminum substitution and grain morphology, *Clay Miner.*, *46*, 137–147, doi:10.1180/claymin.2011.046.1.137.

Liu, T. S. (1985), *Loess and the Environment*, China Ocean Press, Beijing.

Liu, T. S., and Z. L. Ding (1998), Chinese loess and the paleomonsoon, *Annu. Rev. Earth Planet. Sci.*, *26*, 111–145, doi:10.1146/annurev.earth.26.1.111.

Love, S. G., and D. E. Brownlee (1993), A direct measurement of the terrestrial mass accretion rate of cosmic dust, *Science*, *262*, 550–553, doi:10.1126/science.262.5133.550.

Lowrie, W. (1990), Identification of ferromagnetic minerals in a rock by coercivity and unblocking temperature properties, *Geophys. Res. Lett.*, *17*, 159–162, doi:10.1029/GL017i002p00159.

Lyons, R., F. Oldfield, and E. Williams (2010), Mineral magnetic properties of surface soils and sands across four North African transects and links to climatic gradients, *Geochem. Geophys. Geosyst.*, *11*, Q08023, doi:10.1029/2010GC003183.

Lyons, R., F. Oldfield, and E. Willams (2012), The possible role of magnetic measurements in the discrimination of Sahara/Sahel dust sources, *Earth Surf. Processes Landforms*, *37*, 594–606, doi:10.1002/esp.2268.

Maher, B. A. (1986), Characterisation of soils by mineral magnetic measurements, *Phys. Earth Planet. Inter.*, *42*, 76–92, doi:10.1016/S0031-9201(86)80010-3.

Maher, B. A. (1988), Magnetic properties of some synthetic submicron magnetites, *Geophys. J.*, *94*, 83–96, doi:10.1111/j.1365-246X.1988.tb03429.x.

Maher, B. A. (1998), Magnetic properties of modern soils and loessic paleosols: Implications for paleoclimate, *Palaeogeogr. Palaeoclimatol. Palaeoecol.*, *137*, 25–54, doi:10.1016/S0031-0182(97)00103-X.

Maher, B. A. (2011), The magnetic properties of Quaternary aeolian dusts and sediments, and their palaeoclimatic significance, *Aeolian Res.*, *3*, 87–144, doi:10.1016/j.aeolia.2011.01.005.

Maher, B. A., and P. F. Dennis (2001), Evidence against dust-mediated control of glacial-interglacial changes in atmospheric CO_2, *Nature*, *411*, 176–180, doi:10.1038/35075543.

Maher, B. A., and M. W. Hounslow (1999), Palaeomonsoons II: Magnetic records of aeolian dust in Quaternary sediments of the Indian Ocean, in *Quaternary Climates, Environments, and Magnetism*, edited by B. A. Maher and R. Thompson, pp. 126–162, Cambridge Univ. Press, Cambridge, U. K., doi:10.1017/CBO9780511535635.005

Maher, B. A., and M. Hu (2006), A high-resolution record of Holocene rainfall variations from the western Chinese Loess Plateau: Antiphase behaviour of the African/Indian and East Asian summer monsoons, *Holocene*, *16*, 309–319, doi:10.1191/0959683606hl929rp.

Maher, B. A., and R. Thompson (1991), Mineral magnetic record of the Chinese loess and paleosols, *Geology*, *19*, 3–6, doi:10.1130/0091-7613(1991)019<0003:MMROTC>2.3.CO;2.

Maher, B. A., and R. Thompson (1992), Paleoclimatic significance of the mineral magnetic record of the Chinese loess and paleosols, *Quat. Res.*, *37*, 155–170, doi:10.1016/0033-5894(92)90079-X.

Maher, B. A., and R. Thompson (1995), Paleorainfall reconstructions from pedogenic magnetic susceptibility variations in the Chinese loess and paleosols, *Quat. Res.*, *44*, 383–391, doi:10.1006/qres.1995.1083.

Maher, B. A., and R. Thompson (Eds.) (1999), *Quaternary Climates, Environments and Magnetism*, Cambridge Univ. Press, Cambridge, U. K., doi:10.1017/CBO9780511535635

Maher, B. A., R. Thompson, and L. P. Zhou (1994), Spatial and temporal reconstructions of changes in the Asian palaeomonsoon: A new mineral magnetic approach, *Earth Planet. Sci. Lett.*, *125*, 461–471, doi:10.1016/0012-821X(94)90232-1.

Maher, B. A., A. Alekseev, and T. Alekseeva (2002), Variation of soil magnetism across the Russian steppe: Its significance for use of soil magnetism as a palaeorainfall proxy, *Quat. Sci. Rev.*, *21*, 1571–1576, doi:10.1016/S0277-3791(02)00022-7.

Maher, B. A., M. Hu, H. M. Roberts, and A. G. Wintle (2003), Holocene loess accumulation and soil development at the western edge of the Chinese Loess Plateau: Implications for magnetic proxies of paleorainfall, *Quat. Sci. Rev.*, *22*, 445–451, doi:10.1016/S0277-3791(02)00188-9.

Maher, B. A., V. V. Karloukovski, and T. J. Mutch (2004), High-field remanence properties of synthetic and natural submicrometre haematites and goethites: Significance for environmental contexts, *Earth Planet. Sci. Lett.*, *226*, 491–505, doi:10.1016/j.epsl.2004.05.042.

Maher, B. A., C. Moore, and J. Matzka (2008), Spatial variation in vehicle-derived metal pollution identified by magnetic and elemental analysis of roadside tree leaves, *Atmos. Environ.*, *42*, 364–373, doi:10.1016/j.atmosenv.2007.09.013.

Maher, B. A., T. J. Mutch, and D. Cunningham (2009a), Magnetic and geochemical characteristics of Gobi Desert surface sediments: Implications for provenance of the Chinese Loess Plateau, *Geology*, *37*, 279–282, doi:10.1130/G25293A.1.

Maher, B. A., S. J. Watkins, G. Brunskill, J. Alexander, and C. R. Fielding (2009b), Sediment provenance in a tropical fluvial and marine context by magnetic 'fingerprinting' of transportable sand fractions, *Sedimentology*, *56*, 841–861, doi:10.1111/j.1365-3091.2008.00999.x.

Maher, B. A., J. Prospero, D. Mackie, D. M. Gaiero, P. P. Hesse, and Y. Balkanski (2010), Global connections between aeolian dust, climate and ocean biogeochemistry at the present day and at the last glacial maximum, *Earth Sci. Rev.*, *99*, 61–97, doi:10.1016/j.earscirev.2009.12.001.

Maillot, F., G. Morin, Y. Wang, D. Bonnin, P. Ildefonse, C. Chaneac, and G. Calas (2011), New insight into the structure of nanocrystalline ferrihydrite: EXAFS evidence for tetrahedrally coordinated iron(III), *Geochim. Cosmochim. Acta*, *75*, 2708–2720, doi:10.1016/j.gca.2011.03.011.

Malki, M., E. González-Toril, J. L. Sanz, F. Gómez, N. Rodríguez, and R. Amils (2006), Importance of the iron cycle in biohydrometallurgy, *Hydrometallurgy*, *83*, 223–228, doi:10.1016/j.hydromet.2006.03.053.

Mamet, B., and A. Preat (2006), Iron-bacterial mediation in Phanerozoic red limestones: State of the art, *Sediment. Geol.*, *185*, 147–157, doi:10.1016/j.sedgeo.2005.12.009.

Manceau, A. (2009), Evaluation of the structural model for ferrihydrite derived from real-space modeling of high-energy X-ray diffraction data, *Clay Miner.*, *44*, 19–34, doi:10.1180/claymin.2009.044.1.19.

Manceau, A. (2011), Critical evaluation of the revised akdalaite-model for ferrihydrite, *Am. Mineral.*, *96*, 521–533, doi:10.2138/am.2011.3583.

Mann, S., N. H. C. Sparks, R. B. Frankel, D. A. Bazylinski, and H. W. Jannasch (1990), Biomineralization of ferrimagnetic greigite (Fe_3S_4) and iron pyrite (FeS_2) in a magnetotactic bacterium, *Nature*, *343*, 258–261, doi:10.1038/343258a0.

Maslin, M. A., et al. (2000), Palaeoreconstruction of the Amazon River freshwater and sediment discharge using sediments recovered at Site 942 on the Amazon Fan, *J. Quat. Sci.*, *15*, 419–434, doi:10.1002/1099-1417(200005)15:4<419::AID-JQS541>3.0.CO;2-L.

Matzka, J., and B. A. Maher (1999), Magnetic biomonitoring of roadside leaves: Identification of spatial and temporal variations in vehicle-derived particulates, *Atmos. Environ.*, *33*, 4565–4569, doi:10.1016/S1352-2310(99)00229-0.

Mayergoyz, I. D. (1986), Mathematical models of hysteresis, *IEEE Trans. Magn.*, *22*, 603–608, doi:10.1109/TMAG.1986.1064347.

Mazaud, A., C. Kissel, C. Laj, M. A. Sicre, E. Michel, and J. L. Turon (2007), Variations of the ACC-CDW during MIS3 traced by magnetic grain deposition in midlatitude south Indian Ocean cores: Connections with the northern hemisphere and with central Antarctica, *Geochem. Geophys. Geosyst.*, *8*, Q05012, doi:10.1029/2006GC001532.

Mazaud, A., E. Michel, F. Dewilde, and J. L. Turon (2010), Variations of the Antarctic Circumpolar Current intensity during the past 500 ka, *Geochem. Geophys. Geosyst.*, *11*, Q08007, doi:10.1029/2010GC003033.

Mead, G., L. Tauxe, and J. L. LaBrecque (1986), Oligocene paleoceanography of the South Atlantic, *Paleoceanography*, *1*, 273–284, doi:10.1029/PA001i003p00273.

Mehra, O. P., and M. L. Jackson (1958), Iron oxide removal from soils and clays by a dithionite−citrate system buffered with sodium bicarbonate, *Clays Clay Miner.*, *7*, 317–327, doi:10.1346/CCMN.1958.0070122.

Michel, F. M., L. Ehm, S. M. Antao, P. L. Lee, P. J. Chupas, G. Liu, D. R. Strongin, M. A. A. Schoonen, B. L. Phillips, and J. B. Parise (2007), The structure of ferrihydrite, a nanocrystalline material, *Science*, *316*, 1726–1729, doi:10.1126/science.1142525.

Michel, F. M., V. Barrón, J. Torrent, M. P. Morales, C. J. Serna, J. F. Boilye, Q. S. Liu, A. Ambrosinig, C. A. Cismasu, and G. E. Brown (2010), Ordered ferrimagnetic form of ferrihydrite reveals links between structure, composition and magnetism, *Proc. Natl. Acad. Sci. U. S. A.*, *107*, 2787–2792, doi:10.1073/pnas.0910170107.

Mikhaylova, A., M. Davidson, J. E. T. Channell, Y. Guyodo, C. Batich, and J. Dobson (2005), Detection, identification and mapping of iron anomalies in brain tissue using X-Ray absorption spectroscopy, *J. R. Soc. Interface*, *2*, 33–37, doi:10.1098/rsif.2004.0011.

Miller, D. A., and R. A. White (1998), A conterminous United States multilayer soil characteristics dataset for regional climate and hydrology modeling, *Earth Interact.*, *2*, 1–26, doi:10.1175/1087-3562(1998)002<0001:ACUSMS>2.3.CO;2.

Milliman, J. D., and J. P. M. Syvitski (1992), Geomorphic tectonic control of the sediment discharge to the ocean–the importance of small mountainous rivers, *J. Geol.*, *100*, 525–544, doi:10.1086/629606.

Mitra, S., S. Das, S. Basu, P. Sahu, and K. Mandal (2009), Shape- and field-dependent Morin transitions in structured α–Fe_2O_3, *J. Magn. Magn. Mater.*, *321*, 2925–2931, doi:10.1016/j.jmmm.2009.04.044.

Mohamed, K. J., D. Rey, B. Rubio, M. J. Dekkers, A. P. Roberts, and F. Vilas (2011), Onshore-offshore gradient in reductive early diagenesis in coastal marine sediments of the Ria de Vigo, Northwest Iberian Peninsula, *Cont. Shelf Res.*, *31*, 433–447, doi:10.1016/j.csr.2010.06.006.

Moore, A., S. M. Freake, and I. M. Thomas (1990), Magnetic particles in the lateral line of the Atlantic salmon (*Salmo salar* L.), *Philos. Trans. R. Soc. London, Ser. B*, *329*, 11–15, doi:10.1098/rstb.1990.0145.

Moreau, M. G., I. Cojan, and J. Ory (1994), Mechanisms of remanent magnetization acquisition in marl and limestone alternations. Case study: Upper Cretaceous (Chron 31–30), Sopelana, Basque Country, *Earth Planet. Sci. Lett.*, *123*, 15–37, doi:10.1016/0012-821X(94)90254-2.

Moreno, E., L. Sagnotti, J. Dinarès-Turell, A. Winkler, and A. Cascella (2003), Biomonitoring of traffic air pollution in Rome using magnetic properties of tree leaves, *Atmos. Environ.*, *37*, 2967–2977, doi:10.1016/S1352-2310(03)00244-9.

Morin, F. J. (1950), Magnetic susceptibility of αFe_2O_3 and αFe_2O_3 with added titanium, *Phys. Rev.*, *78*, 819–820, doi:10.1103/PhysRev.78.819.2.

Morse, J. W., and Q. W. Wang (1997), Pyrite formation under conditions approximating those in anoxic sediments: II. Influence of precursor iron minerals and organic matter, *Mar. Chem.*, *57*, 187–193, doi:10.1016/S0304-4203(97)00050-9.

Moskowitz, B. M. (1995), Biomineralization of magnetic minerals, *Rev. Geophys.*, *33*(S1), 123–128, doi:10.1029/95RG00443.

Moskowitz, B. M., R. B. Frankel, and D. A. Bazylinski (1993), Rock magnetic criteria for the detection of biogenic magnetite, *Earth Planet. Sci. Lett.*, *120*, 283–300, doi:10.1016/0012-821X(93)90245-5.

Moskowitz, B. M., M. Jackson, and C. Kissel (1998), Low-temperature magnetic behavior of titanomagnetites, *Earth Planet. Sci. Lett.*, *157*, 141–149, doi:10.1016/S0012-821X(98)00033-8.

Moskowitz, B. M., D. A. Bazylinski, R. Egli, R. B. Frankel, and K. J. Edwards (2008), Magnetic properties of marine magnetotactic bacteria in a seasonally stratified coastal pond (Salt Pond, MA, USA), *Geophys. J. Int.*, *174*, 75–92, doi:10.1111/j.1365-246X.2008.03789.x.

Mullins, C. E. (1977), Magnetic susceptibility of soil and its significance in soil science—A review, *J. Soil Sci.*, *28*, 223–246, doi:10.1111/j.1365-2389.1977.tb02232.x.

Musgrave, R. J., N. L. Bangs, J. C. Larrasoaña, E. Gràcia, J. A. Hollamby, and M. E. Vega (2006), Rise of the base of the gas hydrate zone since the last glacial recorded by rock magnetism, *Geology*, *34*, 117–120, doi:10.1130/G22008.1.

Muxworthy, A., W. Williams, and D. Virdee (2003), The effect of magnetostatic interactions on the hysteresis parameters of single-domain and pseudo-single domain grains, *J. Geophys. Res.*, *108*(B11), 2517, doi:10.1029/2003JB002588.

Muxworthy, A., D. Heslop, and W. Williams (2004), Influence of magnetostatic interactions on first-order-reversal-curve (FORC) diagrams: A micromagnetic approach, *Geophys. J. Int.*, *158*, 888–897, doi:10.1111/j.1365-246X.2004.02358.x.

Muxworthy, A. R. (2001), Effect of grain interactions on the frequency dependence of magnetic susceptibility, *Geophys. J. Int.*, *144*, 441–447, doi:10.1046/j.1365-246x.2001.00342.x.

Muxworthy, A. R., J. Matzka, and N. Petersen (2001), Comparison of magnetic parameters of urban atmospheric particulate matter with pollution and meteorological data, *Atmos. Environ.*, *35*, 4379–4386, doi:10.1016/S1352-2310(01)00250-3.

Muxworthy, A. R., J. G. King, and D. Heslop (2005), Assessing the ability of first-order reversal curve (FORC) diagrams to unravel complex magnetic signals, *J. Geophys. Res.*, *110*, B01105, doi:10.1029/2004JB003195.

Nagy, E. A., and J.-P. Valet (1993), New advances for paleomagnetic studies of sediment cores using U-channels, *Geophys. Res. Lett.*, *20*, 671–674, doi:10.1029/93GL00213.

Neretin, L. N., M. E. Böttcher, B. B. Jørgensen, I. I. Volkov, H. Lüschen, and K. Kilgenfeldt (2004), Pyritization processes and greigite formation in the advancing sulphidization front in the Upper Pleistocene sediments of the Black Sea, *Geochim. Cosmochim. Acta*, *68*, 2081–2093, doi:10.1016/S0016-7037(03)00450-2.

Nesje, A., A. E. Bjune, J. Bakke, S. O. Dahl, O. Lie, and H. J. B. Birks (2006), Holocene palaeoclimate reconstructions at Vanndalsvatnet, western Norway, with particular reference to the 8200 cal. yr BP event, *Holocene*, *16*, 717–729, doi:10.1191/0959683606hl954rp.

Nishitani, T., and M. Kono (1983), Curie-temperature and lattice constant of oxidized titanomagnetite, *Geophys. J. R. Astron. Soc.*, *74*, 585–600.

Nolan, S. R., J. Bloemendal, J. F. Boyle, R. T. Jones, F. Oldfield, and M. Whitney (1999), Mineral magnetic and geochemical records of Late Glacial climatic change from two northwest European carbonate lakes, *J. Paleolimnol.*, *22*, 97–107, doi:10.1023/A:1008097518004.

Oldfield, F. (1991), Environmental magnetism—A personal perspective, *Quat. Sci. Rev.*, *10*, 73–85, doi:10.1016/0277-3791(91)90031-O.

Oldfield, F., and J. Bloemendal (2011), Rock-magnetic properties confirm the eolian origin of Miocene sequences from the west of the Chinese Loess Plateau, *Sediment. Geol.*, *234*, 70–75, doi:10.1016/j.sedgeo.2010.11.009.

Oldfield, F., T. A. Rummery, R. Thompson, and D. E. Walling (1979), Identification of suspended sediment sources by means of magnetic measurements: Some preliminary results, *Water Resour. Res.*, *15*, 211–218, doi:10.1029/WR015i002p00211.

Oldfield, F., B. A. Maher, J. Donoghue, and J. Pierce (1985), Particle-size related, mineral magnetic source-sediment linkages in the Rhode River catchment, Maryland, USA, *J. Geol. Soc.*, *142*, 1035–1046, doi:10.1144/gsjgs.142.6.1035.

Oldfield, F., I. Darnley, G. Yates, D. E. France, and J. Hilton (1992), Storage diagenesis versus sulphide authigenesis: Possible implications in environmental magnetism, *J. Paleolimnol.*, *7*, 179–190, doi:10.1007/BF00181713.

Oldfield, F., R. Wake, J. Boyle, R. Jones, S. Nolan, Z. Gibbs, P. Appleby, E. Fisher, and G. Wolff (2003), The late-Holocene history of Gormire Lake (NE England) and its catchment: A multiproxy reconstruction of past human impact, *Holocene*, *13*, 677–690, doi:10.1191/0959683603hl654rp.

Oldfield, F., Q. Hao, J. Bloemendal, Z. Gibbs-Eggar, S. Patil, and Z. Guo (2009), Links between particle size and magnetic grain size: General observations and some implications for Chinese loess studies, *Sedimentology*, *56*, 2091–2106, doi:10.1111/j.1365-3091.2009.01071.x.

Openshaw, S., A. Latham, and J. Shaw (1997), Speleothem palaeosecular variation records from China: Their contribution to the coverage of Holocene palaeosecular variation data in East Asia, *Earth Planets Space*, *49*, 485–505.

O'Reilly, W. (1984), *Rock and Mineral Magnetism*, Chapman and Hall, New York, doi:10.1007/978-1-4684-8468-7

Orgeira, M. J., and R. Compagnucci (2006), Correlation between paleosol-soil magnetic signal and climate, *Earth Planets Space*, *58*, 1373–1380.

Özdemir, Ö., D. J. Dunlop, and B. M. Moskowitz (1993), The effect of oxidation on the Verwey transition in magnetite, *Geophys. Res. Lett.*, *20*, 1671–1674, doi:10.1029/93GL01483.

Paasche, Ø., and R. Løvlie (2011), Synchronized postglacial colonization by magnetotactic bacteria, *Geology*, *39*, 75–78, doi:10.1130/G31525.1.

Paasche, Ø., R. Løvlie, S. O. Dahl, J. Bakke, and A. Nesje (2004), Bacterial magnetite in lake sediments: Late glacial to Holocene climate and sedimentary changes in northern Norway, *Earth Planet. Sci. Lett.*, *223*, 319–333, doi:10.1016/j.epsl.2004.05.001.

Pan, Y., R. X. Zhu, J. Shaw, Q. S. Liu, and B. Guo (2001), Can relative paleointensities be determined from the normalized magnetization of the wind-blown loess of China?, *J. Geophys. Res.*, *106*, 19,221–19,232, doi:10.1029/2001JB000360.

Pan, Y., N. Petersen, M. Winklhofer, A. F. Davila, Q. Liu, T. Frederichs, M. Hanzlik, and R. Zhu (2005), Rock magnetic properties of uncultured magnetotactic bacteria, *Earth Planet. Sci. Lett.*, *237*, 311–325, doi:10.1016/j.epsl.2005.06.029.

Parés, J. M., N. J. C. Hassold, D. K. Rea, and B. A. van der Pluijm (2007), Paleocurrent directions from paleomagnetic reorientation of magnetic fabrics in deep-sea sediments at the Antarctic Peninsula Pacific margin (ODP Sites 1095, 1101), *Palaeogeogr. Palaeoclimatol. Palaeoecol.*, *242*, 261–269.

Passier, H. F., and M. J. Dekkers (2002), Iron oxide formation in the active oxidation front above sapropel S1 in the eastern Mediterranean Sea as derived from low-temperature magnetism, *Geophys. J. Int.*, *150*, 230–240, doi:10.1046/j.1365-246X.2002.01704.x.

Passier, H. F., G. J. de Lange, and M. J. Dekkers (2001), Magnetic properties and geochemistry of the active oxidation front and the youngest sapropel in the eastern Mediterranean Sea, *Geophys. J. Int.*, *145*, 604–614, doi:10.1046/j.0956-540x.2001.01394.x.

Peck, J. A., and J. W. King (1996), Magnetofossils in the sediment of Lake Baikal, Siberia, *Earth Planet. Sci. Lett.*, *140*, 159–172, doi:10.1016/0012-821X(96)00027-1.

Perkins, A. M. (1996), Observations under electron microscopy of magnetic minerals extracted from speleothems, *Earth Planet. Sci. Lett.*, *139*, 281–289, doi:10.1016/0012-821X(96)00013-1.

Petermann, H., and U. Bleil (1993), Detection of live magnetic bacteria in South Atlantic deep-sea sediments, *Earth Planet. Sci. Lett.*, *117*, 223–228, doi:10.1016/0012-821X(93)90128-V.

Peters, C., and M. J. Dekkers (2003), Selected room temperature magnetic parameters as a function of mineralogy, concentration and grain size, *Phys. Chem. Earth*, *28*, 659–667, doi:10.1016/S1474-7065(03)00120-7.

Peters, C., J. Walden, and W. E. N. Austin (2008), Magnetic signature of European margin sediments: Provenance of ice-rafted debris and the climatic response of the British ice sheet during Marine Isotope Stages 2 and 3, *J. Geophys. Res.*, *113*, F03007, doi:10.1029/2007JF000836.

Petersen, N., T. von Dobeneck, and H. Vali (1986), Fossil bacterial magnetite in deep-sea sediments from the South Atlantic Ocean, *Nature*, *320*, 611–615, doi:10.1038/320611a0.

Petrovský, E., and B. B. Ellwood (1999), Magnetic monitoring of pollution of air, land and waters, in *Quaternary Climates, Environments and Magnetism*, edited by B. A. Maher and R. Thompson, pp. 279–322, Cambridge Univ. Press, Cambridge, U. K., doi:10.1017/CBO9780511535635.009.

Pike, C. R., A. P. Roberts, and K. L. Verosub (1999), Characterizing interactions in fine magnetic particle systems using first order reversal curves, *J. Appl. Phys.*, *85*, 6660–6667, doi:10.1063/1.370176.

Pike, C. R., A. P. Roberts, and K. L. Verosub (2001a), First-order reversal curve diagrams and thermal relaxation effects in magnetic particles, *Geophys. J. Int.*, *145*, 721–730, doi:10.1046/j.0956-540x.2001.01419.x.

Pike, C. R., A. P. Roberts, M. J. Dekkers, and K. L. Verosub (2001b), An investigation of multi-domain hysteresis mechanisms using FORC diagrams, *Phys. Earth Planet. Inter.*, *126*, 11–25, doi:10.1016/S0031-9201(01)00241-2.

Pillans, B., and I. Wright (1990), 500,000-Year paleomagnetic record from New Zealand loess, *Quat. Res.*, *33*, 178–187, doi:10.1016/0033-5894(90)90017-F.

Pirrung, M., C. D. Hillenbrand, B. Diekmann, D. Fütterer, H. Grobe, and G. Kuhn (2002), Magnetic susceptibility and ice-rafted debris in surface sediments of the Atlantic sector of the Southern Ocean, *Geo Mar. Lett.*, *22*, 170–180, doi:10.1007/s00367-002-0109-7.

Pope, R. J. J., and A. C. Millington (2000), Unraveling the patterns of alluvial fan development using mineral magnetic analysis: Examples from the Sparta Basin, Lakonia, southern Greece, *Earth Surf. Processes Landforms*, *25*, 601–615, doi:10.1002/1096-9837(200006)25:6<601::AID-ESP94>3.0.CO;2-M.

Porter, S. C., and Z. S. An (1995), Correlation between climate events in the North Atlantic and China during the last glaciation, *Nature*, *375*, 305–308, doi:10.1038/375305a0.

Pósfai, M., B. M. Moskowitz, B. Arató, D. Schüler, C. Flies, D. A. Bazylinski, and R. B. Frankel (2006), Properties of intracellular magnetite crystals produced by *Desulfovibrio magneticus* strain RS-1, *Earth Planet. Sci. Lett.*, *249*, 444–455, doi:10.1016/j.epsl.2006.06.036.

Poulton, S. W., M. D. Krom, and R. Raiswell (2004), A revised scheme for the reactivity of iron (oxyhydr) oxide minerals towards dissolved sulfide, *Geochim. Cosmochim. Acta*, *68*, 3703–3715, doi:10.1016/j.gca.2004.03.012.

Prakash Babu, C. P., J. N. Pattan, K. Dutta, N. Basavaiah, G. V. Ravi Prasad, D. K. Ray, and P. Govil (2010), Shift in detrital sedimentation in the eastern Bay of Bengal during the late Quaternary, *J. Earth Syst. Sci.*, *119*, 285–295, doi:10.1007/s12040-010-0022-9.

Pugh, R. S., I. N. McCave, C. D. Hillenbrand, and G. Kuhn (2009), Circum-Antarctic age modeling of Quaternary marine cores under the Antarctic Cirumpolar Current: Ice-core dust-magnetic correlation, *Earth Planet. Sci. Lett.*, *284*, 113–123, doi:10.1016/j.epsl.2009.04.016.

Radhakrishnamurty, C., and S. D. Likhite (1993), Frequency dependence of low-temperature susceptibility peak in some titanomagnetites, *Phys. Earth Planet. Inter.*, *76*, 131–135, doi:10.1016/0031-9201(93)90062-E.

Raiswell, R., M. Tranter, L. G. Benning, M. Siegert, R. De'ath, P. Huybrechts, and T. Payne (2006), Contribution from glacially derived sediment to the global iron (oxyhydr)oxide cycle: Implications for iron delivery to the oceans, *Geochim. Cosmochim. Acta*, *70*, 2765–2780, doi:10.1016/j.gca.2005.12.027.

Rea, D. K. (1994), The paleoclimatic record provided by eolian deposition in the deep sea: The geologic history of wind, *Rev. Geophys.*, *32*, 159–195, doi:10.1029/93RG03257.

Rey, D., N. López-Rodríguez, B. Rubio, F. Vilas, K. Mohamed, O. Pazos, and M. F. Bógalo (2000), Magnetic properties of estuarine-like sediments: The study case of the Galician Rias, *J. Ib. Geol.*, *26*, 151–170.

Rey, D., K. J. Mohamed, A. Bernabeu, B. Rubio, and F. Vilas (2005), Early diagenesis of magnetic minerals in marine transitional environments: Geochemical signatures of hydrodynamic forcing, *Mar. Geol.*, *215*, 215–236, doi:10.1016/j.margeo.2004.12.001.

Reynolds, R. L., N. S. Fishman, and M. R. Hudson (1991), Sources of aeromagnetic anomalies over Cement oil field (Oklahoma), Simpson oil field (Alaska), and the Wyoming-Idaho-Utah thrust belt, *Geophysics*, *56*, 606–617.

Reynolds, R. L., M. L. Tuttle, C. A. Rice, N. S. Fishman, J. A. Karachewski, and D. W. Sherman (1994), Magnetization and geochemistry of greigite-bearing Cretaceous strata, North Slope Basin, Alaska, *Am. J. Sci.*, *294*, 485–528, doi:10.2475/ajs.294.4.485.

Reynolds, R. L., J. G. Rosenbaum, P. van Metre, M. Tuttle, E. Callender, and A. Goldin (1999), Greigite (Fe_3S_4) as an indicator of drought–The 1912–1994 sediment magnetic record from White Rock Lake, Dallas, Texas, USA, *J. Paleolimnol.*, *21*, 193–206, doi:10.1023/A:1008027815203.

Roberts, A. P. (1995), Magnetic properties of sedimentary greigite (Fe_3S_4), *Earth Planet. Sci. Lett.*, *134*, 227–236, doi:10.1016/0012-821X(95)00131-U.

Roberts, A. P. (2006), High-resolution magnetic analysis of sediment cores: Strengths, limitations and strategies for maximizing the value of long-core magnetic data, *Phys. Earth Planet. Inter.*, *156*, 162–178.

Roberts, A. P., and B. J. Pillans (1993), Rock magnetism of Middle/Lower Pleistocene marine sediments, Wanganui Basin, New Zealand, *Geophys. Res. Lett.*, *20*, 839–842, doi:10.1029/93GL00802.

Roberts, A. P., and G. M. Turner (1993), Diagenetic formation of ferrimagnetic iron sulphide minerals in rapidly deposited marine sediments, South Island, New Zealand, *Earth Planet. Sci. Lett.*, *115*, 257–273, doi:10.1016/0012-821X(93)90226-Y.

Roberts, A. P., and R. Weaver (2005), Multiple mechanisms of remagnetization involving sedimentary greigite (Fe_3S_4), *Earth Planet. Sci. Lett.*, *231*, 263–277, doi:10.1016/j.epsl.2004.11.024.

Roberts, A. P., Y. Cui, and K. L. Verosub (1995), Wasp-waisted hysteresis loops: Mineral magnetic characteristics and discrimination of components in mixed magnetic systems, *J. Geophys. Res.*, *100*, 17,909–17,924, doi:10.1029/95JB00672.

Roberts, A. P., R. L. Reynolds, K. L. Verosub, and D. P. Adam (1996), Environmental magnetic implications of greigite (Fe_3S_4) formation in a 3 m.y. lake sediment record from Butte Valley, northern California, *Geophys. Res. Lett.*, *23*, 2859–2862, doi:10.1029/96GL02831.

Roberts, A. P., J. S. Stoner, and C. Richter (1999), Diagenetic magnetic enhancement of sapropels from the eastern Mediterranean Sea, *Mar. Geol.*, *153*, 103–116, doi:10.1016/S0025-3227(98)00087-5.

Roberts, A. P., C. R. Pike, and K. L. Verosub (2000), First-order reversal curve diagrams: A new tool for characterizing the magnetic properties of natural samples, *J. Geophys. Res.*, *105*, 28,461–28,475, doi:10.1029/2000JB900326.

Roberts, A. P., Q. S. Liu, C. J. Rowan, L. Chang, C. Carvallo, J. Torrent, and C. S. Horng (2006), Characterization of hematite (α-Fe_2O_3), goethite (α-FeOOH), greigite (Fe_3S_4), and pyrrhotite (Fe_7S_8) using first-order reversal curve diagrams, *J. Geophys. Res.*, *111*, B12S35, doi:10.1029/2006JB004715.

Roberts, A. P., F. Florindo, J. C. Larrasoaña, M. A. O'Regan, and X. Zhao (2010), Complex polarity pattern at the (former) Plio-Pleistocene global stratotype section at Vrica (Italy): Remagnetization by magnetic iron sulphides, *Earth Planet. Sci. Lett.*, *292*, 98–111, doi:10.1016/j.epsl.2010.01.025.

Roberts, A. P., L. Chang, C. J. Rowan, C. S. Horng, and F. Florindo (2011a), Magnetic properties of sedimentary greigite (Fe_3S_4): An update, *Rev. Geophys.*, *49*, RG1002, doi:10.1029/2010RG000336.

Roberts, A. P., F. Florindo, G. Villa, L. Chang, L. Jovane, S. M. Bohaty, J. C. Larrasoaña, D. Heslop, and J. D. Fitz Gerald (2011b), Magnetotactic bacterial abundance in pelagic marine environments is limited by organic carbon flux and availability of dissolved iron, *Earth Planet. Sci. Lett.*, *310*, 441–452, doi:10.1016/j.epsl.2011.08.011.

Roberts, A. P., E. J. Rohling, K. M. Grant, J. C. Larrasoaña, and Q. S. Liu (2011c), Atmospheric dust variability from major global source regions over the last 500,000 years, *Quat. Sci. Rev.*, *30*, 3537–3541, doi:10.1016/j.quascirev.2011.09.007.

Robertson, D. J., and D. E. France (1994), Discrimination of remanence-carrying minerals in mixtures, using isothermal remanent magnetisation acquisition curves, *Phys. Earth Planet. Inter.*, *82*, 223–234, doi:10.1016/0031-9201(94)90074-4.

Robinson, S. G. (1986), The Late Pleistocene palaeoclimatic record of North Atlantic deep-sea sediments revealed by mineral-magnetic masurements, *Phys. Earth Planet. Inter.*, *42*, 22–47, doi:10.1016/S0031-9201(86)80006-1.

Robinson, S. G., M. A. Maslin, and I. N. McCave (1995), Magnetic susceptibility variations in Upper Pleistocene deep-sea sediments of the N. E. Atlantic: Implications for ice rafting and paleocirculation at the Last Glacial Maximum, *Paleoceanography*, *10*, 221–250, doi:10.1029/94PA02683.

Robinson, S. G., J. T. S. Sahota, and F. Oldfield (2000), Early diagenesis in North Atlantic abyssal plain sediments characterized by rock-magnetic and geochemical indices, *Mar. Geol.*, *163*, 77–107, doi:10.1016/S0025-3227(99)00108-5.

Rochette, P., and G. Fillion (1989), Field and temperature behavior of remanence in synthetic goethite: Paleomagnetic implications, *Geophys. Res. Lett.*, *16*, 851–854, doi:10.1029/GL016i008p00851.

Rochette, P., G. Fillion, J.-L. Mattéi, and M. J. Dekkers (1990), Magnetic transition at 30–34 Kelvin in pyrrhotite: Insight into a widespread occurrence of this mineral in rocks, *Earth Planet. Sci. Lett.*, *98*, 319–328, doi:10.1016/0012-821X(90)90034-U.

Rochette, P., P. E. Mathe, L. Esteban, H. Rakoto, J. L. Bouchez, Q. S. Liu, and J. Torrent (2005), Non-saturation of the defect moment of goethite and fine-grained hematite up to 57 Teslas, *Geophys. Res. Lett.*, *32*, L22309, doi:10.1029/2005GL024196.

Rochette, P., G. Fillion, and M. J. Dekkers (2011), Interpretation of low-temperature data part 4: The low-temperature magnetic transition of monoclinic pyrrhotite, *IRM Q.*, *21*, 1–11.

Rohling, E. J., K. Grant, C. Hemleben, M. Kucera, A. P. Roberts, I. Schmeltzer, H. Schulz, M. Siccha, M. Siddall, and G. Trommer (2008), New constraints on the timing of sea level fluctuations during early to middle marine isotope stage 3, *Paleoceanography*, *23*, PA3219, doi:10.1029/2008PA001617.

Rohling, E. J., K. Grant, M. Bolshaw, A. P. Roberts, M. Siddall, C. Hemleben, and M. Kucera (2009), Antarctic temperature and global sea level closely coupled over the past five glacial cycles, *Nat. Geosci.*, *2*, 500–504, doi:10.1038/ngeo557.

Rose, A. W., and G. C. Bianchi-Mosquera (1993), Adsorption of Cu, Pb, Zn, Co, Ni and Ag on goethite and hematite: A control on metal mobilization from red beds into stratiform copper deposits, *Econ. Geol.*, *88*, 1226–1236, doi:10.2113/gsecongeo.88.5.1226.

Rosenbaum, J. G., and R. L. Reynolds (2004), Basis for paleoenvironmental interpretation of magnetic properties of sediment from Upper Klamath Lake (Oregon): Effects of weathering and mineralogical sorting, *J. Paleolimnol.*, *31*, 253–265, doi:10.1023/B:JOPL.0000019228.46421.f4.

Rousse, S., C. Kissel, C. Laj, J. Eiríksson, and K. L. Knudsen (2006), Holocene centennial to millennial-scale climatic variability: Evidence from high-resolution magnetic analyses of the last 10 cal kyr off North Iceland (core MD88–2275), *Earth Planet. Sci. Lett.*, *242*, 390–405, doi:10.1016/j.epsl.2005.07.030.

Rowan, C. J., and A. P. Roberts (2006), Magnetite dissolution, diachronous greigite formation, and secondary magnetizations from pyrite oxidation: Unravelling complex magnetizations in Neogene marine sediments from New Zealand, *Earth Planet. Sci. Lett.*, *241*, 119–137, doi:10.1016/j.epsl.2005.10.017.

Rowan, C. J., A. P. Roberts, and T. Broadbent (2009), Reductive diagenesis, magnetite dissolution, greigite growth and paleomagnetic smoothing in marine sediments: A new view, *Earth Planet. Sci. Lett.*, *277*, 223–235, doi:10.1016/j.epsl.2008.10.016.

Rustad, J. R., and A. R. Felmy (2005), The influence of edge sites on the development of surface charge on goethite nanoparticles: A molecular dynamics investigation, *Geochim. Cosmochim. Acta*, *69*, 1405–1411, doi:10.1016/j.gca.2004.08.030.

Ryves, D. B., V. J. Jones, P. Guilizzoni, A. Lami, A. Marchetto, R. W. Battarbee, R. Bettinetti, and E. C. Devoy (1996), Late Pleistocene and Holocene environmental changes at Lake Albano and Lake Nemi (central Italy) as indicated by algal remains, in *Palaeoenvironmental Analysis of Italian Crater Lake and Adriatic Sediments (PALICLAS)*, vol. 55, edited by P. Guilizzoni and F. Oldfield, pp. 119–148, Ist. Ital. di Idrobiologia, Verbiana-Pallanza, Italy.

Sagnotti, L., P. Rochette, and M. Jackson, and the MAG-NET Science Team (2003), Inter-laboratory calibration of low-field magnetic and anhysteretic susceptibility measurements, *Phys. Earth Planet. Inter.*, *138*, 25–38, doi:10.1016/S0031-9201(03)00063-3.

Sagnotti, L., P. Macrí, R. Egli, and M. Mondino (2006), Magnetic properties of atmospheric particulate matter from automatic air sampler stations in Latium (Italy): Toward a definition of magnetic fingerprints for natural and anthropogenic PM10 sources, *J. Geophys. Res.*, *111*, B12S22, doi:10.1029/2006JB004508.

Salomé, A. L., and L. Meynadier (2004), Magnetic properties of rivers, sands and rocks from Martinique Islands: Tracers of weathering?, *Phys. Chem. Earth*, *29*, 933–945, doi:10.1016/j.pce.2004.06.002.

Sander, S. G., and A. Koschinsky (2011), Metal flux from hydrothermal vents increased by organic complexation, *Nat. Geosci.*, *4*, 145–150, doi:10.1038/ngeo1088.

Sandgren, P., and I. Snowball (2002), Application of mineral magnetic techniques to paleolimnology, in *Tracking Environmental Change Using Lake Sediments: Physical and Geochemical Methods*, vol. 2, edited by W. M. Last and J. P. Smol, pp. 217–237, Kluwer Acad., Dordrecht, Netherlands.

Schabes, M. E., and H. N. Bertram (1988), Magnetization processes in ferromagnetic cubes, *J. Appl. Phys.*, *64*, 1347, doi:10.1063/1.341858.

Schüler, D., and E. Baeuerlein (1996), Iron-limited growth and kinetics of iron uptake in *Magnetospirillum gryphiswaldense*, *Arch. Microbiol.*, *166*, 301–307, doi:10.1007/s002030050387.

Schumann, D., et al. (2008), Gigantism in unique biogenic magnetite at the Paleocene–Eocene Thermal Maximum, *Proc. Natl. Acad. Sci. U. S. A.*, *105*, 17,648–17,653, doi:10.1073/pnas.0803634105.

Schütz, G., W. Wagner, W. Wilhelm, P. Kienle, R. Zeller, R. Frahm, and G. Materlik (1987), Absorption of circularly polarized X rays in iron, *Phys. Rev. Lett.*, *58*, 737–740, doi:10.1103/PhysRevLett.58.737.

Schwartz, M., S. P. Lund, D. E. Hammond, R. Schwartz, and K. Wong (1997), Early sediment diagenesis on the Blake/Bahama Outer Ridge, North Atlantic Ocean, and its effects on sediment magnetism, *J. Geophys. Res.*, *102*, 7903–7914, doi:10.1029/96JB03218.

Scourse, J. D., I. R. Hall, I. N. McCave, J. R. Young, and C. Sugden (2000), The origin of Heinrich layers: Evidence from H2 for European precursor events, *Earth Planet. Sci. Lett.*, *182*, 187–195, doi:10.1016/S0012-821X(00)00241-7.

Šimša, Z., F. Zounová, and S. Krupička (1985), Initial permeability of single crystal magnetite and Mn-ferrite, *Czech. J. Phys.*, *35*, 1271–1281, doi:10.1007/BF01597013.

Singer, M. J., K. L. Verosub, P. Fine, and J. TenPas (1996), A conceptual model for the enhancement of magnetic susceptibility in soils, *Quat. Int.*, *34–36*, 243–248, doi:10.1016/1040-6182(95)00089-5.

Sinha, R., P. S. Bhattacharjee, S. J. Sangode, M. R. Gibling, S. K. Tandon, M. Jain, and D. Godfrey-Smith (2007), Valley and interfluve sediments in the Southern Ganga plains, India: Exploring facies and magnetic signatures, *Sediment. Geol.*, *201*, 386–411, doi:10.1016/j.sedgeo.2007.07.004.

Skumryev, V., H. J. Blythe, J. Cullen, and J. M. D. Coey (1999), AC susceptibility of a magnetite crystal, *J. Magn. Magn. Mater.*, *196–197*, 515–517, doi:10.1016/S0304-8853(98)00863-4.

Snowball, I. F. (1991), Magnetic hysteresis properties of greigite (Fe_3S_4) and a new occurrence in Holocene sediments from Swedish Lappland, *Phys. Earth Planet. Inter.*, *68*, 32–40, doi:10.1016/0031-9201(91)90004-2.

Snowball, I. F. (1994), Bacterial magnetite and the magnetic properties of sediments in a Swedish lake, *Earth Planet. Sci. Lett.*, *126*, 129–142, doi:10.1016/0012-821X(94)90246-1.

Snowball, I. F., and R. Thompson (1988), The occurrence of greigite in the sediments of Loch Lomond, *J. Quat. Sci.*, *3*, 121–125, doi:10.1002/jqs.3390030203.

Snowball, I. F., and R. Thompson (1990), A stable chemical remanence in Holocene sediments, *J. Geophys. Res.*, *95*, 4471–4479, doi:10.1029/JB095iB04p04471.

Snowball, I. F., P. Sandgren, and G. Petterson (1999), The mineral magnetic properties of an annually laminated Holocene lake sediment sequence in northern Sweden, *Holocene*, *9*, 353–362, doi:10.1191/095968399670520633.

Snowball, I. F., L. Zillén, and P. Sandgren (2002), Biogenic magnetite in Swedish varved lake sediments and its potential as a biomarker of environmental change, *Quat. Int.*, *88*, 13–19, doi:10.1016/S1040-6182(01)00069-6.

Spassov, S., F. Heller, R. Kretzschmar, M. E. Evans, L. P. Yue, and D. K. Nourgaliev (2003), Detrital and pedogenic magnetic mineral phases in the loess/palaeosol sequence at Lingtai (Central Chinese Loess Plateau), *Phys. Earth Planet. Inter.*, *140*, 255–275, doi:10.1016/j.pepi.2003.09.003.

Stacey, F. D. (1962), A generalized theory of thermoremanence, covering the transition from single domain to multi-domain magnetic grains, *Philos. Mag.*, *7*, 1887–1900, doi:10.1080/14786436208213853.

Stacey, F. D., and S. K. Banerjee (1974), *The Physical Principles of Rock Magnetism*, Elsevier, New York.

Stanford, J. D., E. J. Rohling, S. Hunter, A. P. Roberts, S. O. Rasmussen, E. Bard, J. McManus, and R. G. Fairbanks (2006), Meltwater injections and deep circulation in the North Atlantic, *Paleoceanography*, *21*, PA4103, doi:10.1029/2006PA001340.

Stanford, J. D., E. J. Rohling, S. Bacon, A. P. Roberts, F. E. Grousset, and M. Bolshaw (2011), A new concept for the paleoceanographic evolution of Heinrich event 1 in the North Atlantic, *Quat. Sci. Rev.*, *30*, 1047–1066, doi:10.1016/j.quascirev.2011.02.003.

Stein, R., et al. (2004), Arctic (palaeo) river discharge and environmental change: Evidence from the Holocene Kara Sea sedimentary record, *Quat. Sci. Rev.*, *23*, 1485–1511, doi:10.1016/j.quascirev.2003.12.004.

Stockhausen, H., and N. Thouveny (1999), Rock-magnetic properties of Eemian maar lake sediments from Massif central, France: A climatic signature?, *Earth Planet. Sci. Lett.*, *173*, 299–313, doi:10.1016/S0012-821X(99)00237-X.

Stolz, J. F., S. B. R. Chang, and J. L. Kirschvink (1986), Magnetotactic bacteria and single-domain magnetite in hemipelagic sediments, *Nature*, *321*, 849–851, doi:10.1038/321849a0.

Stoner, J. S., and J. T. Andrews (1999), The North Atlantic as a Quaternary magnetic archive, in *Quaternary Climates, Environments, and Magnetism*, edited by B. A. Maher and R. Thompson, pp. 49–80, Cambridge Univ. Press, Cambridge, U. K., doi:10.1017/CBO9780511535635.003.

Stoner, J. S., J. E. T. Channell, and C. Hillaire-Marcel (1996), The magnetic signature of rapidly deposited detrital layers from the deep Labrador Sea: Relationships to North Atlantic Heinrich Layers, *Paleoceanography*, *11*, 309–325, doi:10.1029/96PA00583.

Stoner, J. S., J. E. T. Channell, and C. Hillaire-Marcel (1998), A 200 kyr geomagnetic chronostratigraphy for deep Labrador Sea sediments: Indirect correlation to SPECMAP, *Earth Planet. Sci. Lett.*, *159*, 165–181, doi:10.1016/S0012-821X(98)00069-7.

Straub, S. M., and H. U. Schmincke (1998), Evaluating the tephra input into Pacific Ocean sediments: Distribution in space and time, *Geol. Rundsch.*, *87*, 461–476, doi:10.1007/s005310050222.

Strzyszcz, Z., T. Magiera, and F. Heller (1996), The influence of industrial emissions on the magnetic susceptibility of soils in Upper Silesia, *Stud. Geophys. Geod.*, *40*, 276–286, doi:10.1007/BF02300743.

Suavet, C., P. Rochette, J. Gattacceca, and L. Folco (2008), Micrometeorites: A possible bias on the sedimentary magnetic record, *Geochem. Geophys. Geosyst.*, *9*, Q11002, doi:10.1029/2008GC002160.

Sugiura, N. (1979), ARM, TRM and magnetic interactions: Concentration dependence, *Earth Planet. Sci. Lett.*, *42*, 451–455, doi:10.1016/0012-821X(79)90054-2.

Sun, J., and T. S. Liu (2000), Multiple origins and interpretations of the magnetic susceptibility signal in Chinese wind-blown sediments, *Earth Planet. Sci. Lett.*, *180*, 287–296, doi:10.1016/S0012-821X(00)00175-8.

Sun, Y., J. Chen, S. C. Clemens, Q. Liu, J. Ji, and R. Tada (2006a), East Asian monsoon variability over the last seven glacial cycles recorded by a loess sequence from the northwestern Chinese Loess Plateau, *Geochem. Geophys. Geosyst.*, *7*, Q12Q02, doi:10.1029/2006GC001287.

Sun, Y., S. C. Clemens, Z. An, and Z. Yu (2006b), Astronomical timescale and palaeoclimatic implication of stacked 3.6-Myr monsoon records from the Chinese Loess Plateau, *Quat. Sci. Rev.*, *25*, 33–48, doi:10.1016/j.quascirev.2005.07.005.

Sun, Y., R. Tada, J. Chen, Q. Liu, S. Toyoda, A. Tani, J. Ji, and Y. Isozaki (2008), Tracing the provenance of fine-grained dust deposited on the central Chinese Loess Plateau, *Geophys. Res. Lett.*, *35*, L01804, doi:10.1029/2007GL031672.

Sweeney, R. E., and I. R. Kaplan (1973), Pyrite framboid formation: Laboratory synthesis and marine sediments, *Econ. Geol.*, *68*, 618–634, doi:10.2113/gsecongeo.68.5.618.

Szönyi, M., L. Sagnotti, and A. M. Hirt (2008), A refined biomonitoring study of airborne particulate matter pollution in Rome, with magnetic measurements on *Quercus ilex* tree leaves, *Geophys. J. Int.*, *173*, 127–141, doi:10.1111/j.1365-246X.2008.03715.x.

Tarduno, J. A. (1994), Temporal change of magnetic dissolution in the pelagic realm: Gauging paleoproductivity?, *Earth Planet. Sci. Lett.*, *123*, 39–48, doi:10.1016/0012-821X(94)90255-0.

Tarduno, J. A., and S. Wilkison (1996), Non-steady state magnetic mineral reduction, chemical lock-in, and delayed remanence acquisition in pelagic sediments, *Earth Planet. Sci. Lett.*, *144*, 315–326, doi:10.1016/S0012-821X(96)00174-4.

Tarduno, J. A., W. L. Tiang, and S. Wilkison (1998), Biogeochemical remanent magnetization in pelagic sediments of the western equatorial Pacific Ocean, *Geophys. Res. Lett.*, *25*, 3987–3990, doi:10.1029/1998GL900079.

Tauxe, L. (1993), Sedimentary records of relative paleointensity of the geomagnetic field—Theory and practice, *Rev. Geophys.*, *31*, 319–354, doi:10.1029/93RG01771.

Tauxe, L. (2010), *Essentials of Paleomagnetism*, Univ. of Calif. Press, Berkeley.

Tauxe, L., C. Constable, L. Stokking, and C. Badgley (1990), Use of anisotropy to determine the origin of the characteristic remanence in Siwalik red beds of northern Pakistan, *J. Geophys. Res.*, *95*, 4391–4404, doi:10.1029/JB095iB04p04391.

Tauxe, L., H. N. Bertram, and C. Seberino (2002), Physical interpretation of hysteresis loops: Micromagnetic modeling of fine particle magnetite, *Geochem. Geophys. Geosyst.*, *3*(10), 1055, doi:10.1029/2001GC000241.

Thompson, R. (1973), Palaeolimnology and palaeomagnetism, *Nature*, *242*, 182–184, doi:10.1038/242182a0.

Thompson, R., and F. Oldfield (1986), *Environmental Magnetism*, Allen and Unwin, Winchester, Mass., doi:10.1007/978-94-011-8036-8

Thompson, R., R. W. Battarbee, P. E. O'Sullivan, and F. Oldfield (1975), Magnetic susceptibility of lake sediments, *Limnol. Oceanogr.*, *20*, 687–698, doi:10.4319/lo.1975.20.5.0687.

Thompson, R., J. Bloemendal, J. A. Dearing, F. Oldfield, T. A. Rummery, J. A. Stober, and G. M. Turner (1980), Environmental applications of magnetic measurements, *Science*, *207*, 481–486, doi:10.1126/science.207.4430.481.

Thouveny, N., et al. (1994), Climate variations in Europe over the past 140 kyr deduced from rock magnetism, *Nature*, *371*, 503–506, doi:10.1038/371503a0.

Thouveny, N., E. Moreno, D. Delanghe, L. Candon, Y. Lancelot, and N. J. Shackleton (2000), Rock magnetic identification of Heinrich layers on the Portuguese margin, *Earth Planet. Sci. Lett.*, *180*, 61–75, doi:10.1016/S0012-821X(00)00155-2.

Tian, L. X., W. Lin, S. Y. Zhang, and Y. X. Pan (2010), Bat head contains soft magnetic particles: Evidence from magnetism, *Bioelectromagnetics*, *31*, 499–503, doi:10.1002/bem.20590.

Tiedemann, R., M. Sarnthein, and N. J. Shackleton (1994), Astronomical timescale for the Pliocene Atlantic $\delta^{18}O$ and dust flux records of Ocean Drilling Program Site 659, *Paleoceanography*, *9*, 619–638, doi:10.1029/94PA00208.

Till, J., M. J. Jackson, J. G. Rosenbaum, and P. Solheid (2011), Magnetic properties in an ash flow tuff with continuous grain size variation: A natural reference for magnetic particle granulometry, *Geochem. Geophys. Geosyst.*, *12*, Q07Z26, doi:10.1029/2011GC003648.

Torii, M., T. Q. Lee, K. Fukuma, T. Mishima, T. Yamazaki, H. Oda, and N. Ishikawa (2001), Mineral magnetic study of the Taklimakan desert sands and its relevance to the Chinese loess, *Geophys. J. Int.*, *146*, 416–424, doi:10.1046/j.0956-540x.2001.01463.x.

Torrent, J., V. Barrón, and Q. S. Liu (2006), Magnetic enhancement is linked to and precedes hematite formation in aerobic soil, *Geophys. Res. Lett.*, *33*, L02401, doi:10.1029/2005GL024818.

Trauth, M. H., J. C. Larrasoaña, and M. Mudelsee (2009), Trends, rhythms and events in Plio-Pleistocene African climate, *Quat. Sci. Rev.*, *28*, 399–411, doi:10.1016/j.quascirev.2008.11.003.

Tric, E., C. Laj, C. Jehanno, J. P. Valet, C. Kissel, A. Mazaud, and S. Iaccarino (1991), High-resolution record of the Upper Olduvai transition from Po Valley (Italy) sediments: Support for dipolar transition geometry?, *Phys. Earth Planet. Inter.*, *65*, 319–336, doi:10.1016/0031-9201(91)90138-8.

van der Post, K. D., F. Oldfield, E. Y. Haworth, P. R. J. Crooks, and P. G. Appleby (1997), A record of accelerated erosion in the recent sediments of Blelham Tarn in the English Lake District, *J. Paleolimnol.*, *18*, 103–120, doi:10.1023/A:1007922129794.

van Dongen, B. E., A. P. Roberts, S. Schouten, W. T. Jiang, F. Florindo, and R. D. Pancost (2007), Formation of iron sulfide nodules during anaerobic oxidation of methane, *Geochim. Cosmochim. Acta*, *71*, 5155–5167, doi:10.1016/j.gca.2007.08.019.

van Santvoort, P. J. M., G. J. de Lange, C. G. Langereis, M. J. Dekkers, and M. Paterne (1997), Geochemical and paleomagnetic evidence for the occurrence of "missing" sapropels in eastern Mediterranean sediments, *Paleoceanography*, *12*, 773–786, doi:10.1029/97PA01351.

Vasiliev, I., C. Franke, J. D. Meeldijk, M. J. Dekkers, C. G. Langereis, and W. Krijgsman (2008), Putative greigite magnetofossils from the Pliocene epoch, *Nat. Geosci.*, *1*, 782–786, doi:10.1038/ngeo335.

Venuti, A., F. Florindo, A. Carburlotto, M. W. Hounslow, C.-D. Hillenbrand, E. Strada, F. M. Talarico, and A. Cavallo (2011), Late Quaternary sediments from deep-sea sediment drifts on the Antarctic Peninsula Pacific margin: Climatic control on the provenance of minerals, *J. Geophys. Res.*, *116*, B06104, doi:10.1029/2010JB007952.

Verosub, K. L., and A. P. Roberts (1995), Environmental magnetism: Past, present, and future, *J. Geophys. Res.*, *100*, 2175–2192, doi:10.1029/94JB02713.

Verosub, K. L., P. Fine, M. J. Singer, and J. TenPas (1993), Pedogenesis and paleoclimate: Interpretation of the magnetic susceptibility record of Chinese loess-paleosol sequences, *Geology*, *21*, 1011–1014, doi:10.1130/0091-7613(1993)021<1011:PAPIOT>2.3.CO;2.

Verwey, E. J. (1939), Electronic conduction of magnetite (Fe_3O_4) and its transition point at low temperature, *Nature*, *144*, 327–328, doi:10.1038/144327b0.

Vidic, N. J., K. L. Verosub, and M. J. Singer (2003), The Chinese loess perspective on Marine Isotope Stage 11 as an extreme interglacial, in *Earth's Climate and Orbital Eccentricity: The Marine Isotope Stage 11 Question*, *Geophys. Monogr. Ser.*, vol. 137, edited by A. W. Droxler, R. Z. Poore, and L. H. Burckle, pp. 231–240, AGU, Washington, D. C., doi:10.1029/137GM17.

Vigliotti, L. (1997), Magnetic properties of light and dark sediment layers from the Japan Sea: Diagenetic and paleoclimatic implications, *Quat. Sci. Rev.*, *16*, 1093–1114, doi:10.1016/S0277-3791(96)00118-7.

Vincent, K. R., W. B. Bull, and O. A. Chadwick (1994), Construction of a soil chronosequence using the thickness of pedogenic carbonate coatings, *J. Geosci. Educ.*, *42*, 316–324.

Walden, J., F. Oldfield, and J. Smith (Eds.) (1999), Environmental magnetism: A practical guide, *Tech. Guide 6*, Quat. Res. Assoc., London.

Walden, J., K. H. White, S. H. Kilcoyne, and P. M. Bentley (2000), Analyses of iron oxide assemblages within Namib dune sediments using high field remanence measurements (9 T) and Mössbauer analysis, *J. Quat. Sci.*, *15*, 185–195, doi:10.1002/(SICI)1099-1417(200002)15:2<185::AID-JQS503>3.0.CO;2–5.

Walden, J., E. Wadsworth, W. E. N. Austin, C. Peters, J. D. Scourse, and I. R. Hall (2007), Compositional variability of ice-rafted debris in Heinrich layers 1 and 2 on the northwest European continental slope identified by environmental magnetic analyses, *J. Quat. Sci.*, *22*, 163–172, doi:10.1002/jqs.1020.

Walling, D. E., M. R. Peart, F. Oldfield, and R. Thompson (1979), Suspended sediment sources identified by magnetic measurements, *Nature*, *281*, 110–113, doi:10.1038/281110a0.

Wang, C., X. Hu, Y. Huang, M. Wagreight, R. Scott, and W. Hay (2011), Cretaceous oceanic red beds as possible consequence of oceanic anoxic events, *Sediment. Geol.*, *235*, 27–37, doi:10.1016/j.sedgeo.2010.06.025.

Watson, J. H. P., B. A. Cressey, A. P. Roberts, D. C. Ellwood, J. M. Charnock, and A. K. Soper (2000), Structural and magnetic studies on heavy-metal-adsorbing iron sulphide nanoparticles produced by sulphate-reducing bacteria, *J. Magn. Magn. Mater.*, *214*, 13–30, doi:10.1016/S0304-8853(00)00025-1.

Waychunas, G. A. (1991), Crystal chemistry of oxides and oxyhydroxides, *Rev. Mineral. Geochem.*, *25*, 11–68.

Weaver, R., A. P. Roberts, and A. J. Barker (2002), A late diagenetic (syn-folding) magnetization carried by pyrrhotite: Implications for paleomagnetic studies from magnetic iron sulphide-bearing sediments, *Earth Planet. Sci. Lett.*, *200*, 371–386, doi:10.1016/S0012-821X(02)00652-0.

Weber, M. E., M. Wiedicke-Hombach, H. R. Kudrass, and H. Erlenkeuser (2003), Bengal Fan sediment transport activity and response to climate forcing inferred from sediment physical properties, *Sediment. Geol.*, *155*, 361–381, doi:10.1016/S0037-0738(02)00187-2.

Weeks, R., C. Laj, L. Endignoux, M. Fuller, A. Roberts, R. Manganne, E. Blanchard, and W. Goree (1993), Improvements in long-core measurement techniques: Applications in palaeomagnetism and palaeoceanography, *Geophys. J. Int.*, *114*, 651–662, doi:10.1111/j.1365-246X.1993.tb06994.x.

White, K., and J. Walden (1997), The rate of iron oxide enrichment in arid zone alluvial fan soils, Tunisian southern Atlas, measured by mineral magnetic techniques, *Catena*, *30*, 215–227, doi:10.1016/S0341-8162(97)00021-0.

Whitmeyer, S. J., L. S. Fichter, and E. J. Pyle (2007), New directions in Wilson Cycle concepts: Supercontinent and tectonic rock cycles, *Geosphere*, *3*, 511–526, doi:10.1130/GES00091.1.

Williams, T., T. van de Flierdt, S. R. Hemming, E. Chung, M. Roy, and S. L. Goldstein (2010), Evidence for iceberg armadas from East Antarctica in the Southern Ocean during the late Miocene and early Pliocene, *Earth Planet. Sci. Lett.*, *290*, 351–361, doi:10.1016/j.epsl.2009.12.031.

Williams, W., and D. J. Dunlop (1989), Three-dimensional micromagnetic modelling of ferromagnetic domain structure, *Nature*, *337*, 634–637, doi:10.1038/337634a0.

Williams, W., and D. J. Dunlop (1995), Simulation of magnetic hysteresis in pseudo-single-domain grains of magnetite, *J. Geophys. Res.*, *100*, 3859–3871, doi:10.1029/94JB02878.

Williamson, D., A. Jelinowska, C. Kissel, P. Tucholka, E. Gibert, F. Gasse, M. Massault, M. Taieb, E. Van Campo, and K. Wieckowski (1998), Rock magnetic proxies of erosion/oxidation cycles in Late Quaternary maar lake sediments (Lake Tritrivakely, Madagascar):

Paleoenvironmental implications, *Earth Planet. Sci. Lett.*, *155*, 205–219, doi:10.1016/S0012-821X(97)00217-3.

Williamson, D., et al. (1999), Magnetic signatures of hydrological change in a tropical maar-lake (Lake Massoko, Tanzania): Preliminary results, *Phys. Chem. Earth*, *9*, 799–803.

Wilson, J. T. (1966), Did the Atlantic close and then re-open?, *Nature*, *211*, 676–681.

Wiltschko, W., and R. Wiltschko (2005), Magnetic orientation and magnetoreception in birds and other animals, *J. Comp. Physiol.*, *191*, 675–693, doi:10.1007/s00359-005-0627-7.

Worm, H. U. (1998), On the superparamagnetic-stable single domain transition for magnetite, and frequency dependence of susceptibility, *Geophys. J. Int.*, *133*, 201–206, doi:10.1046/j.1365-246X.1998.1331468.x.

Worm, H.-U., and M. Jackson (1999), The superparamagnetism of Yucca Mountain Tuff, *J. Geophys. Res.*, *104*, 25,415–25,425, doi:10.1029/1999JB900285.

Yamazaki, T. (2008), Magnetostatic interactions in deep-sea sediments inferred from first-order reversal curve diagrams: Implications for relative paleointensity normalization, *Geochem. Geophys. Geosyst.*, *9*, Q02005, doi:10.1029/2007GC001797.

Yamazaki, T. (2009), Environmental magnetism of Pleistocene sediments in the North Pacific and Ontong-Java Plaeau: Temporal variations of detrital and biogenic components, *Geochem. Geophys. Geosyst.*, *10*, Q07Z04, doi:10.1029/2009GC002413.

Yamazaki, T. (2012), Paleoposition of the Intertropical Convergence Zone in the eastern Pacific inferred from glacial-interglacial changes in terrigenous and biogenic magnetic mineral fractions, *Geology*, *40*, 151–154, doi:10.1130/G32646.1.

Yamazaki, T., and N. Ioka (1997a), Cautionary note on magnetic grain-size estimation using the ratio of ARM to magnetic susceptibility, *Geophys. Res. Lett.*, *24*, 751–754, doi:10.1029/97GL00602.

Yamazaki, T., and N. Ioka (1997b), Environmental rock-magnetism of pelagic clay: Implications for Asian eolian input to the North Pacific since the Pliocene, *Paleoceanography*, *12*, 111–124, doi:10.1029/96PA02757.

Yamazaki, T., and H. Kawahata (1998), Organic carbon flux controls the morphology of magnetofossils in marine sediments, *Geology*, *26*, 1064–1066, doi:10.1130/0091-7613(1998)026<1064:OCFCTM>2.3.CO;2.

Yang, S., F. Ding, and Z. Ding (2006), Pleistocene chemical weathering history of Asian arid and semi-arid regions recorded in loess deposits of China and Tajikistan, *Geochim. Cosmochim. Acta*, *70*, 1695–1709, doi:10.1016/j.gca.2005.12.012.

Yu, Y., and D. J. Dunlop (2003), Decay-rate dependence of anhysteretic remanence: Fundamental origin and paleomagnetic applications, *J. Geophys. Res.*, *108*(B12), 2550, doi:10.1029/2003JB002589.

Zachos, J., M. Pagani, L. Sloan, E. Thomas, and K. Billups (2001), Trends, rhythms, and aberrations in global climate 65 Ma to Present, *Science*, *292*, 686–693, doi:10.1126/science.1059412.

Zhang, C., B. Huang, J. D. A. Piper, and R. Luo (2008), Biomonitoring of atmospheric particulate matter using magnetic properties of *Salixmatsudana* tree ring cores, *Sci. Total Environ.*, *393*, 177–190, doi:10.1016/j.scitotenv.2007.12.032.

Zhang, W., H. Jiang, C. Dong, Q. Yan, L. Yu, and Y. Yu (2011), Magnetic and geochemical characterization of iron pollution in subway dusts in Shanghai, China, *Geochem. Geophys. Geosyst.*, *12*, Q06Z25, doi:10.1029/2011GC003524.

Zheng, Y., C. Kissel, H. B. Zheng, C. Laj, and K. Wang (2010), Sedimentation on the inner shelf of the East China Sea: Magnetic properties, diagenesis and paleoclimate implications, *Mar. Geol.*, *268*, 34–42, doi:10.1016/j.margeo.2009.10.009.

Zhou, L. P., F. Oldfield, A. G. Wintle, S. G. Robinson, and J. T. Wang (1990), Partly pedogenic origin of magnetic variations in Chinese loess, *Nature*, *346*, 737–739, doi:10.1038/346737a0.

Zhu, R. X., Y. X. Pan, and Q. S. Liu (1999), Geomagnetic excursions recorded in Chinese loess in the last 70,000 years, *Geophys. Res. Lett.*, *26*, 505–508, doi:10.1029/1999GL900019.